REGULATION AND FUNCTION OF P GRANULE DYNAMICS DURING GERMLINE DEVELOPMENT IN C. ELEGANS

by

Jennifer T. Wang

A dissertation submitted to The Johns Hopkins University in conformity with the requirements of the degree of Doctor of Philosophy

Baltimore, Maryland

March, 2014

Abstract

Germ granules are conserved cytoplasmic RNA-protein particles unique to the germline. We have used *C. elegans* germ granules, known as P granules, as a model system to understand the function and regulation of germ granules during embryonic development. We show that PPTR-1, a regulatory subunit of PP2A, is specifically required for P granule segregation during the asymmetric cell divisions of the germline lineage. In the *pptr-1* mutant, we find that germ cells are properly specified despite dramatic P granule segregation defects, indicating that P granule asymmetry is not required for germ cell fate specification.

To elucidate the mechanisms of P granule segregation, we have used PPTR-1 as a tool for identification of novel players in P granule segregation. We find $PP2A^{PPTR-1}$ acts downstream of known polarity pathways, and participates in a phosphorylation/dephosphorylation cycle with the kinase MBK-2. This cycle is critical for P granule segregation and asymmetry in the early embryo. The substrates of MBK-2 and $PP2A^{PPTR-1}$, MEG-1 and GEI-12, localize to sub P granular domains scaffolding constitutive P granule components. This work identifies novel regulators of P granule segregation and highlights the crucial role of post-translational modifications on intrinsically disordered proteins in RNA granule assembly.

Thesis Advisor: Geraldine Seydoux, PhD

Thesis Reader: Jin Zhang, PhD

Preface

I would like to thank my wonderful advisor, Geraldine Seydoux, whose fearless mentorship helped guide my course through graduate school. Geraldine's clear thinking and tireless dedication are inspirational, and it is always a joy to discuss science with her. I have grown as a scientist and a human being in her lab, and I am lucky to have met such an incredible role model in academia and in life. Many thanks are due to past and current members of the Seydoux lab for fun discussions about science and non-science topics. My lab family has been an incredible source of strength and mentorship throughout graduate school. Special thanks to Katya Voronina, my rotation mentor, seminar buddy, and fellow P granule lover, for countless hours of scientific scheming and dreaming. I have learned a lot from BCMB and MBG faculty members in classes, seminars, and discussions, and I thank my thesis committee members: Jin Zhang, Joe Gall, Denise Montell, and Carolyn Machamer. I would also like to thank my family, especially my parents, who have never refused my education, no matter the cost or hardship. Finally, and most importantly, many, many thanks to Marc Griffin, who makes everything possible. This thesis is dedicated to him.

Note to readers

Throughout this text, all gene names are italicized and all proteins are in capitals according to convention in *C. elegans*.

Table of Contents

List of Figures

List of Tables

Introduction
Germ Cell Specification

Abstract

The germline of *C. elegans* derives from a single founder cell, the germline blastomere P_4. P_4 is the product of four asymmetric cleavages that divide the zygote into distinct somatic and germline (P) lineages. P_4 inherits a specialized cytoplasm ("germ plasm") containing maternally-encoded proteins and RNAs. The germ plasm has been hypothesized to specify germ cell fate, but the mechanisms involved remain unclear. Three processes stand out: 1) inhibition of mRNA transcription to prevent activation of somatic development, 2) translational regulation of the *nanos* homolog *nos-2* and of other germ plasm mRNAs, and 3) establishment of a unique, partially-repressive chromatin. Together, these processes ensure that the daughters of P_4, the primordial germ cells Z2 and Z3, gastrulate inside the embryo, associate with the somatic gonad, initiate the germline transcriptional program, and proliferate during larval development to generate ~2000 germ cells by adulthood.

1. Introduction to the embryonic germ lineage (P lineage)

1.1. Embryonic origin of the germline:

P_4 arises in the 24-cell stage from a series of 4 asymmetric divisions starting in the zygote (P_0) (Fig. 1). Each division generates a larger, somatic blastomere (AB, EMS, C and D) and a smaller, germline blastomere (P_1, P_2, P_3, P_4). Laser ablation of the P_4 nucleus yields sterile worms with no germ cells (Sulston et al 1983), confirming that P_4 is the sole founder of the germ line and that no other cell can replace P_4.

In the 88-cell stage, P_4 divides once to generate two daughters: the primordial germ cells Z2 and Z3. Soon after their birth, Z2 and Z3 gastrulate into the embryo interior

(Harrell and Goldstein 2011). Z2 and Z3 do not divide further during embryogenesis, and remain close to each other and to the intestine. By the 2-fold stage, Z2 and Z3 extend protrusions towards two intestinal cells (Sulston et al 1983). Intestinal cells have been suggested to provide sustenance to Z2 and Z3 until the gonad is formed.

In mid-embryogenesis, the somatic gonadal precursors Z1 and Z4 migrate towards Z2 and Z3 to form the gonad primordium (Sulston et al 1983). Z2 and Z3 resume divisions only in the first (L1) larval stage after the larva begins feeding. Z2 and Z3 will eventually generate ~2000 germ cells by adulthood (Kimble and White 1981).

1.2. Characteristics of the P blastomeres:

1.2.1. *Asymmetric divisions:*

P_0, P_1, P_2, P_3 all divide asymmetrically. Before each division, the spindle becomes displaced towards one side of the cell. The P granules, RNA-rich organelles specific to the germline, and several associated cytoplasmic proteins and RNAs (collectively referred to as "germ plasm"; Table 1) also accumulate on that same side. As a result, each division generates daughters of unequal size with the smaller daughter inheriting most of the germ plasm (Gonczy and Rose 2005, Strome 2005).

In the first two divisions, the spindle becomes displaced towards the posterior pole of the embryo, such that P_1 and P_2 are born in the posterior. The posterior pole is defined in the zygote P_0 by the position of the sperm centrosome, which orients the distribution of the PAR polarity regulators (Gonczy and Rose 2005). In the P_2 blastomere, the polarity axis is reversed by signaling from the somatic blastomere EMS, and P_3 and P_4 are born towards the anterior (Schierenberg 1987, Arata et al 2010). As a result, P_4 is

born next to the descendants of the E (intestinal) lineage. Unlike P_0-P_3, P_4 divides symmetrically into two equal size daughters (Z2 and Z3) that both inherit germ plasm.

1.2.2. *Long cell cycle times:*

P blastomeres have longer cell cycle times than their somatic sisters. For example, P_1 divides 2 minutes after AB, in part due to enhanced activity of DNA replication checkpoint in P_1 (Encalada et al 2000, Brauchle et al 2003), and in part due to higher levels of cell cycle regulators (PLK-1 and Cdc25.1) in AB (Rivers et al 2008, Budirahardja and Gonczy 2008). P_4 divides about 70 minutes after its birth (Sulston et al 1983). Z2 and Z3 undergo DNA and centrosome duplication, but remain arrested in G2 until after hatching (Fukuyama et al 2006).

1.2.3. *No mRNA transcription:*

mRNA transcription begins in the 3 to 4-cell stage in somatic blastomeres, but appears to remain off in the germline blastomeres until gastrulation. In a survey of 16 mRNAs, no newly transcribed mRNAs were detected in P_0-P_4 by in situ hybridization (Seydoux et al 1996). During the transcription cycle, the serine-rich repeats in the carboxy-terminal tail of RNA polymerase II become phosphorylated, first on Serine 5 during initiation and then on Serine 2 during elongation. These phosphoepitopes are reduced (Pser5) or completely absent (Pser2) in the germline blastomeres (Seydoux and Dunn 1997). Both phospho-epitopes appear transiently in Z2 and Z3 shortly after their birth, but return to low/background levels by the 1.5 fold stage and do not reappear until after hatching (Furuhashi et al 2010). Z2 and Z3 also lose the active chromatin marks H3K4me2, H3K4me3 and H4K8ac (Schaner et al 2003). Z2 and Z3 are not completely

transcriptionally silent, however: zygotic expression of several germline genes have been detected in Z2 and Z3. These include P granule components (*pgl-1*, *glh-1,* and *glh-4*), the nanos ortholog *nos-1*, and meiotic genes (*htp-3, rec-8*) (Subramaniam and Seydoux 1999, Kawasaki et al 2004, Takasaki et al 2007, Spencer et al 2011). In contrast to mRNA transcription, transcription of ribosomal RNAs has been detected in all P blastomeres with the possible exception of P_4 (Seydoux and Dunn 1997).

1.2.4. *Maintenance of maternal mRNAs:*

In situ hybridization and RNA profiling studies have uncovered two classes of maternal mRNAs in early embryos: maternal mRNAs that are maintained in all blastomeres, and maternal mRNAs that are rapidly turned over in somatic blastomeres and maintained only in germline blastomeres (Seydoux and Fire 1994, Seydoux et al 1996, Baugh et al 2003). Some in the latter class are also enriched in P granules. For example, the Nanos homolog *nos-2* is partitioned to both germline and somatic blastomeres during the first two divisions. Between the 4 cell and 8 cell stages, *nos-2* is turned over in somatic blastomeres and maintained in the P lineage, where it is enriched in P granules. By the 28-cell stage, *nos-2* RNA remains only in P_4 where it is finally translated (Subramaniam and Seydoux 1999, Tenenhaus et al 2001).

2. Cellular mechanisms of germ cell specification

Two general modes of germline specification have been described in animals: induction by extracellular signals and induction by germ plasm, a specialized cytoplasm inherited from the oocyte (Seydoux and Braun 2006). In this section, we describe evidence for each of these mechanisms acting in *C. elegans*.

2.1. Asymmetric segregation of the germ plasm

Several lines of evidence suggest that *C. elegans* embryos possess germ plasm. As described above, the germline-specific P granules and associated RNAs and RNA-binding proteins co-segregate to the same side of the P blastomere before each asymmetric cleavage (Table 1). P or "germ" granules have been reported in the germline of many different animals, including mammals, and are considered to be intimately associated with germ cell fate (Strome and Lehmann 1997).

Embryo manipulations support the view that at least some aspects of P cell fate are specified by factors that are asymmetrically localized in the zygote. Using a laser microbeam to create holes in the eggshell, Schierenberg (1988) extruded "partial embryos" containing cytoplasm from only the anterior or posterior of the zygote. Partial embryos containing anterior cytoplasm divided symmetrically, whereas partial embryos containing posterior cytoplasm divided asymmetrically, similar to the P blastomeres. However, mixing of posterior cytoplasm into anterior cytoplasm was not sufficient to confer asymmetric divisions. Delaying cell division eliminated the ability of posterior cytoplasm to support asymmetric divisions. Together these observations suggest that the germ plasm is required for germ cell fate but is not sufficient to induce germ cell fate when diluted with "somatic cytoplasm". In contrast, in *Drosophila*, injection of germ plasm in the anterior pole of the embryo is sufficient to create ectopic germ cells (Mahowald and Illmensee 1974).

Asymmetric distribution of the germ plasm is controlled by the PAR network of polarity regulators, which regulates anterior-posterior polarity in P_0 and most likely also

in P_1, P_2 and P_3 (see below). The PAR proteins PAR-1 and PAR-2 segregate with the germ plasm, and both are maintained in the P lineage through the asymmetric divisions leading to P_4 (Guo and Kemphues 1995, Boyd et al 1996). PAR-1 and PAR-2 become enriched at the cell periphery on the side of the germ plasm during each asymmetric division. Strong mutations in the *par* genes disrupt all polarity in the 1-cell stage and lead to embryonic lethality. Hypomorphic *par* mutations, however, lead to viable but sterile worms that lack all germ cells (Kemphues et al 1988, Guo and Kemphues 1995, Spilker et al 2009). These observations suggest that asymmetric segregation of the germ plasm is required to specify P_4 as the germline founder cell.

2.1.1. *MEX-5 and MEX-6: germ plasm antagonists*

The PAR network regulate germ plasm asymmetry through the action of the PAR-1 kinase and its substrates MEX-5 and MEX-6, two highly related and partially redundant RNA-binding proteins that segregate opposite the germ plasm. Phosphorylation by PAR-1 stimulates MEX-5 (and presumably MEX-6) diffusion in the posterior cytoplasm of the zygote, causing MEX-5 to become enriched in the anterior (Tenlen et al 2008, Griffin et al 2011). As a result, the AB blastomere inherits high levels of MEX-5/6 and low levels of PAR-1, and the P_1 blastomere inherit low levels of MEX-5/6 and high levels of PAR-1. This pattern is repeated during the divisions of P_1, P_2 and P_3 (Schubert et al 2000, Guo and Kemphues 1995). MEX-5 and MEX-6 promote both asymmetric partitioning of the germ plasm to germ cells during cell division, and asymmetric degradation of the germ plasm from the soma after cell division.

2.1.2. *Asymmetric partitioning of the germ plasm during division*

Examination of P granule dynamics in live zygotes has revealed that P granule partitioning depends both on MEX-5/6-driven granule disassembly in the anterior cytoplasm, and PAR-1-driven granule assembly in the posterior cytoplasm (Cheeks et al 2004, Brangwynne et al 2009, Gallo et al 2010). P granule proteins that become dispersed in the anterior cytoplasm are reincorporated into granules in the posterior cytoplasm. As a result, P_1 inherits more P granule proteins than AB (Gallo et al 2010). After polarity reversal in P_2, P granules appear to segregate using a different mechanism involving association with the P cell nuclei (Hird et al 1996). PAR-1 and MEX-5/6 also promote the posterior enrichment of germ plasm proteins that are only loosely associated with P granules, such as PIE-1 and POS-1 (Table 1), but the mechanisms involved are not known (Schubert et al 2000). MEX-5/6 also promote anterior enrichment of PLK-1 and CDC-25, which contribute to the fast cell cycle of the AB blastomere (Rivers et al 2008, Budirahardja and Gonczy 2008).

2.1.3. *Asymmetric degradation of the germ plasm after division*

Asymmetric enrichment of the germ plasm during division is not absolute and low levels of germ plasm RNAs and proteins are inherited by all somatic blastomeres. These low levels are rapidly turned over, and this degradation depends on MEX-5 and MEX-6. In *mex-5;mex-6* embryos, germ plasm proteins are uniformly partitioned to all blastomeres. Heat shock induced expression of MEX-5 in single blastomere is sufficient to degrade germ plasm proteins in that cell (Schubert et al 2000). The potent anti-germ plasm effect of MEX-5 may explain why embryonic manipulations resulting in mixing of the germ plasm with anterior cytoplasm as described above (Schierenberg 1988), is not sufficient to induce “germ cell fate”.

The mechanisms by which MEX-5 and MEX-6 promote germ plasm degradation are not well understood. MEX-5 activity requires phosphorylation by the Polo kinases PLK-1 and PLK-2, which directly bind to, and segregate with, MEX-5. Phosphorylation of MEX-5 by Polo kinase is primed by MBK-2, a kinase that becomes activated at the oocyte to embryo transition. This requirement may explain why MEX-5 promotes germ plasm turn-over in embryos, but not in oocytes where MEX-5 is also present (Nishi et al 2008). Activation of mRNA degradation in somatic blastomeres is temporally correlated with the recruitment of LSM-1 and CCF-1 (CAF1/Pop2 subunit of the CCR4/NOT deadenylase complex) to P bodies, cytoplasmic granules that have been implicated in the decapping and deadenylation of mRNAs. In *mex-5; mex-6* (RNAi) embryos, LSM-1 is not recruited to P bodies and maternal mRNAs are stabilized. Consistent with a role for deadenylation, RNAi depletion of *let-711*/Not-1, a component of CCR4/NOT deadenylase, also interferes with LSM-1 recruitment and mRNA degradation (Gallo et al 2008). Whether LSM-1 is required for this process, however, has not yet been examined.

During the first division of each somatic blastomere, MEX-5 and MEX-6 also stimulate their own degradation and the degradation of other CCCH zinc finger proteins (POS-1, PIE-1, and MEX-1). CCCH protein degradation depends on ZIF-1, a substrate recognition subunit for the CUL-2 E3 ubiquitin ligase. ZIF-1 recognizes specific CCCH fingers in MEX-5, MEX-1, POS-1 and PIE-1. A fusion between GFP and the PIE-1 first zinc finger (GFP:ZF1) is symmetrically segregated to somatic and germline blastomeres, but degraded in each somatic lineage in a ZIF-1-dependent manner (DeRenzo et al 2003). The distribution of ZIF-1 protein is not known, but a reporter containing the *zif-1* 3' UTR is activated in each somatic lineage, suggesting that ZIF-1 activity is restricted to somatic

blastomeres by translational regulation of the *zif-1* mRNA. *zif-1* translation is inhibited in oocytes and zygotes by OMA-1 and OMA-2, two redundant RNA binding proteins that regulate several aspects of the oocyte-to-embryo transition (Detwiler et al 2001; Robertson and Lin, Chapter 12). OMA-1 and OMA-2 bind specifically to the *zif-1* 3' UTR and interact with the eIF4E-binding protein and translational repressor SPN-2. In the embryo, OMA-1 and OMA-2 repression is lifted by MBK-2 (Guven-Ozkan et al 2010). MBK-2 phosphorylates OMA-1 and OMA-2, which leads to 1) displacement of SPN-2 from the *zif-1* 3' UTR and 2) degradation of OMA-1 and OMA-2 during the first cleavage by an unknown activity (Guven-Ozkan et al 2010, Pellettieri et al 2003, Stitzel et al 2006). How ZIF-1 translation is restricted to somatic blastomeres after OMA-1/2 repression is lifted is not known, but may involve MEX-5 and MEX-6, since MEX-5 and MEX-6 are required for ZIF-1-dependent degradation (DeRenzo et al 2003).

2.1.4. *Self-propagation of germ plasm and anti-germ plasm?*

The properties of MEX-5 and MEX-6 suggest that in *C. elegans* the distinction between soma and germline depends both on maintenance of the germ plasm in the P lineage, and on the active degradation of germ plasm in somatic lineages ("anti-germ plasm activity"). In *par-1* mutants, MEX-5 and MEX-6 remain uniform and germ plasm RNAs and CCCH proteins are degraded in all cells by the 4-cell stage. Presumably, in wild-type embryos, PAR-1 maintains MEX-5 and MEX-6 at low enough levels in the P blastomeres to avoid degradation of the germ plasm. PAR-1 is maintained in all germline blastomeres and in Z2 and Z3, suggesting that PAR-1 is required continuously in the embryonic germ lineage to maintain the germ plasm. Intriguingly, in the zygote, MEX-5/6 activity is required for maximal enrichment of PAR-1 in the posterior (Cuenca et al

2003). One possibility is that mutual regulation/exclusion by PAR-1 and MEX-5/6 functions in a continuous loop to ensure that germ plasm asymmetry is reestablished in each P blastomere.

2.2. Asymmetric segregation of P granules: not essential?

The P granules are the only components of the germ plasm that persist in all germ cells throughout development (except in sperm). P or "germ" granules have been observed in the germ plasm and/or germ cells of all animals examined (Strome and Lehmann 1997). By electron microscopy in zygotes, P granules appear as round, electron-dense structures without membranes and dispersed throughout the cytoplasm (Wolf et al 1983). Starting in P_2, P granules associate with the cytoplasmic face of the nuclear envelope, where they will remain until gametogenesis. Like nuclei, P granules exclude macromolecules larger than 70 kD and greater, suggesting that they extend the nuclear pore environment of the nuclear membrane into the cytoplasm (Updike et al 2011).

P granules contain both constitutive components present at all stages of development and stage-specific components. Constitutive components include the RGG domain RNA binding proteins PGL-1 and PGL-3 (Kawasaki et al 1998, Kawasaki et al 2004) and the Vasa-related RNA helicases GLH-1,2,3 and 4 (Roussell et al 1993, Kuznicki et al 2000). PGL-1/3 are the core scaffolding components of P granules and can assemble into granules when expressed on their own in tissue culture cells (Hanazawa et al 2011). Mutations in *pgl* and *glh* genes interfere with larval germ cell proliferation and gamete formation (Kawasaki et al 2004, Spike et al 2008). The most severe defects are

seen when the worms are raised at high temperature or when mutations in multiple genes are combined. For example, *pgl-1* mutants are fertile at 20°C but sterile with underproliferated germlines at 26°C. Double loss of *pgl-1* and *pgl-3* leads to sterility even at low temperature (Kawasaki et al 2004). In mutant combination, however, germ cells are still formed, suggesting that P granule proteins are required primarily for germ cell proliferation and/or differentiation, and not for germ cell fate specification (Kawasaki et al 2004, Spike et al 2008). The redundancy and strong maternal contribution of PGL and GLH proteins, however, has made it difficult to exclude a potential role for P granules in germ cell fate specification in embryos.

In embryos, several germ plasm proteins are enriched on P granules (e.g. PIE-1, POS-1, MEX-1, MEX-3, MEG-1, MEG-2, Sm proteins), raising the possibility that P granules organize the germ plasm. Dynamic association of PIE-1 with P granules has been suggested to drive PIE-1 partitioning into P blastomeres by slowing down PIE-1 diffusion in the cytoplasm destined for P blastomeres (Daniels et al., 2009). Mutants that mislocalize P granules to somatic blastomeres or misexpress P granule components in somatic cells, however, do not make extra germ cells, suggesting that P granules on their own are not sufficient to assemble germ plasm and/or specify germ cell fate (Strome et al 1995, Tabara et al 1999, Mello et al 1992). Mutants that mislocalized P granules often fail to form primordial germ cells (ie. *mes-1*), but because these mutants also missegregate other germ plasm components, a specific requirement for P granules could not be inferred.

Recently, a gene required specifically for the asymmetric partitioning of P granules was identified. *pptr-1* codes for a regulatory subunit of the phosphatase PP2A.

In *pptr-1* mutants, P granules disassemble during each embryonic cell division. As a result, P granule components, including PGL-1/3, GLH-1/2/4 and the P granule-associated mRNAs *cey-2* and *nos-2* are partitioned equally to somatic and germline blastomeres. Surprisingly, other germ plasm components (including PAR-1, MEX-5/6 and PIE-1) still segregate asymmetrically in *pptr-1* mutants, demonstrating that P granules are in fact not essential to organize germ plasm. Consistent with normal MEX-5 and MEX-6 partitioning, *nos-2* and *cey-2* mRNAs are quickly degraded in each somatic blastomere in *pptr-1* mutants. After MEX-5 and MEX-6 turn over in the somatic lineages, PGL and GLH proteins reassemble into granules during interphase, but these granules appear in all cells and become progressively smaller with each division. By the time of the birth of Z2 and Z3, all cells have either very small or undetectable granules. (Gallo and Wang et al 2010)

The PGL granules inherited by somatic blastomeres in *pptr-1* mutants are eventually eliminated by autophagy after gastrulation (Zhang et al 2009). During mid-embryogenesis, when zygotic transcription of P granule components begins, Z2 and Z3 assemble new P granules. At that time, Z2 and Z3 also initiate expression of the *nos-2* paralog *nos-1*, as they do in wild-type (Subramaniam and Seydoux 2009). Consistent with proper specification of Z2 and Z3, 100% of *pptr-1* mutants are fertile when raised at 20^{o}C (Gallo et al 2010). These observations demonstrate that P granule partitioning is not essential to distinguish soma from germline. If P granules harbor factors that promote germ cell fate, these factors must be quickly inactivated in somatic cells, possibly by MEX-5 and MEX-6.

When raised at 26°C, 20% of *pptr-1* mutants grow into sterile adults with underproliferated germlines. The *pptr-1* phenotype is reminiscent of the phenotype of *pgl* and *glh* mutants, and is exacerbated by mutations in *pgl-1*: 15% of *pptr-1;pgl-1* double mutants are sterile at 20°C (Gallo et al 2010). These observations suggest that asymmetric inheritance of maternal P granules, although not essential, serves as a back-up mechanism to ensure that Z2 and Z3 have sufficient P granule material before starting to divide in the larva. Because *pptr-1* mutants *missegregate* but do not *eliminate* all maternal P granule components, the possibility remains that P granules also *contribute* to germ cell fate specification, perhaps as permissive rather than instructive cues.

2.3. Cell-to-cell signaling: also required?

Specification of the embryonic germ lineage also depends on at least one cell-cell interaction. MES-1 is a transmembrane protein that functions with SRC-1 to mediate bidirectional signaling between EMS and P_2. This signaling is required to polarize the EMS spindle and to reverse the polarity of P_2 to ensure that P_3 arises in the anterior (Strome et al 1995, Berkowitz and Strome 2000, Bei et al 2002). In the absence of MES-1, P_3 divides symmetrically, and P_4 adopts the somatic fate of its sister D. Both cells inherit P granules and other germ plasm components (Strome et al 1995). The P_4 to D transformation could be due to "dilution" of the germ plasm below a certain threshold necessary to induce germ cell fate. If so, MES-1 signaling could contribute to germ cell fate indirectly by promoting P_3 polarity. Consistent with this possibility, MES-1 has been shown to be required for the proper localization of PAR-2 (Arata et al 2010). Another possibility, however, is that signaling by MES-1 also induces other changes in P_2 and P_3 required directly to specify or maintain "germ cell fate". Because no experiment has yet

shown that the germ plasm is sufficient to induce germ cell fate in *C. elegans*, the possibility that other mechanisms are involved, including induction by cell-cell interactions, cannot be excluded at this time.

3. Molecular mechanisms of germ cell specification

While no single molecular mechanism has been shown yet to be *sufficient* to induce germ cell fate, several have been suggested to be *required* for the proper development of P blastomeres and/or Z2 and Z3. We consider each of these in turn below.

3.1. Translational regulation of maternal RNAs

Several germ plasm components are RNA-binding proteins (Table 1). Mutations in these proteins lead to embryonic lethality and cell fate transformations affecting both somatic and germline blastomeres. POS-1 and MEX-3 regulate the translation of several mRNAs and are required to maintain germ plasm asymmetry (Tabara et al 1999, Jadhav et al 2008, Mello et al 1992, Draper et al 1996). The complex phenotypes of these mutants make it difficult to evaluate their direct contribution to germ cell fate. Because each RNA-binding protein exhibits a unique pattern of perdurance within the germ plasm, one possibility is that they function combinatorially to specify the fate of each germline blastomere and their somatic daughters.

Analysis of the *nos-2* mRNA supports the view that multiple RNA-binding proteins cooperate to regulate the translation of mRNAs in the germ plasm. As described above, *nos-2* mRNA is maintained throughout the P lineage but translated only in P_4. Silencing of *nos-2* translation requires SPN-4, OMA-1,OMA-2, MEX-3, 5 and 6, and activation requires PIE-1 and POS-1 (Jadhav et al 2008, Tenenhaus et al 2001,

D'agostino et al 2006). OMA-1, OMA-2 and MEX-3 silence *nos-2* during oogenesis, whereas SPN-4 is required primarily to silence *nos-2* in embryos. POS-1 and SPN-4 compete for binding to the *nos-2* 3' UTR; when SPN-4 levels fall below a threshold in P_4, POS-1 prevails and activates *nos-2* translation (Jadhav et al 2008).

The role of PIE-1 in the translational activation of *nos-2* is less understood, but is distinct from PIE-1's role in transcriptional repression (described below). A *pie-1* transgene with mutations in the second zinc finger (PIE-1^{ZF2-}) rescues the transcriptional defects of a *pie-1* null mutation, but is not sufficient to activate *nos-2* translation in P_4. (see below). In embryos expressing PIE-1^{ZF2-}, Z2 and Z3 form normally, but do not gastrulate efficiently. In some embryos, Z2 and Z3 are never incorporated into the embryo proper, and are left behind by the crawling larva at hatching (Tenenhaus et al 2001).

These observations support the view that germ plasm proteins, such as PIE-1, promote the translation of mRNAs required for the proper development and/or specification of Z2 and Z3. The identity of these mRNAs is not yet known. In embryos where *nos-2* is depleted by RNAi, Z2 and Z3 gastrulate normally, and only occasionally fail to associate with the somatic gonad, suggesting that PIE-1 also regulates other mRNAs besides *nos-2*.

Analysis of MEG-1 and MEG-2 supports the view that regulation of germ plasm mRNAs is essential for the proper specification of Z2 and Z3. MEG-1 and MEG-2 are two partially redundant novel proteins that associate with P granules specifically in the P_2, P_3 and P_4 blastomeres. Loss of *meg-1* and *meg-2* leads to germ cell death in the L3 stage

(Leacock and Reinke 2008). Interestingly, *meg-1* interacts genetically with *nos-2*. *nos-2(RNAi);meg-1(vr10)* animals show the most severe phenotype reported for Z2 and Z3: the cells never proliferate, lose perinuclear P granules and die by the first larval stage in an apoptosis-independent manner (Kapelle and Reinke 2011). Since MEG-1 and NOS-2 expression overlaps only in P_4, events critical for germ cell fate specification likely occur first in this cell.

NOS-2 levels are partially reduced in *meg-1* embryos, raising the possibility that like other germ plasm components, MEG-1 regulate the expression of germ plasm RNAs. MEG-1 does not contain any recognizable RNA-binding motif, but shows complex genetic interactions with RNA-binding proteins that function during larval germline development (Leacock and Reinke 2008, Kapelle and Reinke 2011). One possibility is that RNA regulation by the MEGs and other germ plasm components initiates the network of protein-RNA regulation that drive germ cell proliferation (see Chapter 8, Nousch and Eckmann, 2012).

By mid embryogenesis, Z2 and Z3 initiate the transcription of *nos-1*, another Nanos homolog which functions partially redundantly with *nos-2*. Embryos lacking both *nos-1* and *nos-2* do not down-regulate marks of active transcription in Z2 and Z3 and all germ cells degenerate during the L3 and L4 larval stages (Subramaniam and Seydoux 1999, Furuhashi et al 2010). Nanos family members are RNA-binding proteins that often function with the PUF family of translational regulators (Parisi and Lin 2000), so *nos-2* and *nos-1* likely function by regulating the translation of other mRNAs, but the identity of these targets is not known.

Biochemical experiments have begun to define the RNA-binding specificity of some germ plasm proteins (POS-1, MEX-3, MEX-5, Pagano et al 2007, Farley et al 2008, Pagano et al 2009). These types of approaches, together with the identification of RNAs bound by germ plasm proteins *in vivo*, may help elucidate the complex network of protein-RNA interactions that specify the fate of Z2 and Z3.

3.2. Inhibition of mRNA transcription

As described above, the germline blastomeres P_0-P_4 maintain many maternally-inherited mRNAs, but do not transcribe any mRNAs *de novo*. RNA polymerase II is present in these cells, but kept inactive by two distinct mechanisms.

3.2.1. Inhibition of TAF-4 by OMA-1 and OMA-2:

In addition to their role as translational regulators (see above), OMA-1 and OMA-2 also function to inhibit transcription in the zygote. OMA-1 and OMA-2 interact with TAF-4, a component of the TFIID transcription complex. To activate transcription, TAF-4 must bind to TAF-12 in the nucleus. OMA-1 and 2 compete with TAF-12 for binding to TAF-4, and sequester TAF-4 in the cytoplasm (Guven-Ozkan et al 2008). OMA-1 and OMA-2 are made during oogenesis, but become competent to bind TAF-4 only in the zygote due to phosphorylation by MBK-2, a kinase activated during the oocyte-to-embryo transition (see above). Phosphorylation by MBK-2 also induces degradation of OMA-1/2 by the two-cell stage (Pellettieri et al 2003, Stitzel et al 2006). Regulation by MBK-2 ensures that OMA-1/2 inhibit zygotic transcription specifically in the zygote and early 2-cell stage. OMA-1/2 turnover in the 2-cell stage releases TAF-4 and activates

mRNA transcription in the somatic blastomeres ABa and Abp by the three-cell stage (Guven-Ozkan et al 2008, also see Chapter 12, Egg-to-embryo transition).

3.2.2. Inhibition of RNA polymerase II phosphorylation by PIE-1

In the germline blastomeres P_2, P_3 and P_4, transcription remains repressed through the action of PIE-1. Unlike other germ plasm components, which are primarily cytoplasmic, PIE-1 also accumulates in the nuclei of each P blastomere (Mello et al 1996). In *pie-1* mutants, high levels of CTD phosphorylation appear prematurely in P_2, P_3 and P_4 (Seydoux and Dunn 1997). Studies in mammalian cells have shown that PIE-1 inhibits P-TEF-b, the cyclin T-Cdk9 complex that phosphorylates Serine 2 in the CTD repeats of RNA polymerase. PIE-1 binds to cyclin T and inhibits P-TEF-b kinase activity using a pseudo-substrate motif that resembles a non-phosphorylatable version of the CTD (Batchelder et al 1999). Genetic studies have shown that this activity, although functional in the germline blastomeres, is not essential to promote germ cell fate. A *pie-1* transgene with mutations in the pseudo-substrate motif fails to repress Serine 2 phosphorylation as expected, but still inhibits Serine 5 phosphorylation and mRNA transcription. In fact, such a transgene is sufficient to rescue a *pie-1* loss of function mutant to viability and fertility (Ghosh et al 2008). These observations suggest that PIE-1 uses redundant mechanisms to inhibit RNA polymerase II activity and promote germ cell fate.

Why inhibit mRNA transcription in germline blastomeres? The phenotype of *pie-1* null mutants provides one clue. In *pie-1* mutants, P_2 adopts the fate of its somatic sister EMS. *pie-1* embryos die as disorganized embryos with excess intestine and pharyngeal cells (EMS fates) and no germ cells (Mello et al 1992). This cell fate transformation

depends on the transcription factor SKN-1. SKN-1 is maternally encoded and present at high levels in both P_2 and EMS (Bowerman et al 1993). One hypothesis therefore is that repression of mRNA transcription serves to protect germline blastomeres from transcription factors like SKN-1 that would otherwise induce somatic development (Seydoux et al 1996).

Since the original observations in *C. elegans*, inhibition of RNA polymerase II phosphorylation has been observed in the embryonic germlines of Drosophila, Xenopus, ascidians, and mice (Nakamura and Seydoux 2008, Hanyu-Nakamura et al 2008, Shirae-Kurabayashi et al 2011, Kumano et al 2011, Venkatarama et al 2010). The factors responsible have been identified in Drosophila and Ciona and, remarkably, bear no resemblance to OMA-1/2 or PIE-1 (Hanyu-Nakamura et al 2008, Shirae-Kurabayashi et al 2011, Kumano et al 2011). Inhibition of RNA polymerase II appears, therefore, to be conserved characteristic of germline development that depends on multiple mechanisms that have diverged during animal evolution.

3.3. Chromatin regulation

While the chromatin of P_0-P_3 resemble that of somatic blastomeres, the chromatin of P_4, and Z2 and Z3 adopts a distinct compact configuration. PSer2 and PSer5 appear in Z2 and Z3 at birth coincident with degradation of PIE-1 at that time (Seydoux and Dunn 1997). By mid-embryogenesis, however, PSer2 and PSer5 levels are low again and Z2 and Z3 also become negative for the "active" chromatin marks H3K4me2, H3K4me3 and H4K8ac (Furuhashi et al 2010, Schaner et al 2003). PSer2, PSer5 and H3K4me reappear in Z2 and Z3 after hatching (Furuhashi et al 2010). These observations suggest that Z2

and Z3 remain in a relatively transcriptionally-repressed state during embryogenesis, although unlike P_0-P_4, they are capable of transcribing at least a few messages (see section 1.2.3). Loss of H3K4me depends on *nos-1* and *nos-2* (Schaner et al 2003). Whether the unique chromatin of Z2 and Z3 depends on their arrest in G2 is also not known (Fukuyama et al 2007).

Genetic screens designed to identify maternal factors required for fertility identified 4 genes coding for chromatin regulators: MES-2, 3, 4, and 6. Mutations in these genes are maternal-effect sterile (MES): homozygous mothers are fertile but give rise to sterile progeny ("grandchildless", phenotype). Z2 and Z3 cells are made in embryos derived from *mes/mes* mothers, and proliferate during the first two larval stages but die by necrosis in the L3 and L4 stages (Capowski et al 1991, Paulsen et al 1995). In *mes-4* mutants, Z2 and Z3 retain pSer 2 (Furuhashi et al 2010), suggesting that these cells are already compromised during embryogenesis. *mes* germ cells are also unable to differentiate: ablation of somatic gonadal cells in the L2 stage, which causes wild-type germ cells to differentiate prematurely, only causes *mes-3* germ cells to stop proliferating (Paulsen et al 1995).

MES-2/3/6 forms a complex related to Enhancer of Zeste that methylates Lys 27 of histone H3, a repressive mark that accumulates on the X chromosome (Xu et al 2001, Bender et al 2004). Consistently, the X is mostly inactive in germ cells (with the exception of oocytes; Schaner and Kelly 2006, Reinke 2006, Spencer et al 2011). MES-4 methylates Lys 36 of histone H3, and MES-4 accumulates preferentially on autosomes (Bender et al 2006). This specificity depends on MES-2/3/6: in *mes-2, 3* and *6* mutants, MES-4 binds all along the X chromosome and the X is inappropriately activated in germ

cells (Fong et al 2002, Bender et al 2006). Chromatin immunoprecipitation experiments revealed that, in embryos, MES-4 associates preferentially with genes that were active in the maternal germ line. For example, MES-4 associates with meiotic genes that are transcribed in germ cells but not in embryos, and does not associate with genes that are transcribed in embryos but not in the maternal germline (Rechtsteiner et al 2010). H3K36 methylases typically mark genes in a transcription-dependent manner. Surprisingly, MES-4 appears unable to establish the H3K36 mark *de novo*, but is able to maintain the mark in the embryonic germ lineage even though RNA polymerase II is not active in the P blastomeres (Furuhashi et al 2010, Rechtsteiner et al 2010). Although further analysis is necessary to clarify the link between genes bound by *mes-4* and those that are misregulated in *mes-4* mutants, the results so far suggest that MES-4 functions as an "epigenetic memory factor" that marks genes expressed in the maternal germline for the next generation. Maternal contribution of another chromatin-associated protein, MRG-1, is also required for robust germ cell proliferation in the progeny (Takasaki et al 2007), suggesting that inheritance of a specific chromatin state is key for germ cell development.

MES-4 is inherited maternally and segregated to all blastomeres. After the 100-cell stage, MES-4 is maintained primarily in Z2 and Z3 (Fong et al 2002). The mechanisms that allow high levels of MES-4 to persist only in the germline are not known. Genetic evidence suggest that MES-4 is also active, at least transiently, in somatic lineages and is antagonized there by the synMuv B class of chromatin regulators. In synMuvB mutants, intestinal cells express germline genes and this ectopic expression requires MES-4 (Unhavaithaya et al 2002, Wang et al 2005). When grown at high temperatures, synMuv B mutants arrest as starved larvae, perhaps because germline gene

expression compromises intestinal function (Petrella et al 2011). One possibility is that maternal MES-4 initially confers competence for the germline transcriptional program to all blastomeres, including the intestinal founder cell (E blastomere). During embryogenesis, this competence is erased by the synMuv B complex in somatic lineages, but not in the P lineage, perhaps because that lineage activates transcription later and maintains maternal MES-4 for longer.

3.4. Epigenetic licensing by maternal RNA

A recent report suggests that activation of the germline transcriptional program also depends on maternal inheritance of specific germline transcripts. The *fem-1* gene is required for masculinization of the germline and soma (Doniach and Hodgkin 1984). Mothers homozygous for deletions that remove the *fem-1* gene produce progeny with feminized germlines, even when these progeny inherit a wild-type copy of the *fem-1* gene from their father. This maternal effect can be rescued by injecting *fem-1* RNA in the maternal germline. Remarkably, rescue is observed even when the injected RNA lacks a start codon, spans only short sub-regions of the *fem-1* gene, or is antisense to the *fem-1* transcript (Johnson and Spence 2011), indicating that inheritance of maternal *fem-1* RNA, but not FEM-1 protein, is needed to "*license*" zygotic expression of the *fem-1* gene. One possibility is that new germline transcripts are continuously compared to maternally-inherited transcripts to avoid expression of potentially toxic "intruder genes". Whether this phenomenon is specific to *fem-1* or extends to other germline genes remains to be determined.

4. Conclusions and remaining questions

While the precise molecular mechanisms that specify germ cell fate remain elusive, several themes have emerged. First key to the delineation of distinct soma and germ lineages is the PAR-1-MEX-5/6 polarity axis. MEX-5/6 promote the disassembly and degradation of germ plasm components in somatic lineages and PAR-1 stabilizes the germ plasm in the germ lineage, in part by physically excluding MEX-5 and MEX-6. The distinction between soma and germline, therefore, involves both active turnover of the germ plasm in somatic cells and protection of the germ plasm in the P blastomeres. Second, although P granules contribute to the proliferation and viability of germ cells during post-embryonic development, P granules are unlikely to be sufficient to *specify* germ cell fate during embryogenesis. We suggest instead that germ cell fate is specified by the collective action of RNAs and RNA-binding proteins found throughout the germ plasm. In the germline blastomeres, these factors mediate two important functions: 1) inhibition of mRNA transcription which prevents somatic transcription factors from activating somatic development and 2) translation of *nos-2* and other maternal mRNAs whose products promote gastrulation of the primordial germ cells, adhesion to the intestine, and a unique partially-repressive chromatin configuration. In Z2 and Z3, the chromatin regulator MES-4, perhaps with the help of "licensing RNAs" in the germ plasm, transmits the "memory" of the maternal germline transcriptional program.

The task of germ cell specification in the embryo may be viewed as a careful balancing act between the need to generate new (somatic) cell types and the need to preserve the germ cell program of the oocyte. In this context, the P_0-P_3 blastomeres may be considered an intermediate cell type, similar to the epiblast cells of the mammalian

embryo, where the potential for soma and germline fates temporarily co-exist. Global silencing of transcription and of the translation of certain germline mRNAs (e.g. *nos-2*) in these cells ensures that neither program takes over. P_4 in contrast may be considered the first cell where the germ cell fate program is returned to its original state, but how this program is implemented to modify the chromatin of P_4 is not known.

We also do not yet know when P_4 and/or Z2 and Z3 first activate the germline-specific transcription program. In many studies, "germ cell fate" is evaluated using markers present in germ plasm (such as P granules), but such markers do not necessarily indicate active commitment to germ cell fate. For example, Subramaniam et al. concluded that *nos-1* and *nos-2* are not required for germ cell fate because in *nos-1;nos-2* larvae, the dying "germ cells" still expressed certain germline-specific markers, but whether these markers were maternally inherited or expressed de novo in those cells was not determined (Subramaniam et al 1999). Because maternal products can perdure in the germline into larval stages (Kawasaki et al 1998), it will be important in future studies to use markers indicative of an "active germline program" such as germline-specific chromatin marks or zygotic transcripts (as in Schaner et al 2003, Takasaki et al 2007). Sequencing of RNAs isolated from Z2 and Z3 dissected from mid-stage embryos has confirmed that these cells already produce several germline-specific transcripts (Gerstein et al 2010, Spencer et al 2011). Analyses of the zygotic transcriptome of Z2 and Z3 may provide further insights into the molecular mechanisms that specify germ cell fate.

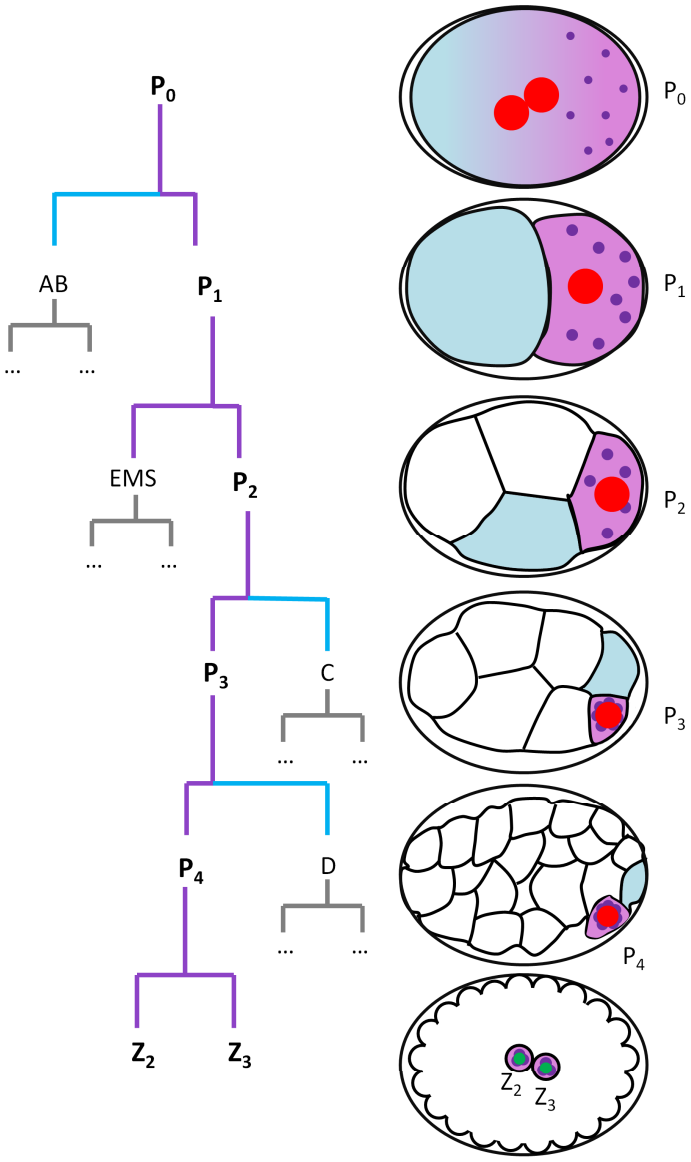

Figure 1: Embryonic origin of the germline

Abbreviated embryonic lineage from the 1-cell stage to the ~88-cell stage and embryo schematics corresponding to each stage shown in the lineage tree. Germ plasm is denoted in purple, germ granules are darker purple dots. High levels of MEX-5/6 inherited by somatic blastomers are denoted in blue. Red nuclei are not competent for mRNA transcription.

Table 1: Proteins in germ plasm

Protein	Domains	Protein localization	Loss of function phenotype	Proposed function	References
PIE-1	CCCH fingers	P blastomeres Nuclear, cytoplasmic, P granules , centrosomes	Maternal-effect embryonic lethality P_2 transformed to EMS fate No germ cells	Repression of RNA Polymerase II Translational control of mRNAs	Mello et al 1992, Seydoux et al 1996, Tenenhaus et al 2001
POS-1	CCCH fingers	P blastomeres Cytoplasmic, P granules	Maternal-effect embryonic lethality Complex cell fate transformations No germ cells	Translational control of mRNAs	Tabara et al 1999
MEX-1	CCCH fingers	P blastomeres Cytoplasmic, P granules	Maternal effect embryonic lethality Complex cell fate transformations No germ cells	Unknown	Mello et al 1992, Guedes and Priess 1997
MEX-3	KH domain	Present in oocytes through 4 cell stage Cytoplasmic in multiple cell types P granules in P_1 through P_4	Maternal effect embryonic lethality D transformed to P4, as a result more than 2 Z2/Z3 like cells are formed	Translational control of mRNAs	Draper et al 1996
MES-1	Receptor tyrosine kinase related	In P_2 at junction with EMS contact In P_3 at junction with E contact	Maternal effect sterility P_4 transformed to D fate No germ cells	Signaling from EMS to P_2 to reverse polarity in P_2	Strome et al 1995, Berkowitz and Strome 2000
Sm proteins	LSm fold	P granules	Embryonic arrest at 50 to 100 cell stage Mislocalization of PIE-1, P granules Symmetric divisions and short cell cycles	Regulation of mRNAs	Barbee et al 2002, Barbee and Evans 2002
PAR-1	KIN1/MARK kinase	Cortical - P blastomeres and Z2 and Z3 until morphogenesis	Maternal effect embryonic lethality No germ cells	Polarization of P blastomeres	Kemphues et al 1988, Guo and Kemphues 1995
MES-2/3/6	Polycomb orthologs	Nuclear in both somatic and germ cells in embryos. Persists in Z2 and Z3 in embryos and L1 larvae.	Maternal effect sterility Germ cell death at L3 and L4 stages	Repression of X chromosome transcription	Bender et al 2004, Strome 2005
MES-4	SET domain	Chromatin, preferentially autosomes. Present in somatic and germ cells in early embryogenesis,	Maternal effect sterility Germ cell death at L3 and L4 stages	Transmission of germline transcriptional program from mother to progeny	Fong et al 2002, Bender et al 2006, Rechtsteiner et al 2010

		persists in Z2 and Z3		Repression of X chromosome transcription	
NOS-1/2	Nanos orthologs	NOS-1: expressed in Z2 and Z3 from zygotic mRNA NOS-2: expressed in P_4 from maternal mRNA Cytoplasmic	Z2 and or Z3 outside somatic gonad Germ cell death at L3 stage	Regulation of mRNAs	Subramaniam and Seydoux 1999
MEG-1/2	Novel	P granules from P_2 through P_4	Maternal effect sterility Germ cell death at L3 stage	Unknown	Leacock and Reinke 2008
PGL-1/2/3	RGG box	Constitutive P granule components	Sterility with variable phenotypes	Unknown, primarily post-embryonic	Kawasaki et al 2004
GLH-1/2/3/4	DEAD box helicase	Constitutive P granule components	Sterility with variable phenotypes	Unknown, primarily post-embryonic	Spike et al 2008

Anti germ plasm:

Protein	**Domains**	**Protein localization**	**Loss of function phenotype**	**Proposed function**	**References**
MEX-5/6	CCCH fingers	High levels in somatic founder blastomeres - cytoplasmic High/low levels in Ant/Post cytoplasm of P blastomeres – cytoplasmic and enriched on P granules and centrosomes	Embryonic lethality Complex cell fate transformations No germ cells	Dispersal of P granules in dividing P blastomeres Degradation of germ plasm in somatic blastomeres	Schubert et al., 2000 Gallo et al., 2011

References

Arata Y, Lee J-Y, Goldstein B, Sawa H (2010) Extracellular control of PAR protein localization during asymmetric cell division in the C. elegans embryo. Development 137:3337-45.

Barbee S a, Evans TC (2006) The Sm proteins regulate germ cell specification during early C. elegans embryogenesis. Developmental biology 291:132-43.

Barbee S, Lublin A (2002) A novel function for the Sm proteins in germ granule localization during C. elegans embryogenesis. Current biology 12:1502-1506.

Batchelder C, Dunn M a, Choy B, et al. (1999) Transcriptional repression by the Caenorhabditis elegans germ-line protein PIE-1. Genes & development 13:202-12.

Baugh LR, Hill AA, Slonim DK, et al. (2003) Composition and dynamics of the Caenorhabditis elegans early embryonic transcriptome. Development 130:889-900.

Bei Y, Hogan J, Berkowitz L a, et al. (2002) SRC-1 and Wnt signaling act together to specify endoderm and to control cleavage orientation in early C. elegans embryos. Developmental cell 3:113-25.

Bender L, Cao R, Zhang Y, Strome S (2004) The MES-2/MES-3/MES-6 Complex and Regulation of Histone H3 Methylation in C. elegans. Current Biology 14:1639-1643.

Bender LB, Suh J, Carroll CR, et al. (2006) MES-4: an autosome-associated histone methyltransferase that participates in silencing the X chromosomes in the C. elegans germ line. Development 133:3907-17.

Berkowitz L a, Strome S (2000) MES-1, a protein required for unequal divisions of the germline in early C. elegans embryos, resembles receptor tyrosine kinases and is localized to the boundary between the germline and gut cells.

Bowerman B, Draper BW, Mello CC, Priess JR (1993) The maternal gene skn-1 encodes a protein that is distributed unequally in early C. elegans embryos. Cell 74:443-52.

Boyd L, Guo S, Levitan D, et al. (1996) PAR-2 is asymmetrically distributed and promotes association of P granules and PAR-1 with the cortex in C. elegans embryos. Development 122:3075-84.

Brangwynne CP, Eckmann CR, Courson DS, et al. (2009) Germline P granules are liquid droplets that localize by controlled dissolution/condensation. Science 324:1729-32.

Brauchle M, Baumer K, Gönczy P (2003) Differential activation of the DNA replication checkpoint contributes to asynchrony of cell division in C. elegans embryos. Current biology 13:819–827.

Budirahardja Y, Gönczy P (2008) PLK-1 asymmetry contributes to asynchronous cell division of C. elegans embryos. Development 135:1303-13.

Capowski EE, Martin P, Garvin C, Strome S (1991) Identification of grandchildless loci whose products are required for normal germ-line development in the nematode Caenorhabditis elegans. Genetics 129:1061-72.

Cheeks RJ, Canman JC, Gabriel WN, et al. (2004) C. elegans PAR proteins function by mobilizing and stabilizing asymmetrically localized protein complexes. Current Biology 14:851–862.

Ciosk R, DePalma M, Priess JR (2006) Translational regulators maintain totipotency in the Caenorhabditis elegans germline. Science 311:851-3.

Cuenca AA, Schetter A, Aceto D, et al. (2003) Polarization of the C. elegans zygote proceeds via distinct establishment and maintenance phases. Development 130:1255-1265.

Daniels BR, Perkins EM, Dobrowsky TM, et al. (2009) Asymmetric enrichment of PIE-1 in the Caenorhabditis elegans zygote mediated by binary counterdiffusion. The Journal of cell biology 184:473-9.

DeRenzo C, Reese KJ, Seydoux G (2003) Exclusion of germ plasm proteins from somatic lineages by cullin-dependent degradation. Nature 424:685-9.

Detwiler MR, Reuben M, Li X, et al. (2001) Two zinc finger proteins, OMA-1 and OMA-2, are redundantly required for oocyte maturation in C. elegans. Developmental cell 1:187-99.

Draper BW, Mello CC, Bowerman B, et al. (1996) MEX-3 is a KH domain protein that regulates blastomere identity in early C. elegans embryos. Cell 87:205-16.

D'Agostino I, Merritt C, Chen P-L, et al. (2006) Translational repression restricts expression of the C. elegans Nanos homolog NOS-2 to the embryonic germline. Developmental biology 292:244-52.

Encalada SE, Martin PR, Phillips JB, et al. (2000) DNA replication defects delay cell division and disrupt cell polarity in early Caenorhabditis elegans embryos. Developmental biology 228:225-38.

Farley BM, Pagano JM, Ryder SP (2008) RNA target specificity of the embryonic cell fate determinant POS-1. RNA 14:2685-97.

Fong Y, Bender L, Wang W, Strome S (2002) Regulation of the different chromatin states of autosomes and X chromosomes in the germ line of C. elegans. Science 296:2235-8.

Fukuyama M, Rougvie AE, Rothman JH (2006) C. elegans DAF-18/PTEN mediates nutrient-dependent arrest of cell cycle and growth in the germline. Current biology 16:773-9.

Furuhashi H, Takasaki T, Rechtsteiner A, et al. (2010) Trans-generational epigenetic regulation of C. elegans primordial germ cells. Epigenetics & chromatin 3:15.

Gallo CM, Munro E, Rasoloson D, et al. (2008) Processing bodies and germ granules are distinct RNA granules that interact in C. elegans embryos. Developmental biology 323:76-87.

Gallo CM, Wang JT, Motegi F, Seydoux G (2010) Cytoplasmic partitioning of P granule components is not required to specify the germline in C. elegans. Science 330:1685-9.

Gerstein MB, Lu ZJ, Van Nostrand EL, et al. (2010) Integrative analysis of the Caenorhabditis elegans genome by the modENCODE project. Science 330:1775-87.

Ghosh D, Seydoux G (2008) Inhibition of transcription by the Caenorhabditis elegans germline protein PIE-1: genetic evidence for distinct mechanisms targeting initiation and elongation. Genetics 178:235-43. d

Griffin EE, Odde DJ, Seydoux G (2011) Regulation of the MEX-5 Gradient by a Spatially Segregated Kinase/Phosphatase Cycle. Cell 146:955-968.

Guedes S, Priess JR (1997) The C. elegans MEX-1 protein is present in germline blastomeres and is a P granule component. Development 124:731-9.

Guo S, Kemphues K (1995) par-1, a gene required for establishing polarity in C. elegans embryos, encodes a putative Ser/Thr kinase that is asymmetrically distributed. Cell 81:611.

Guven-Ozkan T, Nishi Y, Robertson SM, Lin R (2008) Global transcriptional repression in C. elegans germline precursors by regulated sequestration of TAF-4. Cell 135:149-60.

Guven-Ozkan T, Robertson SM, Nishi Y, Lin R (2010) zif-1 translational repression defines a second, mutually exclusive OMA function in germline transcriptional repression. Development 137:3373-82.

Gönczy P, Rose LS (2005) Asymmetric cell division and axis formation in the embryo. WormBook, ed The C elegans Research Community, Wormbook 1-20.

Hanyu-Nakamura K, Sonobe-Nojima H, Tanigawa A, et al. (2008) Drosophila Pgc protein inhibits P-TEFb recruitment to chromatin in primordial germ cells. Nature 451:730-3.

Harrell JR, Goldstein B (2011) Internalization of multiple cells during C. elegans gastrulation depends on common cytoskeletal mechanisms but different cell polarity and cell fate regulators. Developmental biology 350:1-12.

Hayashi Y, Hayashi M, Kobayashi S (2004) Nanos suppresses somatic cell fate in Drosophila germ line. Proceedings of the National Academy of Sciences of the United States of America 101:10338-42.

Hird SN, Paulsen JE, Strome S (1996) Segregation of germ granules in living Caenorhabditis elegans embryos: cell-type-specific mechanisms for cytoplasmic localisation. Development 122:1303-12.

Jadhav S, Rana M, Subramaniam K (2008) Multiple maternal proteins coordinate to restrict the translation of C. elegans nanos-2 to primordial germ cells. Development 135:1803-12.

Johnson CL, Spence a M (2011) Epigenetic Licensing of Germline Gene Expression by Maternal RNA in C. elegans. Science 333:1311-1314.

Kapelle WS, Reinke V (2011) C. elegans meg-1 and meg-2 differentially interact with nanos family members to either promote or inhibit germ cell proliferation and survival. Genesis 49:380-91.

Kawasaki I, Amiri A, Fan Y, et al. (2004) The PGL family proteins associate with germ granules and function redundantly in Caenorhabditis elegans germline development. Genetics 167:645-61.

Kawasaki I, Shim YH, Kirchner J, et al. (1998) PGL-1, a predicted RNA-binding component of germ granules, is essential for fertility in C. elegans. Cell 94:635-45.

Kemphues KJ, Priess JR, Morton DG, Cheng NS (1988) Identification of genes required for cytoplasmic localization in early C. elegans embryos. Cell 52:311-20.

Kimble JE, White JG (1981) On the control of germ cell development in Caenorhabditis elegans. Developmental biology 81:208-19.

Kumano G, Takatori N, Negishi T, et al. (2011) A Maternal Factor Unique to Ascidians Silences the Germline via Binding to P-TEFb and RNAP II Regulation. Current biology 21:1308-13.

Kuznicki K a, Smith P a, Leung-Chiu WM, et al. (2000) Combinatorial RNA interference indicates GLH-4 can compensate for GLH-1; these two P granule components are critical for fertility in C. elegans. Development 127:2907-16.

Leacock SW, Reinke V (2008) MEG-1 and MEG-2 are embryo-specific P-granule components required for germline development in Caenorhabditis elegans. Genetics 178:295-306.

Mahowald A, Illmensee K (1974) Transplantation of Posterior Polar Plasm in Drosophila. Induction of Germ Cells at the Anterior Pole of the Egg. PNAS 71:1016-1020.

Mello CC, Draper BW, Weintraub H, Priess JF (1992) The pie-1 and mex-1 Genes and Maternal Control of Blastomere in Early C . elegans Embryos. Cell 70:163-176.

Mello CC, Schubert C, Draper B, et al. (1996) The PIE-1 protein and germline specification in C. elegans embryos. Nature 382:710–712.

Nakamura A, Seydoux G (2008) Less is more: specification of the germline by transcriptional repression. Development 135:3817-27.

Nishi Y, Rogers E, Robertson SM, Lin R (2008) Polo kinases regulate C. elegans embryonic polarity via binding to DYRK2-primed MEX-5 and MEX-6. Development 135:687-97.

Pagano JM, Farley BM, McCoig LM, Ryder SP (2007) Molecular basis of RNA recognition by the embryonic polarity determinant MEX-5. The Journal of biological chemistry 282:8883-94.

Pagano JM, Farley BM, Essien KI, Ryder SP (2009) RNA recognition by the embryonic cell fate determinant and germline totipotency factor MEX-3. Proceedings of the National Academy of Sciences 106:20252-7.

Paulsen JE, Capowski EE, Strome S (1995) Phenotypic and molecular analysis of mes-3, a maternal-effect gene required for proliferation and viability of the germ line in C. elegans. Genetics 141:1383-98.

Parisi M, Lin H (2000) Translational repression: a duet of Nanos and Pumilio. Current biology : CB 10:R81-3.

Pellettieri J, Reinke V, Kim SK, Seydoux G (2003) Coordinate activation of maternal protein degradation during the egg-to-embryo transition in C. elegans. Developmental cell 5:451-62.

Petrella LN, Wang W, Spike C a, et al. (2011) synMuv B proteins antagonize germline fate in the intestine and ensure C. elegans survival. Development 138:1069-79.

Rechtsteiner A, Ercan S, Takasaki T, et al. (2010) The histone H3K36 methyltransferase MES-4 acts epigenetically to transmit the memory of germline gene expression to progeny. PLoS Genetics.

Reinke V (2006) Germline genomics. WormBook, ed The C elegans Research Community, Wormbook 1-10.

Rivers DM, Moreno S, Abraham M, Ahringer J (2008) PAR proteins direct asymmetry of the cell cycle regulators Polo-like kinase and Cdc25. The Journal of cell biology 180:877-85.

Roussell DL, Bennett KL (1993) glh-1, a germ-line putative RNA helicase from Caenorhabditis, has four zinc fingers. Proceedings of the National Academy of Sciences 90:9300-4.

Schaner CE, Deshpande G, Schedl PD, Kelly WG (2003) A conserved chromatin architecture marks and maintains the restricted germ cell lineage in worms and flies. Developmental cell 5:747-57.

Schaner CE, Kelly WG (2006) Germline chromatin. WormBook, ed The C elegans Research Community, Wormbook 1-14.

Schierenberg E (1987) Reversal of cellular polarity and early cell-cell interaction in the embryo of Caenorhabditis elegans. Developmental Biology 122:452-463.

Schierenberg E (1988) Localization and segregation of lineage-specific cleavage potential in embryos of Caenorhabditis elegans. Roux's Arch Dev Biol 197:282–293.

Schnabel R, Weigner C, Hutter H, et al. (1996) mex-1 and the general partitioning of cell fate in the early C. elegans embryo. Mechanisms of development 54:133-47.

Schubert CM, Lin R, de Vries CJ, et al. (2000) MEX-5 and MEX-6 function to establish soma/germline asymmetry in early C. elegans embryos. Molecular Cell 5:671-82.

Seydoux G, Braun RE (2006) Pathway to totipotency: lessons from germ cells. Cell 127:891-904.

Seydoux G, Dunn M a (1997) Transcriptionally repressed germ cells lack a subpopulation of phosphorylated RNA polymerase II in early embryos of Caenorhabditis elegans and Drosophila melanogaster. Development 124:2191-201.

Seydoux G, Fire A (1994) Soma-germline asymmetry in the distributions of embryonic RNAs in Caenorhabditis elegans. Development 120:2823-34.

Seydoux G, Mello CC, Pettitt J, et al. (1996) Repression of gene expression in the embryonic germ lineage of C. elegans. Nature 382:713-716.

Sheth U, Pitt J, Dennis S, Priess JR (2010) Perinuclear P granules are the principal sites of mRNA export in adult C . elegans germ cells. Development 1314:1305-1314.

Shimada M, Yokosawa H, Kawahara H (2006) OMA-1 is a P granules-associated protein that is required for germline specification in Caenorhabditis elegans embryos. Genes to cells 11:383-96.

Shirae-Kurabayashi M, Matsuda K, Nakamura A (2011) Ci-Pem-1 localizes to the nucleus and represses somatic gene transcription in the germline of Ciona intestinalis embryos. Development 138:2871-81.

Spencer WC, Zeller G, Watson JD, et al. (2011) A spatial and temporal map of C. elegans gene expression. Genome research 21:325-41.

Spike C, Meyer N, Racen E, et al. (2008) Genetic analysis of the Caenorhabditis elegans GLH family of P-granule proteins. Genetics 178:1973-87.

Spilker AC, Rabilotta A, Zbinden C, et al. (2009) MAP kinase signaling antagonizes PAR-1 function during polarization of the early Caenorhabditis elegans embryo. Genetics 183:965-77.

Stitzel ML, Pellettieri J, Seydoux G (2006) The C. elegans DYRK Kinase MBK-2 Marks Oocyte Proteins for Degradation in Response to Meiotic Maturation. Current biology 16:56-62.

Strome S, Martin P, Schierenberg E, Paulsen J (1995) Transformation of the germ line into muscle in mes-1 mutant embryos of C. elegans. Development 121:2961-72.

Strome S (2005) Specification of the germ line. WormBook, ed The C elegans Research Community, Wormbook 1-10.

Strome S, Lehmann R (2007) Germ versus soma decisions: lessons from flies and worms. Science 316:392-3.

Strome S, Wood WB (1983) Generation of asymmetry and segregation of germ-line granules in early C. elegans embryos. Cell 35:15–25.

Subramaniam K, Seydoux G (1999) nos-1 and nos-2, two genes related to Drosophila nanos, regulate primordial germ cell development and survival in Caenorhabditis elegans. Development 126:4861-71.

Sulston JE, Schierenberg E, White JG, Thomson JN (1983) The embryonic cell lineage of the nematode Caenorhabditis elegans. Developmental biology 100:64-119.

Tabara H, Hill RJ, Mello CC, et al. (1999) pos-1 encodes a cytoplasmic zinc-finger protein essential for germline specification in C. elegans. Development 126:1-11.

Takasaki T, Liu Z, Habara Y, et al. (2007) MRG-1, an autosome-associated protein, silences X-linked genes and protects germline immortality in Caenorhabditis elegans. Development 134:757-67.

Tenenhaus C, Schubert C, Seydoux G (1998) Genetic requirements for PIE-1 localization and inhibition of gene expression in the embryonic germ lineage of Caenorhabditis elegans. Developmental biology 200:212-24.

Tenenhaus C, Subramaniam K, Dunn M a, Seydoux G (2001) PIE-1 is a bifunctional protein that regulates maternal and zygotic gene expression in the embryonic germ line of Caenorhabditis elegans. Genes & development 15:1031-40.

Tenlen JR, Molk JN, London N, et al. (2008) MEX-5 asymmetry in one-cell C. elegans embryos requires PAR-4- and PAR-1-dependent phosphorylation. Development 135:3665-75.

Tsuda M, Sasaoka Y, Kiso M, Abe K, Haraguchi S, Kobayashi S, Saga Y (2003) Conserved role of nanos proteins in germ cell development. Science 301:1239-41.

Tursun B, Patel T, Kratsios P, Hobert O (2011) Direct conversion of C. elegans germ cells into specific neuron types. Science 331:304-8.

Unhavaithaya Y, Shin TH, Miliaras N, et al. (2002) MEP-1 and a homolog of the NURD complex component Mi-2 act together to maintain germline-soma distinctions in C. elegans. Cell 111:991-1002.

Updike D, Strome S (2010) P granule assembly and function in Caenorhabditis elegans germ cells. Journal of andrology 31:53-60.

Updike DL, Hachey SJ, Kreher J, Strome S (2011) P granules extend the nuclear pore complex environment in the C. elegans germ line. The Journal of cell biology 192:939-48.

Venkatarama T, Lai F, Luo X, et al. (2010) Repression of zygotic gene expression in the Xenopus germline. Development 137:651-60.

Voronina E, Seydoux G (2010) The C . elegans homolog of nucleoporin Nup98 is required for the integrity and function of germline P granules. Development 1450:1441-1450.

Wang D, Kennedy S, Conte D, et al. (2005) Somatic misexpression of germline P granules and enhanced RNA interference in retinoblastoma pathway mutants. Nature 436:593-7.

Wolf N, Priess J, Hirsh D (1983) Segregation of germline granules in early embryos of Caenorhabditis elegans: an electron microscopic analysis. Journal of embryology and experimental morphology 73:297-306.

Xu L, Fong Y, Strome S (2001) The Caenorhabditis elegans maternal-effect sterile proteins, MES-2, MES-3, and MES-6, are associated in a complex in embryos. Proceedings of the National Academy of Sciences 98:5061.

Zhang Y, Yan L, Zhou Z, et al. (2009) SEPA-1 mediates the specific recognition and degradation of P granule components by autophagy in C. elegans. Cell 136:308-21.

Chapter 1

Cytoplasmic partitioning of P granule components is not required to specify the germline in C. elegans

This chapter is an edited version of the manuscript, "Cytoplasmic partitioning of P granule components is not required to specify the germline in C. elegans" by Gallo C.M.*, Wang J.T.*, Motegi F., and Seydoux G. *Science*. 2010;330(6011):1685-1689. *Both authors contributed equally to this work.

Summary

Asymmetric segregation of P granules during the first four divisions of the C. elegans embryo is a classic example of cytoplasmic partitioning of germline determinants. It is thought that asymmetric partitioning of P granule components during mitosis is essential to distinguish germline from soma. We have identified a mutant (*pptr-1*) where P granules become unstable during mitosis and P granule proteins and RNAs are distributed equally to somatic and germline blastomeres. Despite symmetric partitioning of P granule components, pptr-1 mutants segregate a germline that uniquely expresses P granules during post-embryonic development. *pptr-1* mutants are fertile, except at high temperatures. Hence, asymmetric inheritance of maternal P granules is not essential to specify germ cell fate. Instead, it may serve to protect the nascent germline from stress.

Results

A general characteristic of germ cells is the presence of cytoplasmic RNA-rich granules called germ granules (1). In C. elegans, germ (P) granules are present in all germ cells except mature sperm, and they segregate asymmetrically with the germline precursors (P blastomeres) during the first embryonic divisions (Fig. 2A) (2). Like embryonic germ granules of other organisms, P granules have been hypothesized to harbor the determinants that specify the germline. However, their function and segregation mechanisms are not fully understood (2, 3).

To monitor P granule dynamics, we used confocal microscopy to image live embryos expressing the P granule protein PGL-1 fused to green fluorescence protein (GFP)(4). We obtained similar results with GFP fusions to two other P granule proteins

PGL-3 and GLH-1 (5, 6). In the live movies, we analyzed granule dynamics (number, size and movement) and the overall distribution of each protein by quantifying total (granular + diffuse cytoplasmic) GFP fluorescence (Figs. 2, 3, 7 and Movies S1 to S3). P granules behaved differently during interphase and mitosis. During interphase, P granules were in a dynamic equilibrium between growing and shrinking phases (Movies S1-S3), with a bias for shrinking in the anterior and a bias for growing in the posterior. By the end of interphase, 85% of P granules in the anterior had disappeared completely or crossed over to the posterior (15%; n=41), and the total number of P granules had increased (Figure 6A). Although most granules became restricted to the posterior (Fig. 3A), levels of GFP::PGL-1 fluorescence remained equal in the anterior and posterior halves of the zygote during interphase (Fig. 3F), indicating that GFP::PGL-1 was still present in the anterior cytoplasm even though not in discrete granules. During mitosis, P granules grew in size, fused with each other, and decreased in number (Fig. 3A, 6 and Movie S1). GFP::PGL-1 fluorescence decreased in the anterior and increased in the posterior, suggesting that GFP::PGL-1 in the anterior cytoplasm was recruited into the posterior granules (Fig. 3F). Using a photoactivatable Dendra::PGL-1 fusion to permanently label a subpopulation of PGL-1, we confirmed that PGL-1 enrichment in the posterior involves redistribution of existing PGL-1 protein from anterior to posterior with no change in total protein levels (Sup. Fig. 3D). Dendra::PGL-1 diffuses throughout the embryo and diffuses fastest in the anterior during mitosis (Fig. 7E, G). We conclude that enrichment of PGL-1 in the posterior of the zygote does not depend on synthesis or degradation, but correlates with rapid recruitment of cytoplasmic PGL-1 into growing granules during mitosis.

P granule asymmetry requires the polarity regulators PAR-1, MEX-5 and MEX-6 (7). PAR-1 is a kinase that segregates with P granules, and MEX-5 and MEX-6 are two redundant RNA binding proteins that segregate opposite P granules in response to PAR-1 asymmetry (8). MEX-5 and MEX-6 are inherited by somatic blastomeres and turned over after 1 or 2 cell divisions (9). We found that PAR-1 and MEX-5/6 promote P granule assembly and disassembly, respectively. In *par-1* zygotes, where MEX-5/6 are uniformly distributed, most P granules disassembled completely throughout the zygote (Fig. 3B). Complete disassembly was dependent on MEX-5/6: in *par-1;mex-5/6* zygotes and in *mex-5/6* zygotes, P granules remained in a dynamic equilibrium between assembly and disassembly throughout the zygote, and P granule number increased (Fig. 3C and D, Fig. 6A). Consistent with MEX-5/-6 having a direct role in P granule disassembly, we observed mCherry::MEX-5 on shrinking PGL-1::GFP granules in wild-type embryos (Fig. 6B and Movie S4). In *mex-5/6* zygotes, we observed large P granules throughout the zygote at meiotic exit and in a small region in the posterior at mitosis (Fig. 3C), consistent with the localization of PAR-1 in *mex-5/6* embryos (10). In contrast, in par-1;mex-5/6 zygotes, P granules were fewer and smaller (Fig. 3D, 6). These results suggest that PAR-1 promotes P granule assembly both directly, by an unknown mechanism most active during mitosis, and indirectly by restricting MEX-5/6 to the anterior (also see (7)).

Our observations are consistent with an earlier study (3), which also concluded that P granule asymmetry is driven primarily by localized assembly and disassembly, rather than by granule movement. That study hypothesized that a local change in the concentration threshold for granule assembly might be sufficient to promote disassembly in the anterior, assembly in the posterior, and enrich PGL-1 in the posterior. Our findings,

however, indicate that disassembly during interphase and assembly during mitosis are regulated independently, and that preferential segregation of PGL-1 to the germline depends primarily on granule assembly during mitosis.

Consistent with this hypothesis, in an RNAi screen for genes required for GFP::PGL-1 asymmetry, we identified a gene necessary to assemble P granules during mitosis (Methods). *pptr-1* encodes a regulatory subunit of the phosphatase PP2A (Methods and (11)). In *pptr-1(tm3103)* embryos, GFP::PGL-1 granules disassembled during mitosis (Fig. 3E) and equal levels of diffuse GFP::PGL-1 were inherited by somatic and germline blastomeres at each division (Fig. 3F and G, 8A, and Movie S5). During interphase, GFP::PGL-1 reassembled into granules in the germline daughter, but remained diffusely distributed in the somatic daughter until after the next division (after MEX-5 and MEX-6 have turned over). As a result of equal partitioning, GFP::PGL-1 granules became progressively fewer and smaller with each P blastomere (Fig. 2B, 8A, 8B). Staining of fixed pptr-1 embryos with antibodies against core P granule proteins (PGL-1, PGL-3, GLH-1, GLH-2, GLH-4, and the P granule epitope OIC1D4) confirmed that P granules disassemble at each division in *pptr-1* mutants (Fig. 4A and 9). Granules reformed during interphase in each P blastomere, but were smaller and fewer than in wild-type, consistent with 50% or more loss of P granule components to somatic blastomeres at each division (Fig. 4). Granules also reappeared in somatic cells after the 4-cell stage, in a pattern matching the dynamics of MEX-5/6 turnover (9). By the 100 cell-stage, only small granules remained and these were not enriched in the primordial germ cells Z2 and Z3. We also monitored the distribution of two P granule-associated mRNAs, *cey-2* and *nos-2*. In wild-type embryos, *cey-2* and *nos-2* mRNAs segregate

preferentially with P granules to the germline blastomeres; lower levels inherited by somatic blastomeres are rapidly degraded after division (12, 13). In *pptr-1* embryos, *cey-2* and *nos-2* mRNAs were equally partitioned to somatic and germline blastomeres, but were still degraded in somatic lineages after division (Fig. 4B, 8C). Similarly, after the 30-cell stage, PGL-1 remaining in somatic lineages is degraded by the autophagy machinery in wild-type (14) and in *pptr-1* embryos (Fig 8B). We conclude that in *pptr-1* embryos, P granule proteins and RNAs are partitioned equally to somatic and germline blastomeres, but behave differently post mitosis in each cell type. In germline blastomeres, P granules components remained stable and were re-assembled into granules, albeit of diminishing size and number with each division. In somatic blastomeres, P granule RNAs were rapidly degraded; P granule proteins reassembled into granules after 1-2 cell cycles, and were turned over after gastrulation.

Segregation of other asymmetric proteins, including PAR-2, PAR-1 and MEX-5, was not affected in *pptr-1* mutants (Fig 10A). Depletion of *mex-5/6* by RNAi in pptr-1 mutants stabilized P granules in the anterior of the zygote and in somatic blastomeres during interphase, but not during mitosis, indicating that MEX-5/6 are active but are not responsible for P granule disassembly during mitosis (Fig 10B). PIE-1 is a transcriptional repressor required to silence transcription in the P lineage (15). In the cytoplasm, PIE-1 is enriched on P granules and this association has been proposed to drive PIE-1's preferential segregation into germline blastomeres (16). Consistent with the lack of P granules, in *pptr-1* embryos, GFP::PIE-1 was not enriched on granules during mitosis, yet was still asymmetrically segregated (Fig. 5A and 10A). We conclude that *pptr-1* is

required specifically for P granule partitioning, but is not required for the segregation of other germ plasm components, which can segregate independently of P granules.

If asymmetric partitioning of P granule components is necessary to distinguish germline from somatic blastomeres, then mutants like *pptr-1* should show defects in germline specification. Primordial germ cells do not form in *par-1*, *mex-5/6* mutants, and *mes-1* mutants (which miss-segregate P granules in the P2 and P3 blastomeres); but these mutants also miss-segregate other factors, notably PIE-1 (17) (18). We found that primordial germ cells form normally in *pptr-1* embryos: by mid-embryogenesis, we detected two cells expressing the germline proteins NOS-1 and PGL-1 as is observed in wild-type (13) (4). NOS-1, which is expressed only zygotically, was expressed at the same level in wild-type and *pptr-1* embryos (Fig. 5A). In contrast, PGL-1, which is expressed both maternally and zygotically at this stage, was lower in *pptr-1* embryos, consistent with mis-segregation of maternal PGL-1 (Fig. 5A). We confirmed that *pptr-1* mutants express PGL-1 zygotically in primordial germ cells using a paternally-inherited *pgl-1* transgene (Fig 11C). Consistent with proper germline specification, at 20°C, 100% of *pptr-1* adults (n=5798) were self-fertile with a full germline. At higher temperatures (24°C and 26°C), however, a minority (~20%) of *pptr-1* adults were sterile (Fig. 5B and C). Sterile *pptr-1* hermaphrodites had underdeveloped gonads with P granule-positive germ cells but no gametes (Fig. 5B). Stunted gonad development at high temperatures is characteristic of mutants lacking maternal PGL or GLH proteins (6, 19), raising the possibility that the sterility of *pptr-1* mutants is caused by the P granule partitioning defect. Consistent with this hypothesis, we found that, at 20°C, 15% of *pptr-1;pgl-1* double mutants (n= 1191) were sterile, in contrast to the single mutants (1.3% n=1959

pgl-1; 0% n=5798 *pptr-1*). Furthermore, both the sterility and P granule defects of *pptr-1* mutants could be rescued by maternal *pptr-1*, but not by zygotic *pptr-1* (Fig. 5C and 12). We conclude that P granule partitioning during embryogenesis is not essential to specify germ cell fate, but is required to promote robust germ cell proliferation and differentiation at high temperatures.

Our findings demonstrate that, in C. elegans, asymmetric partitioning of P granules during division can be uncoupled from the asymmetric partitioning of other germ plasm components (such as PIE-1), and is not essential to distinguish germline from soma. Even after inheriting equal levels of germ granule components, somatic and germline blastomeres maintain distinct fates. Therefore, why are germ granule components partitioned with the germ plasm? Our results suggest that partitioning increases stress resistance in the nascent germline by maximizing the maternal load of germ granule material inherited by primordial germ cells. In this regard, it is interesting that pptr-1 also regulates insulin signaling (10), a pathway important for stress resistance. Many animals (including mammals) do not possess germ plasm and use inductive interactions to specify the germline. In those animals, germ granules are assembled de novo after germ cell specification (20). Our findings suggest that in animals with germ plasm, germ granule assembly is also a consequence, not a cause, of an underlying soma-germline distinction maintained by other factors.

References

1. Chuma S, Hosokawa M, Tanaka T, Nakatsuji N. Mol. Cell. Endocrinol. 2009 Jul 10;306:17.

2. Updike D, Strome S. J. Androl. 2010 Jan-Feb;31:53.

3. Brangwynne CP, et al. Science. 2009 Jun 26;324:1729.

4. Kawasaki I, et al. Cell. 1998;94:635.

5. Gruidl ME, et al. Proc Natl Acad Sci U S A. 1996;93:13837.

6. Kawasaki I, et al. Genetics. 2004 Jun;167:645.

7. Cheeks RJ, et al. Curr. Biol. 2004 May 25;14:851.

8. Munro E, Bowerman B. Cold Spring Harb Perspect Biol. 2009 Oct;1:a003400.

9. Schubert CM, Lin R, de Vries CJ, Plasterk RH, Priess JR. Mol Cell. 2000;5:671.

10. Cuenca AA, Schetter A, Aceto D, Kemphues K, Seydoux G. Development. 2003 Apr;130:1255.

11. Padmanabhan S, et al. Cell. 2009 Mar 6;136:939.

12. Seydoux G, Fire A. Development. 1994;120:2823.

13. Subramaniam K, Seydoux G. Development. 1999;126:4861.

14. Zhang Y, et al. Cell. 2009 Jan 23;136:308.

15. Nakamura A, Seydoux G. Development. 2008 Dec;135:3817.

16. Daniels BR, Perkins EM, Dobrowsky TM, Sun SX, Wirtz D. J. Cell Biol. Feb;17:2009.

17. Gonczy P, Rose LS. WormBook. 2005;1

18. Strome S. WormBook. 2005;1

19. Spike C, et al. Genetics. 2008 Apr;178:1973.

20. Kotaja N, Sassone-Corsi P. Nat Rev Mol Cell Biol. 2007 Jan;8:85.

Supplementary Materials

Methods

Nematode Strains

C. elegans strains (Table 2) were derived from the wild-type Bristol N2 and reared with standard procedures (*6*). All experiments, including movies, were performed at 24°C, unless otherwise indicated. The P granule partitioning defect of *pptr-1* mutants is fully penetrant at 20°C and 24°C, but the low penetrance sterility phenotype is only seen at 24°C and 26°C. *pptr-1* was identified as follows: 231 candidate miRNA pathway genes (*7*) were screened by RNAi for disruption of GFP::PGL-1 expression in embryos. This primary screen identified the PP2A catalytic subunit *let-92.* We then screened by RNAi the 14 PP2A regulatory subunits predicted by WormBase; only *pptr-1(RNAi)* disrupted GFP::PGL-1 distribution. We obtained two deletion alleles of *pptr-1* (*tm2954* and *tm3103*) from the National BioResource Project for the Experimental Animal, Japan and both affected the distribution of endogenous PGL-1 (data not shown). *tm3103* was outcrossed 6 times before use in all the experiments described here. JH2842 and JH2483 were made by crossing JH2108 and JH2841, respectively, with OD57 (*8*).

Transgenics

Gateway cloning (Invitrogen) (*9*) was used to generate all constructs (Table 2). Transgenes were introduced into worms by microparticle bombardment (*10*) . Dendra DNA sequence (*11*) was recoded to conform to *C. elegans* codon usage (*12*) and to

include three synthetic introns (*13*) (Genscript, NJ, USA; Sequence is available upon request).

RNAi-mediated Knockdown

RNAi was performed by feeding (except in Fig. 12 see below). HT115 bacteria transformed with feeding vectors were grown at 37º C in LB + ampicillin (100µg/mL), plated on NNGM (nematode nutritional growth media) + ampicillin (100µg/mL) + IPTG (1mM), and grown overnight at room temperature before adding L4 worms at 25º C for 22-28 hours. For *mex-5/6(RNAi)*, the second exon of *mex-5* and *mex-6* were cloned separately into the gateway feeding vector pCD1.01, and bacteria expressing each were mixed before plating. The *pptr-1(RNAi)* and *par-1(RNAi)* constructs were obtained from the Ahringer RNAi library (*14*). To make *pptr-1* dsRNA, 465 bp of *pptr-1* cDNA was amplified using primers containing T7 promoter sequences and corresponding to exons 1, 2, and 3 of pptr-1. dsRNA was then created using AmpliScribe T7-Flash Transcription Kit (Epicentre) and purified using RNeasy kit (Qiagen).

For Fig. 12, P0 generation mothers were soaked in 0.4 µg/µl of *pptr-1* dsRNA and 5x soaking buffer (*15*) for 22 hours before plating on feeding *pptr-1(RNAi)* prepared as described above.

Live Imaging and Spinning-Disc Confocal Microscopy

Embryos were dissected from gravid adults into egg salts (118 mM NaCl, 10mM Hepes pH 7.5, 2mM $CaCl_2$, 48mM KCl, 2mM $MgCl_2$) and placed on a 3% agarose pad. Time-lapse movies were acquired using a Zeiss Axio Imager fitted with a Yokogawa spinning-

disc confocal scanner (63x 1.4NA plan apochromat lens). Slices were taken every 1µm for a total of 8µm for time-lapse images. Dendra photoconversions were performed using a 120W mercury vapor short arc lamp and an exposure of 2.4 seconds with an excitation of 357nm. Local photoconversions were performed by closing down the field diaphragm of the Zeiss Axio Imager and an exposure time of 4.8 seconds with an excitation of 357nm. All images were acquired with Slidebook software (Intelligent Imaging Innovations). For *par-1* experiments, *par-1(zu310ts)* L4s were shifted from 15 ºC to 25.5 ºC and grown overnight. Embryos were then dissected into 25.5 ºC egg salts and imaged at 26 ºC.

In situ Hybridization

In situ hybridization of *nos-2* and *cey-2* mRNA was performed as described previously (*16*), except that probe hybridization was performed at 46º C.

Immunostaining

Gravid adult hermaphrodites were laid on a slide coated with 0.01% poly-L-lysine and embryos, extruded by squashing with a coverslip, and frozen on pre-chilled aluminum blocks. Cover slips were removed and slides were incubated in -20 °C methanol for 15 minutes, followed by -20 °C acetone for 10 minutes. Slides were preblocked in PBS/0.1% Tween/0.1% BSA (PBT) for 30 minutes, and incubated with primary antibody overnight at 4 °C. Primary antibodies were diluted in PBT as follows: OIC1D4 (1:10, Developmental Studies Hybridoma Bank), K76 (1:10, DSHB), KT3 (1:10, DSHB), chicken anti-GLH-1 (1:100, gift from K. Bennett), chicken anti-GLH-2 (1:200, gift from

K. Bennett), rabbit anti-GLH-4 (1:10, gift from K. Bennett), rabbit anti-PAR-1 (1:200, gift from K. Kemphues), and affinity purified rat anti-NOS-1 (1:15). Secondary antibodies were applied for 2 hours at room temperature in the following dilutions: Cy3-conjugated goat anti-mouse IgG Fc fragment specific (1:100, Jackson Immunoresearch), Cy3-conjugated goat anti-mouse IgM (1:100, Jackson Immunoresearch), Cy3-conjugated goat anti-mouse IgG H+L (1:100, Jackson Immunoresearch), Alexa 568-conjugated goat anti-chicken IgY (1:200, Molecular Probes), Alexa 488-conjugated goat anti-rabbit IgG (1:100, Molecular Probes), Alexa 568-conjugated goat anti-rat IgG (1:100, Molecular Probes), and FITC-conjugated goat anti-GFP (1:200, Abcam).

Images were acquired using a Zeiss Axio Imager fitted with a Yokogawa spinning-disc confocal scanner (63x 1.4NA plan apochromat lens). All fluorescence intensities were below saturation during capture. Z-stack images (0.5um intervals spanning entire embryo) were collapsed (maximum projection) using Slidebook software. Collapsed images were normalized based on minimal and maximal values in *pptr-1* embryos. Consequently, maximal wild-type values are saturated in pictures shown.

Fluorescence Quantification

At least 3 embryos were analyzed for all quantifications. Image analysis was performed using Slidebook software.

For all graphs in Fig. 2 and Fig 7, average fluorescence levels from time-lapse movies were measured from average projections of an 8µm stack (spanning approximately half the embryo). For the GFP fusions and whole embryo photoconversions of Dendra::PGL-1, movies were started at pronuclear formation

(meiotic exit) and the first recorded anterior and posterior values were set to 1 and all other values scaled accordingly (Average variance between anterior and posterior values at meiotic exit was less than 3% with no preference for anterior or posterior). For local photoconversions of Dendra::PGL-1, the value of the converted half of the embryo was set to 1.

For Fig 6A, granules were manually counted. To measure anterior rates of granule disappearance versus movement into the posterior, granules were followed manually through time and Z-stacks (slices 1-8). Only granules that disappeared while in slices 2-7 were counted to rule out movement into a focal plane that was not acquired.

Values in Figure 3 were measured by imaging three different focal planes in 3 embryos for each genotype and stage. Sum fluorescence intensities were measured in the P blastomere and in an identically-sized region positioned over the somatic sister. Fold enrichment was calculated as the average ratio of P cell:soma. Error bars are the standard error of the mean.

Sterility and brood size counts

Sterile animals were identified under the dissecting microscope among synchronized broods (12-24 hour lay) as adult hermaphrodites with empty (clear) uteri. When examined at higher magnification, 10/10 hermaphrodites with clear uteri had an underproliferated gonad as shown in Fig. 5C. M0Z0 and M0Z1 animals were analyzed on the same plates among the brood of *pptr-1/pptr-1* mothers mated to +/+ males carrying the *myo-2GFP transgene* (PD4790): M0Z1 (cross progeny) were GFP+, whereas M0Z0 (self-progeny) were GFP-. Fertile M0Z1 mothers were allowed to self to generate M1Z0,

M1Z1, M1Z2 progeny. All sterile animals were genotyped; totals in each category were estimated from expected Mendelian ratios.

To obtain total brood sizes, mothers were cloned as L4s onto individual plates and passaged to a new plate after 30 hours (1 mother → 2 plates). Progeny from both plates were counted at the L4 stage. *pptr-1/pptr-1* hermaphrodites were crossed with +/+ (N2) males to generate M0Z1 hermaphrodites, and these were selfed to generate M1Z0, M1Z1, M1Z2 hermaphrodites. The genotype of each mother was determined by whole-worm PCR after the mother had laid her complete brood.

Legends for Supplementary Movies

All movies oriented anterior to the left and posterior to the right. Movies were acquired with a Zeiss Axio Imager fitted with a Yokogawa spinning-disc confocal scanner (63x 1.4NA plan apochromat lens). Slices were taken every 1μm for a total of 8μm for time-lapse images. For Movies 1, 4, and 5, images were captured every 8s and movies are shown at 15 frames/sec. For Movies 2 and 3, images were captured every 2 min and movies are shown at 6 frames/sec.

Movie S1. Wild-type Embryo expressing PGL-1::GFP (JH2330, Figure 2C)

Movie S2. Wild-type embryo expressing GFP::PGL-3 (JH2017)

Movie S3. Wild-type embryo expressing GFP::GLH-1 (JH2172)

Movie S4. Wild-type embryo expressing PGL-1::GFP and mCherry::MEX-5 (JH2840, Figure 6)

Movie S5. Combined movie of wild-type and *pptr-1* embryos expressing GFP::PGL-1 and mCherry::H2B (JH2842 and JH2843, respectively; Figure 8A)

References

1. I. Kawasaki *et al.*, *Cell* 94, 635 (1998).
2. G. Seydoux, A. Fire, *Development* 120, 2823 (1994).
3. M. Tijsterman, K. L. Okihara, K. Thijssen, R. H. Plasterk, *Curr. Biol.* 12, 1535 (Sep 3, 2002).
4. T. Sijen *et al.*, *Cell* 107, 465 (Nov 16, 2001).
5. J. Maciejowski *et al.*, *Genetics* 169, 1997 (Apr, 2005).
6. S. Brenner, *Genetics* 77, 71 (1974).
7. D. H. Parry, J. Xu, G. Ruvkun, *Curr. Biol.* 17, 2013 (Dec 4, 2007).
8. K. McNally, A. Audhya, K. Oegema, F. J. McNally, *J. Cell Biol.* 175, 881 (Dec 18, 2006).
9. A. Landy, *Annu. Rev. Biochem.* 58, 913 (1989).
10. V. Praitis, E. Casey, D. Collar, J. Austin, *Genetics* 157, 1217 (Mar, 2001).
11. N. G. Gurskaya *et al.*, *Nat. Biotechnol.* 24, 461 (Apr, 2006).
12. R. A. Green *et al.*, *Methods Cell Biol.* 85, 179 (2008).
13. A. Fire *et al.*, *Nature* 391, 806 (1998).
14. R. S. Kamath *et al.*, *Nature* 421, 231 (Jan 16, 2003).
15. P. G. Okkema, M. Krause, *WormBook*, 1 (2005).
16. G. Seydoux, A. Fire, *Methods Cell Biol.* 48, 323 (1995).

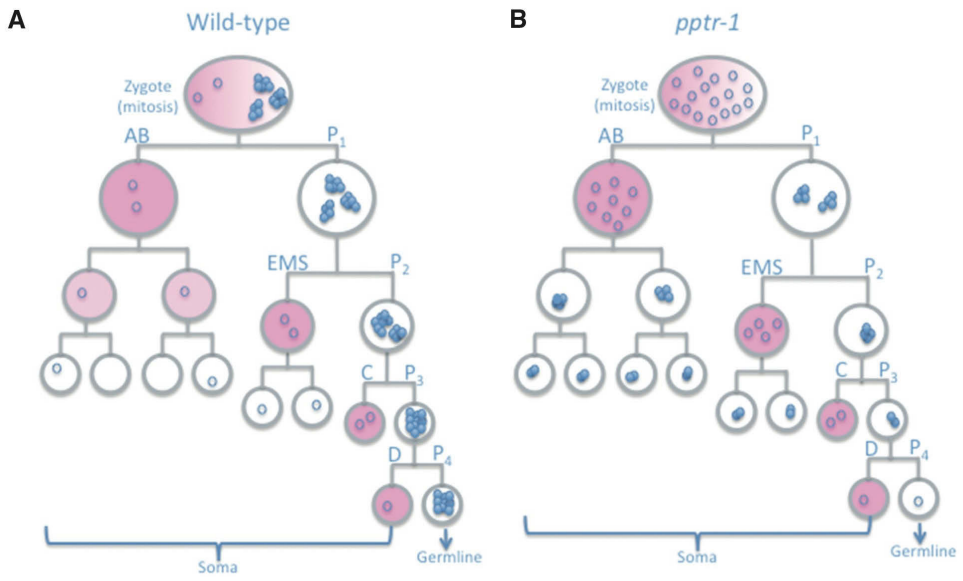

Figure 2. Segregation of the P granule component PGL-1 in C. elegans embryos

A) Abbreviated embryonic lineage showing the divisions that give rise to somatic (AB, EMS, C and D) and germline (P1-P4) blastomeres. All cells are shown in interphase except for the zygote, which is shown in mitosis. Circles represent PGL-1 molecules: open circles represent PGL-1 diffuse in cytoplasm and closed circles represent PGL-1 assembled into granules visible by microscopy. Pink is MEX-5, which promotes granule disassembly; localized granule assembly ensures that the majority of PGL-1 segregates with the germline (Fig. 2). B) In *pptr-1* mutants, PGL-1 granules disassemble at each mitosis and equal numbers of dispersed PGL-1 molecules are segregated to all cells (Fig. 2). During interphase, PGL-1 granules reform in all cells, except in MEX-5-positive somatic blastomeres (pink). Note that somatic PGL-1 granules are not equivalent to true P granules, as they do not contain P granule-associated mRNAs, which are degraded in somatic lineages (Fig. 3).

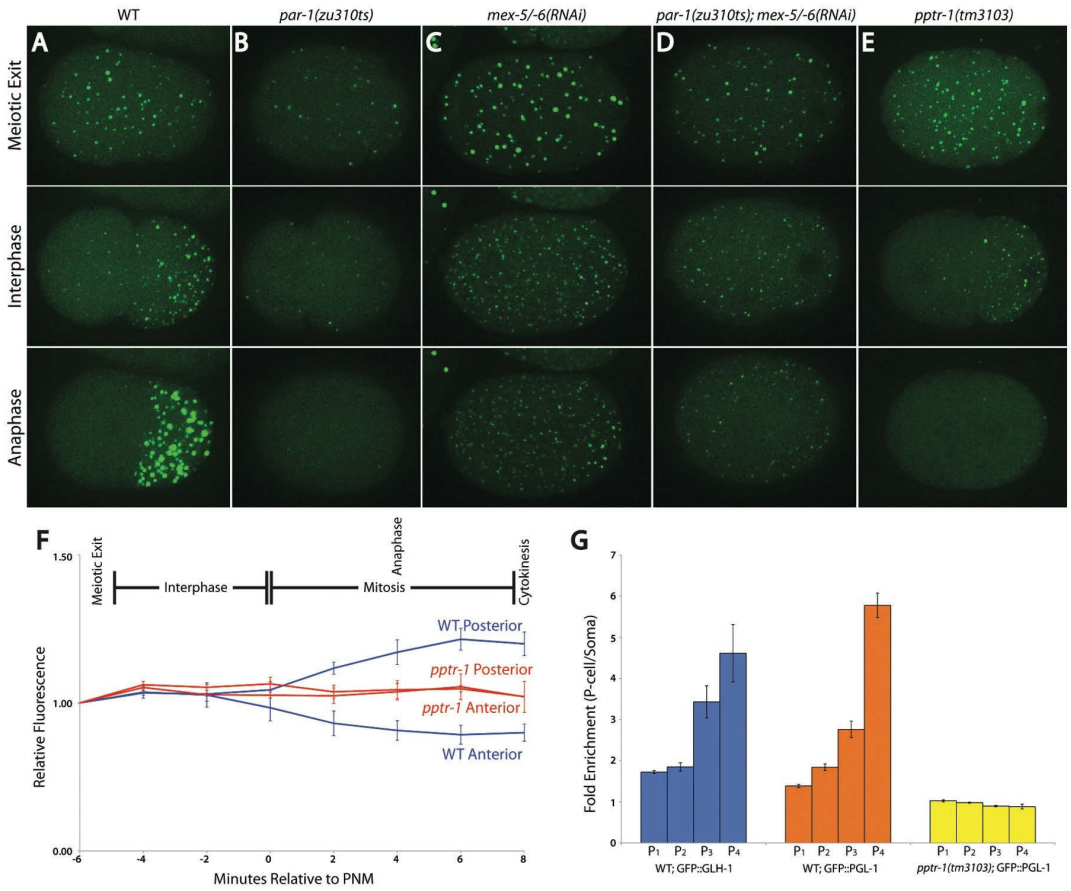

Figure 3. P granule dynamics require *par-1*, *mex-5/6*, and *pptr-1*

A-E) Time-lapse images of zygotes expressing GFP::PGL-1. Image are maximum projections of confocal Z-stacks spanning 8µm (~half of embryo depth). P granule numbers are shown in Sup. Fig. 1. MEX-5 and MEX-6 are uniformly distributed in *par-1* embryos and PAR-1 localizes to a reduced-size posterior domain in *mex-5;mex-6* zygotes (9, 10).

F) GFP::PGL-1 levels over time in wild-type and *pptr-1(tm3103)* zygotes. Error bars are standard deviation of mean values from 3 zygotes. In wild-type embryos, GFP::PGL-1 fluorescence does not decrease in the anterior during interphase, even though the number of visible granules decreases (Fig. 2A), consistent with granule disassembly. During

mitosis, GFP::PGL-1 fluorescence and P granule size increase in the posterior (Sup. Fig. 1), consistent with granule assembly.

G) Fold-enrichment of GFP::PGL-1 and GFP::GLH-1 in each P blastomere over its somatic sister. Enrichment becomes most pronounced with each division in wild-type. No enrichment is observed at any division in *pptr-1* mutants. Error bars are standard deviation from values obtained from 3 focal planes in 3 embryos.

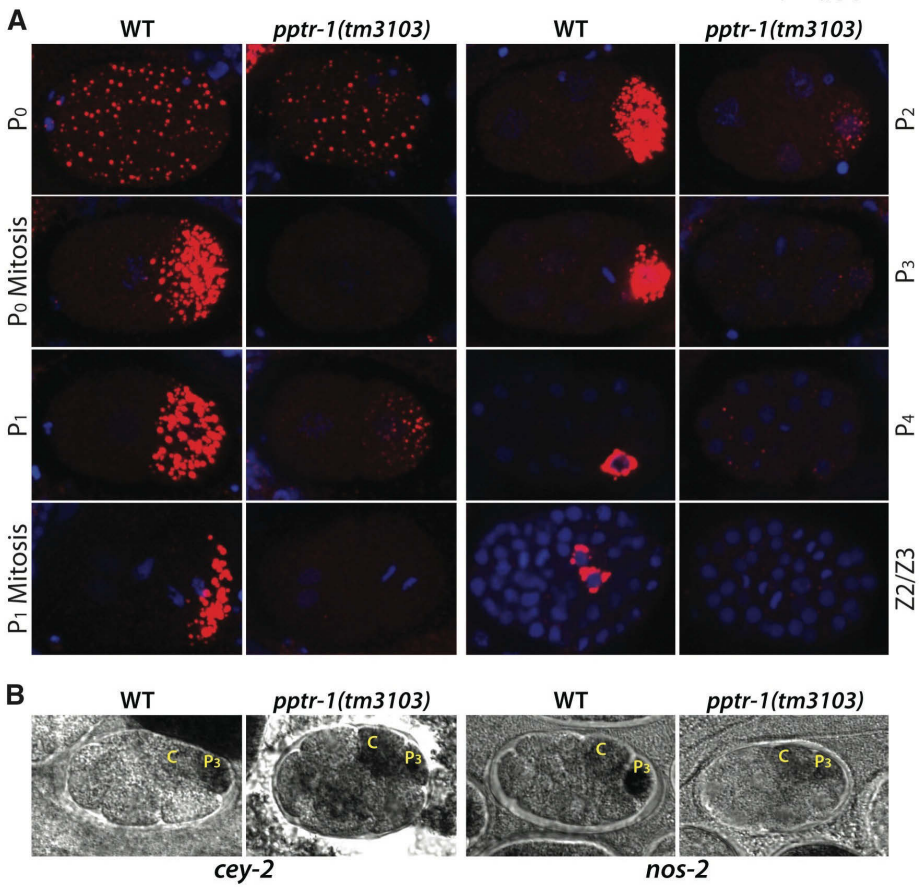

Figure 4. P granule components are segregated equally to germline and somatic blastomeres in *pptr-1* mutants

A) Fixed wild-type and *pptr-1* embryos stained with DAPI (blue) and OIC1D4 (red). Images are maximum projections of confocal Z-stacks (spanning entire embryo), except for P4 and Z2/Z3 images, which show single planes.

B) Wild-type and *pptr-1* embryos stained for *nos-2* and *cey-2* RNAs (black) by in situ hybridization. In *pptr-1* embryos, *nos-2* and *cey-2* RNAs are present at equal levels in P3 and C, indicative of symmetric segregation during the P2 division. In *pptr-1* embryos, as in wild-type, *nos-2* and *cey-2* RNAs levels are lower in all other blastomeres, indicative of rapid degradation of these RNAs in somatic lineages.

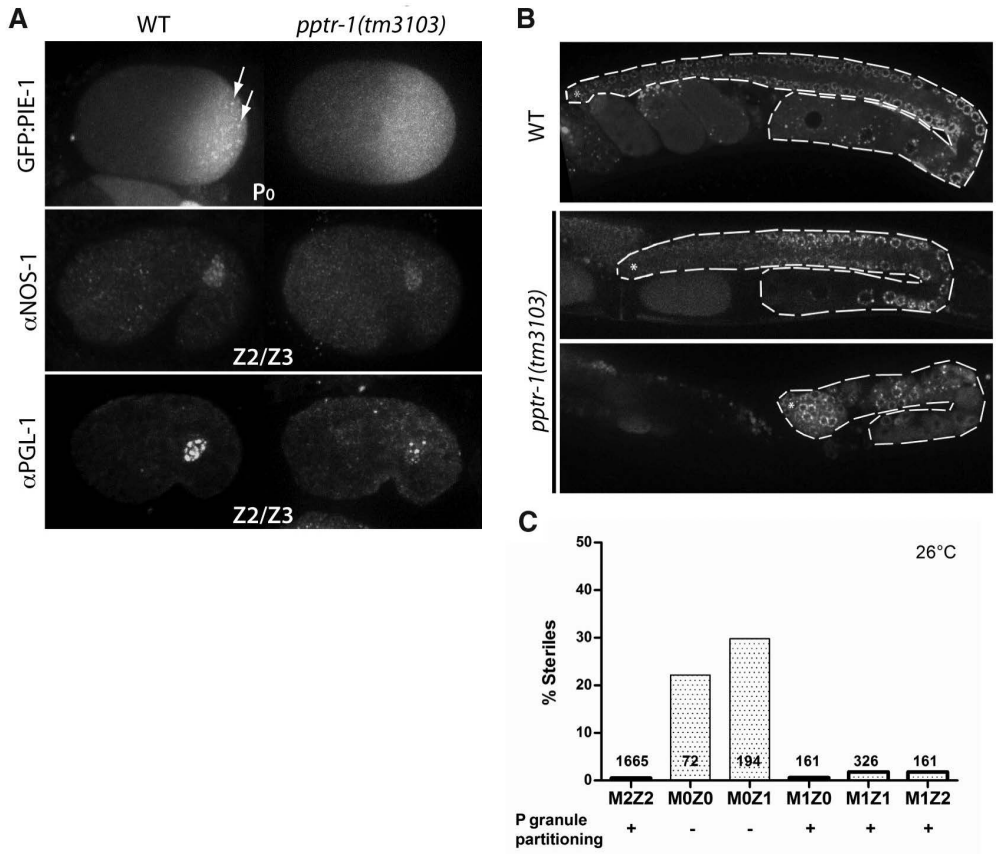

Figure 5. *pptr-1* mutants specify a germline, but a minority are sterile at high temperatures

A) Embryos expressing GFP::PIE-1 or stained with NOS-1 and PGL-1 antibodies. Patterns are identical in wild-type and *pptr-1*, except that *pptr-1* embryos lack GFP::PIE-1 foci seen in wild-type (arrows), and have lower PGL-1 levels.

B) Adult wild-type and *pptr-1* hermaphrodites expressing GFP::PGL-1. Gonads are outlined. Most *pptr-1* hermaphrodites develop a full gonad with gametes (top panel), but at high temperatures a minority (20%) are sterile, with no gametes (lower panel). Fertile *pptr-1* gonads are smaller than wild-type and yield a reduced number of progeny; unlike

the P granule defect, however, the brood size defect is partially rescued by zygotic *pptr-1* (Sup. Fig. 7).

C) Percentage of sterile hermaphrodites and total numbers scored. Wild-type have 2 maternal and 2 zygotic *pptr-1* copies (M2Z2). Mutant *pptr-1* hermaphrodites (M0Z0) were crossed with wild-type males to generate M0Z1, which were allowed to self-fertilize to generate M1Z0, M1Z1 and M1Z2. Only M0Z0 and M0Z1 hermaphrodites show significant sterility, demonstrating maternal requirement. *pptr-1* is also required maternally for P granule partitioning (Sup. Fig. 3).

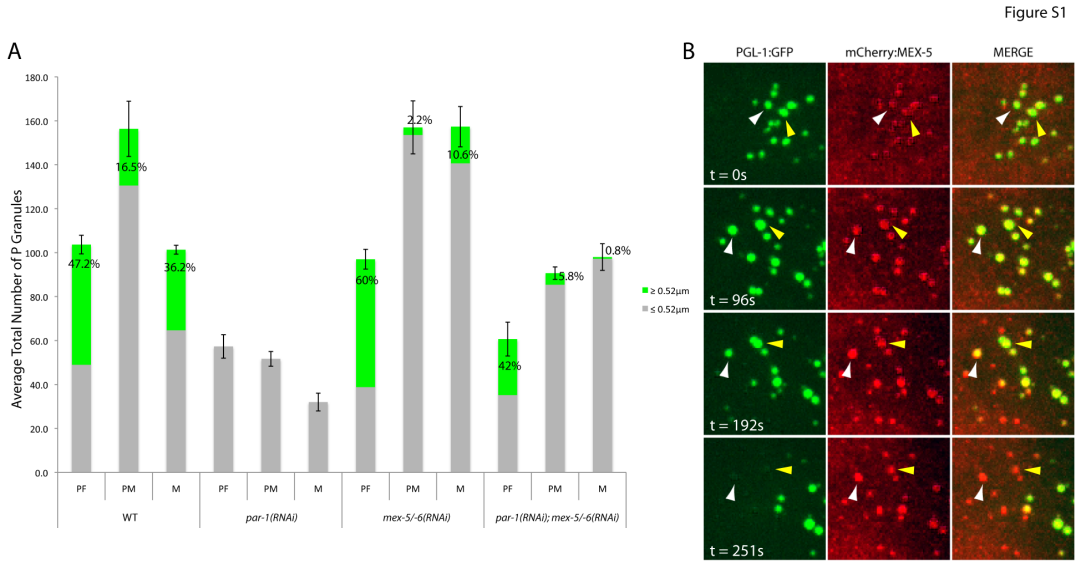

Figure 6: P granule dynamics.

A) Average number of P granules from 3 zygotes filmed from meiotic exit (pronuclear formation, PF), interphase (pronuclear migration, PM), and mitosis (M). Green color in each bar indicates portion of GFP::PGL-1 granules with diameters larger than 0.52µm (numbers show percentage). P granule sizes and numbers are intermediate *in par-1(RNAi);mex-5/6(RNAi)* zygotes compared to *par-1(RNAi)* and *mex-5/6(RNAi)* zygotes, suggesting that PAR-1 promotes P granule assembly both by antagonizing MEX-5 and MEX-6, and by another mechanism.

B) Time-lapse confocal images of the anterior cytoplasm of a zygote expressing PGL-1::GFP and mCherry::MEX-5. Arrows point to two examples of PGL-1::GFP granules that associate with mCherry::MEX-5 before disassembly, leaving mCherry::MEX-5 behind. See movie 4.

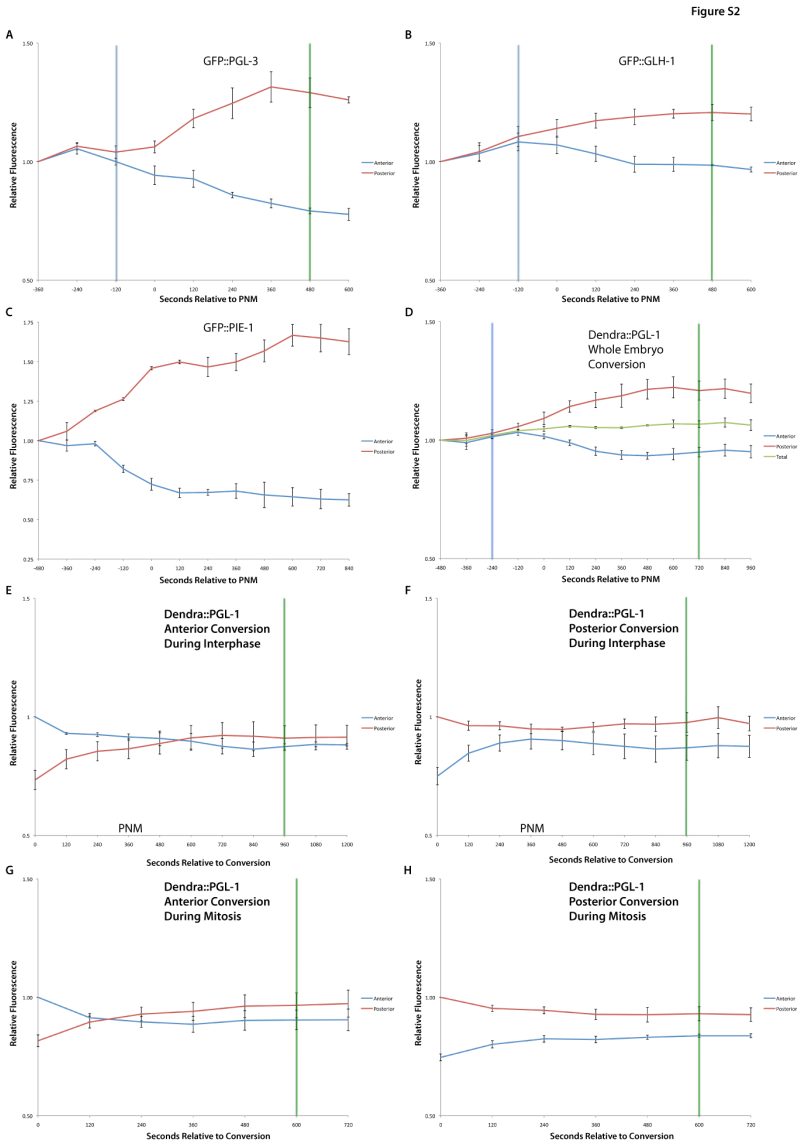

Figure 7. Dynamics of P granule components.

In all experiments, GFP or photoconverted Dendra fluorescence was measured in the anterior and posterior halves of the zygote over time. Error bars are standard deviation of mean values obtained from 3 embryos. Blue lines indicate the first time point at which P granules are restricted to the posterior, and green lines indicate cytokinesis.

A, B, and C) Time zero is pronuclear meeting. Like GFP::PGL-1 (Figure 3F), GFP::PGL-3 and GFP::GLH-1 levels remain equal in the anterior and posterior during interphase,

even though visible granules disappear from the anterior during this time. GFP::PGL-3 and GFP::GLH-1 levels decrease significantly in the anterior only during mitosis (prophase begins shortly before pronuclear meeting). By contrast, GFP::PIE-1 begins to segregate during interphase.

D) Time zero is pronuclear meeting. Dendra::PGL-1 was photoconverted throughout the zygote approximately 10-15 seconds before the first time point. Anterior levels increase and posterior levels decreases during mitosis (with no change in total levels), indicating that GFP::PGL-1 relocalizes from anterior to posterior.

E-H) Dendra::PGL-1 was photoconverted in the region indicated. Time zero is first time point 10-15 seconds after photoconversion. At this time, some photoactivated Dendra::PGL-1 has already diffused into the non-photoconverted half of the embryo. Value in photoconverted half at first time point was set to one and all other values were scaled accordingly. Note that in posterior photoconversion experiments, Dendra::PGL-1 levels remain higher in the posterior throughout the experiment. In anterior photoconversion experiments, Dendra::PGL-1 redistributes from anterior to posterior, and redistribution is faster during mitosis.

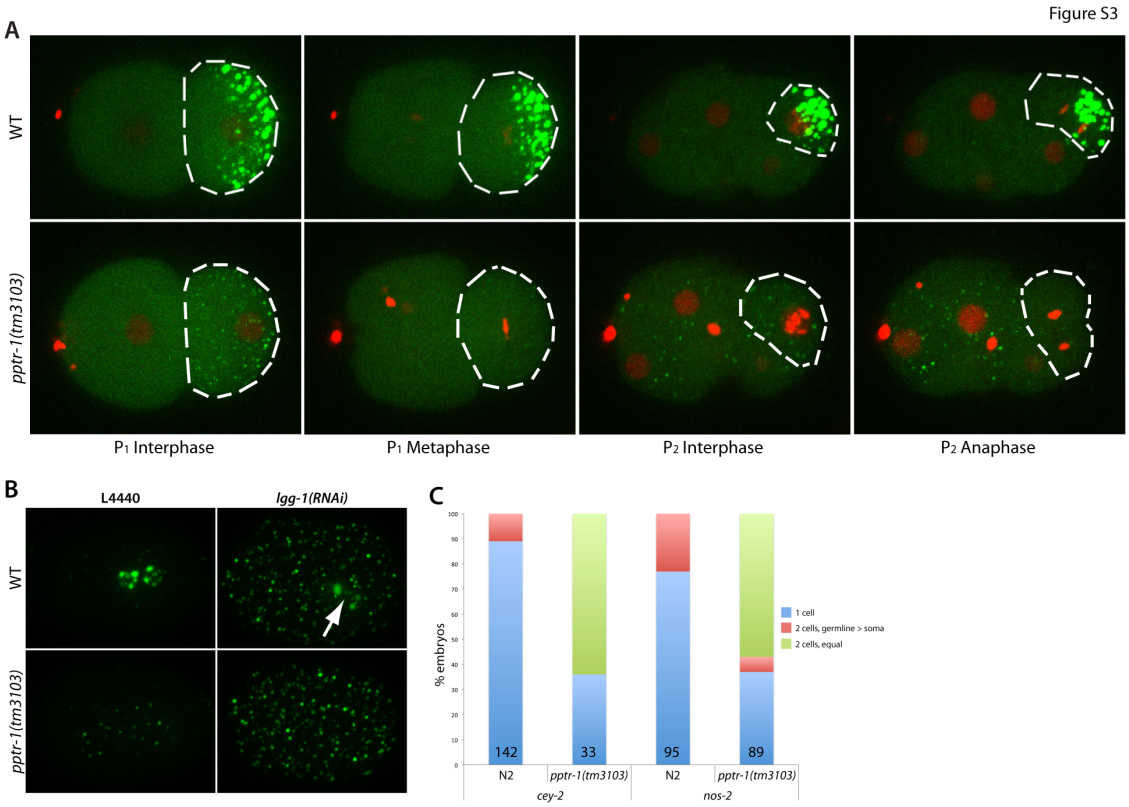

Figure 8: P granule components are segregated symmetrically in *pptr-1* mutants.

A) Time-lapse confocal images from Movie 5 of 2-to-8 cell wild-type and *pptr-1* embryos expressing GFP::PGL-1 (green) and mCherry:Histone H2B (red)**.** The P blastomere is outlined. GFP::PGL-1 granules are present in interphase/prophase and disperse during metaphase/anaphase. Granules are absent in AB (anterior blastomere in first panel) due to high MEX-5/6 levels, and re-appear in the AB daughters (last two panels) in a short period after sufficient MEX-5/6 has turned over and before the cells enter mitosis.

B) Confocal images (maximum projection of confocal Z-stacks spanning 8µm) of 100-cell embryos expressing GFP::PGL-1. At this stage GFP::PGL-1 is restricted to the primordial germ cells Z2 and Z3 in wild-type embryos, but is present in more cells in

pptr-1 embryos. *lgg-1(RNAi)* blocks PGL-1 degradation in somatic cells. Note that GFP::PGL-1 still accumulates preferentially in Z2 and Z3 in *lgg-1(RNAi)* embryos (arrow), but is evenly distributed in all cells in *pptr-1; lgg-1(RNAi)* embryos.
C) Quantification of *nos-2* and *cey-2 in situ* hybridization data. All embryos were scored in the 8-16 cell stage. At this stage, in wild-type embryos, *cey-2* and *nos-2* RNA are detected in 2 cells (P_3 and C, with stronger signal in P_3, due to asymmetric segregation during division) or in just 1 cell (P_3, due to rapid RNA degradation in C). In contrast, in ~60% of *pptr-1* embryos, *nos-2* and *cey-2* RNAs were detected at equal levels in both P_3 and C (green color in graph), a pattern never observed in wild-type. In the remaining embryos, levels were lower or undetectable in C due to rapid RNA degradation in that blastomere as in wild-type.

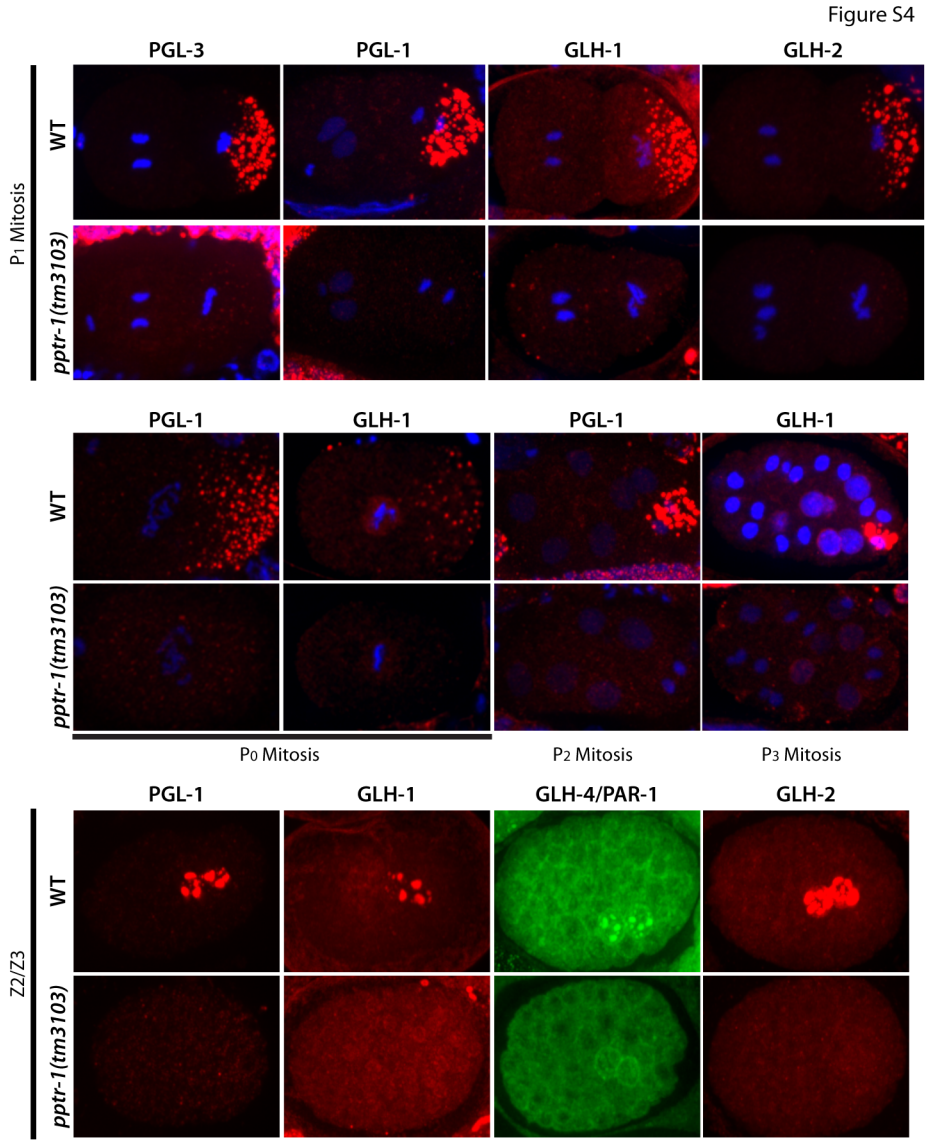

Figure 9: P granule components are segregated symmetrically in *pptr-1* mutants.

Fixed wild-type and *pptr-1* embryos stained with DAPI (blue) and antibodies (red or green) against core P granule proteins as indicated. All images are maximum projections of confocal Z-stacks (spanning entire embryo), except for GLH-1 stainings in P_0, which show a single focal plane. Note the absence of bright asymmetric granules during mitosis. For some antibodies, it is difficult to distinguish diffuse cytoplasmic staining from background.

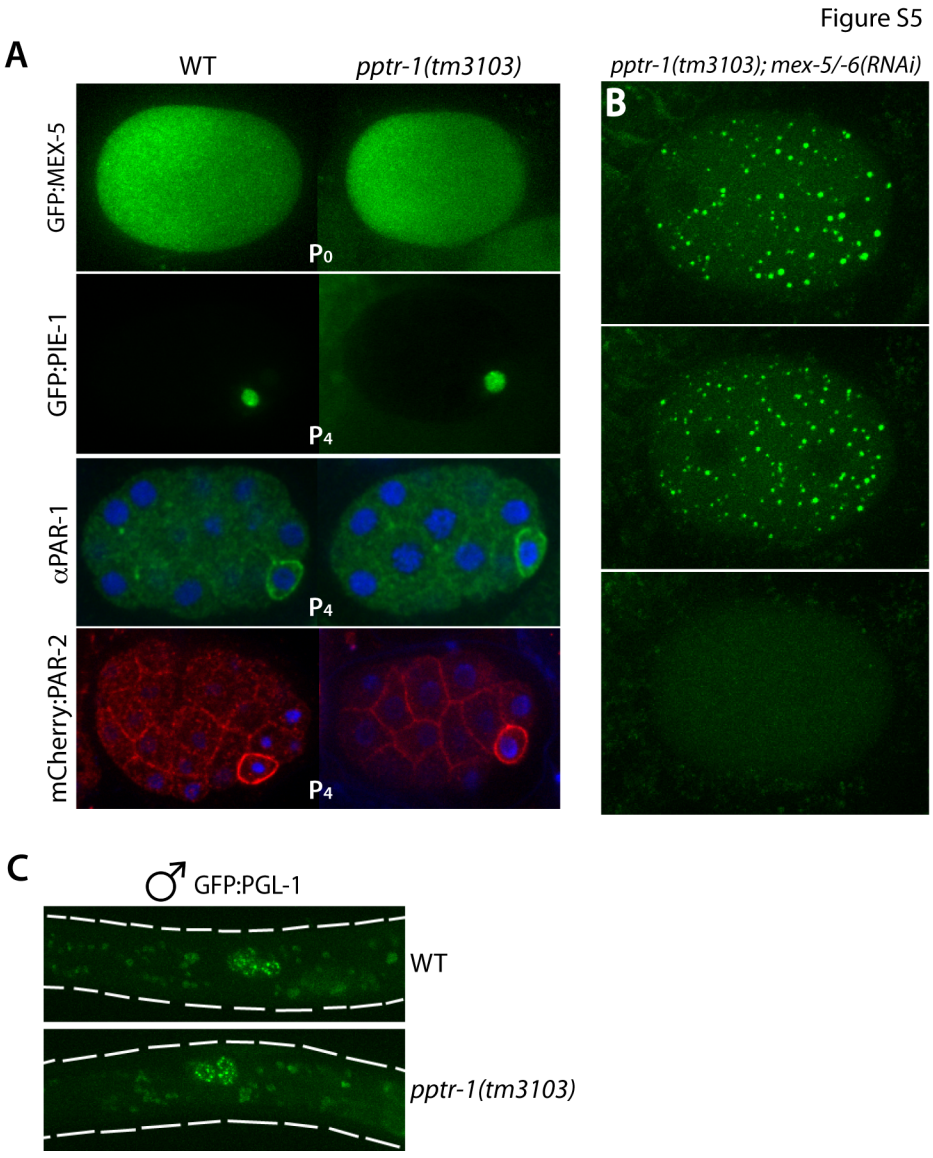

Figure 10: *pptr-1* does not affect other soma-germline asymmetries in embryos.

A**)** Embryos expressing the indicated fusions or stained with the indicated antibodies. Patterns are identical in wild-type and *pptr-1* embryos.

B) GFP::PGL-1 dynamics in *pptr-1;mex-5/6* embryos. MEX-5/6 are required for P granule disassembly in the anterior during interphase in *pptr-1* embryos, but are not required for P granule disassembly during mitosis.

C) Z2 and Z3 descendents in L1 larvae derived from wild-type or *pptr-1* mothers express a paternally-inherited GFP::PGL-1 transgene. L1 was the earliest stage at which we could detect zygotic expression of the GFP::PGL-1 transgene; zygotic expression of endogenous PGL-1, however, can be detected as early as the comma-stage (see PGL-1 panel in Fig. 3 and (*1*)).

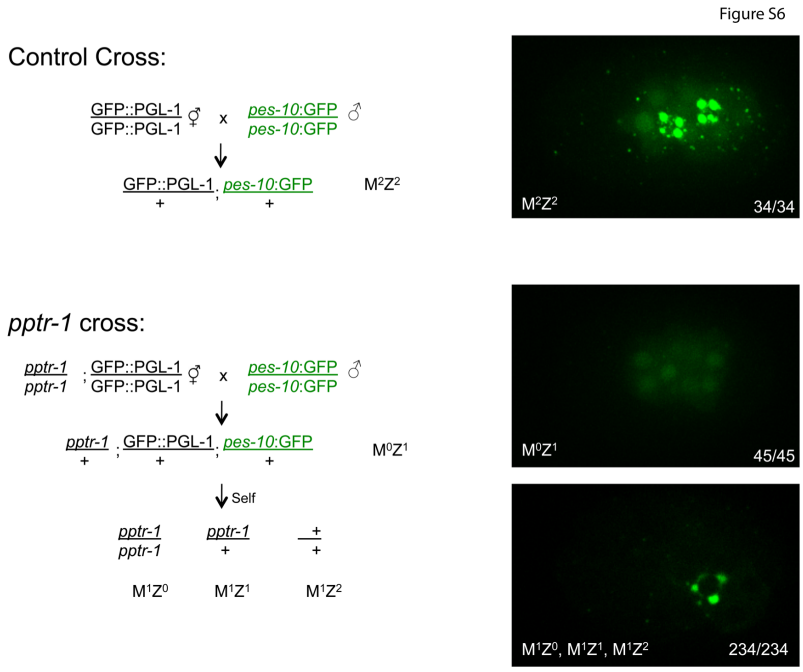

Figure 11: *pptr-1* is required maternally for GFP::PGL-1 enrichment in germline blastomeres.

Wild-type (control) or *pptr-1* hermaphrodites expressing GFP::PGL-1 were crossed with males homozygous for the *pes-10:GFP* transgene, which is transcribed transiently in each somatic lineage (*2*). Cross-progeny embryos (> 100 cell and younger) were identified by *pes-10:GFP* expression (zygotic expression only) and scored for GFP::PGL-1 (maternal expression only at this stage). All cross progeny from wild-type mothers (M2Z2) had normal P granules, whereas all cross progeny from *pptr-1* mothers (M0Z1) showed the *pptr-1* phenotype (no P granule enrichment). The latter were allowed to self-fertilize; all self progeny (M1Z0, M1Z1, M1Z2) had normal P granules demonstrating that the requirement for *pptr-1* with respect to P granule partitioning in embryos is strictly maternal.

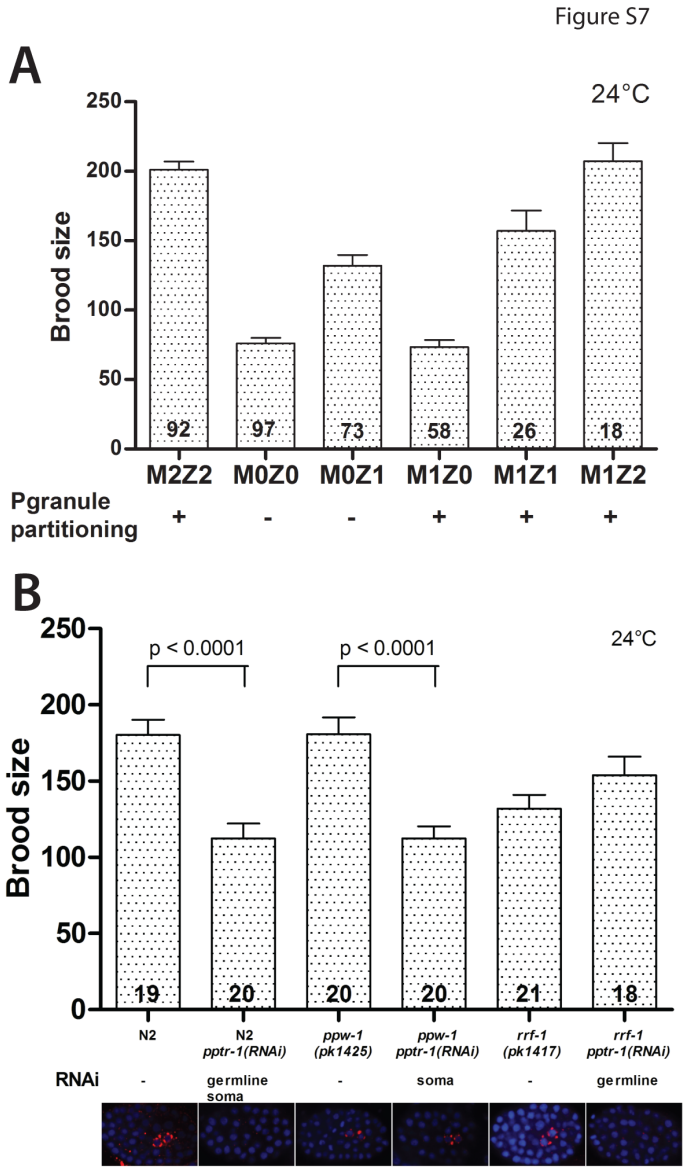

Figure 12. *pptr-1* is required zygotically for maximal brood size.

A) Graph comparing average brood size for mothers (n) with different maternal and zygotic *pptr-1* copy numbers (MZ nomenclature as in Fig. 3 and Sup. Fig. 6). Numbers are number of mothers examined for each genotype, aggregated from at least 2 independent experiments. Error bars are standard error of the mean.

At 24°C, *pptr-1* hermaphrodites (M0Z0) have a small brood size compared to wild-type (M2Z2). This defect is partially rescued by introducing a zygotic copy of *pptr-1* (M0Z1),

but not by introducing a maternal copy (M1Z0). Brood size increases with increased zygotic copy (compare M1Z0, M1Z1 and M1Z2), suggesting that *pptr-1* is required zygotically for maximal brood size and is haploinsufficient.

B) Graph comparing average brood size for mothers (n) of the indicated genotypes. Error bars are standard error of the mean. p values were obtained from an unpaired T-test. RNAi in wild-type, *ppw-1(pk1425)*, and *rrf-1(pk1417)* hermaphrodites depletes *pptr-1* from both soma and germline, soma only, and germline only, respectively (*3, 4*). N2 (wild-type), *rrf-1(pk1417)*, or *ppw-1(pk1425)* L4 hermaphrodites ("P0" generation) were soaked in *pptr-1* dsRNA (Methods), recovered on *pptr-1(RNAi)* plates for 24 hours, and allowed to lay eggs (F1) for 2 hours onto fresh *pptr-1(RNAi)* plates. Gravid P0 mothers were squashed and stained to visualize P granules in F1 embryos (photomicropgraphs below graph). F1 L4 stage hermaphrodites were transferred to fresh *pptr-1(RNAi)* plates for 30 hours and passaged to a second plate to lay remainder of their brood. Total broods were determined by counting number of L4 larvae on both plates (F2s). Note that depletion of *pptr-1* in the soma (*ppw-1* background) does not affect P granule partitioning during embryogenesis but these embryos grow up to have reduced brood size. In contrast, depletion of *pptr-1* in the germline (*rrf-1* background) disrupts embryonic partitioning of P granules, but these embryos grow up to have a normal brood size. *rrf-1* mutants are sterile are high temperatures (*5*) so we could not determine whether depletion of *pptr-1* in the germline also leads to low penetrance sterility at high temperatures as expected.

Table 2. Strains used in this study

Name	Description	Genotype	Reference
JH1999	pie-1 prom::GFP-H2B-nos-2 3'UTR	*unc-119(ed3); axIs1448[pCM1.01]*	D'Agostino et al., 2006
JH2015	pie-1 prom::GFP::PIE-1-pie-1 3'UTR	*unc-119(ed3); axIs1462[pCM4.08]*	Merritt et al., 2008
JH2017	pie-1 prom::GFP::PGL-3-pgl-3 3'UTR	*unc-119(ed3); axIs1464[pCM4.10]*	Merritt et al., 2008
JH2078	pie-1 prom-LAP::MEX-5::pie-1 3'UTR	*unc-119(ed3); axIs1504[pCG2]*	This study
JH2108	pie-1 prom::GFP::PGL-1-pgl-1 3'UTR	*unc-119(ed3); axIs1522[pCM4.11]*	Merritt et al., 2008
JH2172	pie-1 prom::LAP-GLH-1-nos-2 3'UTR	*unc-119(ed3); axIs1485[pEV1.02]*	Gift from E. Voronina
JH2330	nmy-2 prom-PGL-1-GFP-nmy-2 3'UTR; pie-1 prom::mCherry-PATR-1::pie-1 3'UTR	*unc-119(ed3); axIs1488[pCG176]; NA*	Gallo et al., 2008
JH2758	pie-1 prom::mCherry-PAR-2::pie-1 3'UTR	*unc-119(ed3); axIs1929[pFM033]*	Zonies et al., 2010
JH2773	pie-1 prom::Dendra::PGL-1-pgl-1 3'UTR	*unc-119(ed3); axIs1946[pCG391]*	This study
JH2787	*pptr-1* mutant	*pptr-1(tm3103)*	This study
JH2791	*pptr-1* mutant; pie-1 prom::GFP-H2B-nos-2 3'UTR	*pptr-1(tm3103); axIs1448[pCM1.01]*	This study
JH2794	*pptr-1* mutant; pie-1 prom::GFP::PIE-1-pie-1 3'UTR	*pptr-1(tm3103); axIs1462 [pCM4.08]*	This study
JH2835	*pptr-1* mutant; pie-1 prom-LAP::MEX-5::pie-1 3'UTR	*pptr-1(tm3103); axIs1504[pCG2]*	This study
JH2836	nmy-2 prom-PGL-1-GFP-nmy-2 3'UTR	*unc-119(ed3); NA*	Wolke et al., 2007
JH2838	*par-1* ts; nmy-2 prom-PGL-1-GFP-nmy-2 3'UTR	*par-1(zu310ts); NA*	This study
JH2839	*pptr-1* mutant; pie-1 prom::GFP::PGL-1-pgl-1 3'UTR; pie-1 prom::mCherry-PAR-2::pie-1 3'UTR	*pptr-1(tm3103); axIs1522[pCM4.11]; axIs1929[pFM033]*	This study
JH2840	nmy-2 prom-PGL-1-GFP-nmy-2 3'UTR; pie-1 prom::mCherry-MEX-5::pie-1 3'UTR	*unc-119(ed3); NA; axIs1731[pEG56]*	This study
JH2841	*pptr-1* mutant; pie-1 prom::GFP::PGL-1-pgl-1 3'UTR	*pptr-1(tm3103); axIs1522[pCM4.11]*	This study
JH2842	pie-1 prom::GFP::PGL-1-pgl-1 3'UTR; pie-1 prom::mCherry-H2B::pie-1 3'UTR	*unc-119(ed3); axIs1522[pCM4.11]; NA*	This study
JH2843	*pptr-1* mutant; pie-1 prom::GFP::PGL-1-pgl-1 3'UTR; pie-1 prom::mCherry-H2B::pie-1 3'UTR	*pptr-1(tm3103); axIs1522[pCM4.11]; NA*	This study
KK289	*par-1* kinase dead	*par-1(it51) rol-4(sc8)/DnT1*	Gift from K. Kemphues

KK822	*par-1* ts	*par-1(zu310ts)*	Gift from K. Kemphues
NL2098	*rrf-1* mutant	*rrf-1(pk1417)*	Sijen et al., 2001
NL3511	*ppw-1* mutant	*ppw-1(pk1425)*	Tijsterman et al., 2002
PD4790	myo-2 prom::GFP; pes-10 prom::GFP	*mIs12*	Edgley et al., 1999
TH202[#]	glh-1 prom::GLH-1::GFP::glh-1 3'UTR	Recombineered fosmid integrated by bombardment	Brangwynne et al., 2009
TH206*	pgl-1 prom::PGL-1::GFP::pgl-1 3'UTR	Recombineered fosmid integrated by bombardment	Brangwynne et al., 2009

Abbreviations:
Prom – Promoter
3' UTR - 3' untranslated region
All CAPs – coding regions of indicated genes
:: - GATEWAY recombination sequence used for cloning (for JH strains only).
All transgenes (except for *myo-2* and *pes-10*) also contain a wild-type copy of *unc-119* (transformation marker). Note that we used four different GFP::PGL-1 lines: each with different promoter and 3' UTR combinations. All lines behaved identically in movies. Nevertheless for quantification of PGL-1 levels as shown in Fig. 1I,J, Fig. 2B, and Sup. Fig. 2, we specifically used lines with the *pgl-1* 3' UTR (JH2108, JH2773, and JH2841).
TH202 was used for experiments shown in Fig. 2B.
* TH206 was used for experiments shown in Fig. 4B.

Chapter 2

Regulation of P granule asymmetry by phosphorylation of a dynamic scaffold

Introduction

We showed in Chapter 1 (Gallo et al 2010) that a protein phosphatase 2A (PP2A) heterotrimer with the PPTR-1 regulatory subunit is required to stabilize P granules during mitosis (Gallo et al 2010). In this chapter, we sought to understand the molecular mechanisms by which PPTR-1 regulates P granule segregation. We found that PPTR-1 acts redundantly with PPTR-2. Together, these PP2A heterotrimers are the opposing phosphatases to MBK-2 kinase and act downstream of known polarity regulators. In a yeast two hybrid screen for PPTR-1 interactors, we found MBK-2/PPTR-1 substrates that regulate P granule dynamics. We propose that these interactors form a scaffold around canonical P granule components to actively assemble P granules in the posterior of the embryo. I was helped in this work by Dominique Rasoloson (GST pulldown assays), Jarrett Smith (Phos tag assays), and Alexandre Paix (*in situ* hybridization).

Results

PPTR-1 and PPTR-2 redundantly affect P granule dynamics

PPTR-1, a B'/B56 PP2A regulatory subunit, is 61% identical at the amino acid level with PPTR-2, another B'/B56 PP2A regulatory subunit. Knockdown of PPTR-2 by RNAi in wildtype did not affect P granule dynamics. However, knockdown of PPTR-2 in the *pptr-1(tm3103)* mutant resulted in an enhanced P granule hyperdisassembly phenotype. We conclude that PPTR-2 functions partially redundantly with PPTR-1 to stabilize P granules in the posterior cytoplasm of C. elegans zygotes (Figure 13A).

MBK-2 and PP2A are an opposing kinase/phosphatase pair required for P granule dynamics

To place PP2A in a genetic pathway for P granule segregation, we performed epistasis experiments with other mutants that affect P granule dynamics. MBK-2 codes for a serine/threonine kinase. In *mbk-2* mutant zygotes, P granules do not disassemble and large granules remain stabilized throughout the cytoplasm (Pellettieri et al 2003). *pptr-1(tm3103);pptr-2(RNAi);mbk-2(RNAi)* zygotes showed the same phenotype as *mbk-2(RNAi)* zygotes. We conclude that MBK-2 is epistatic to PPTR-1/2, raising the possibility that the two act on the same substrates to promote disassembly (phosphorylation by MBK-2) and reassembly (dephoshorylation by PPTR-1/2) (Figure 13B).

par-1 and *mex-5/6* are polarity regulators that regulates several asymmetries in the zygote. In *par-1* mutant zygotes, all P granules disassemble and in *mex-5/6* mutant zygotes, all P granules disassemble partially. We found that *mbk-2* is epistatic to both, and *pptr-1/2* are epistatic to *mex-5/6* (*pptr-1* could not be tested against *par-1* since the mutants have the same phenotypes) (Figure 13C). These analyses suggest that MBK-2 and PPTR-1 function downstream of the polarity machinery to promote disassembly and reassembly of P granules.

A Yeast-Two-Hybrid Screen for PPTR-1 interactors identifies GEI-12, C36C9.1, and MEG-1

To identify potential targets of MBK-2/PPTR-1/2, we performed a yeast two hybrid screen for proteins that bind to PPTR-1. We first tested several known P granule

components and obtained no positives, although known substrate AKT-1 is phosphorylated (Figure 14). Next, we screened a C. elegans mixed stage cDNA library and obtained 32 positives (Table 3).

We tested each positive by RNAi for an effect on P granule segregation in wild-type zygotes, and for suppression of the *pptr-1* hyperdisassembly phenotype (Table 3). From these secondary screens, we identified two pairs of intrinsically disordered paralogous proteins: GEI-12/C36C9.1, and MEG-1/MEG-2. Each of these proteins codes for serine and asparagine-rich intrinsically disordered proteins (Figure 15 and Table 4). We verified that GEI-12 and C36C9.1 interact with PPTR-1 yeast by GST pulldown (Figure 16A).

GEI-12 and MEG-1 can be phosphorylated in vitro by MBK-2

To determine whether GEI-12 and MEG-1 are substrates of MBK-2 kinase, we expressed recombinant proteins in vitro and performed in vitro kinase assays. Both GEI-12 and MEG-1 can be phosphorylated in vitro by recombinant MBK-2 (Figure 16B).

We identified 3 putative MBK-2 consensus sites in GEI-12, and 1 putative consensus site in MEG-1 using the known MBK-2 consensus site K/R X_{1-3} S/T P (Campbell et al 2002, Himpel et al 2000). We mutated all of these consensus sites to alanine and performed in vitro kinase assays. Although these mutations did not abolish phosphorylation by MBK-2, phosphorylation was reduced compared to wildtype (Figure 16B). Thus, the predicted consensus sites may be phosphorylated by MBK-2 in vivo. Indeed, phosphorylation at the MEG-1 S574 site has been identified in large scale phosphoproteome analyses (Gnad et al 2007).

GEI-12 is phosphorylated in vivo in an MBK-2 dependent manner and dephosphorylated in a PPTR-1 dependent manner.

To determine whether GEI-12 is phosphorylated *in vivo*, we ran embryonic lysates from worms expressing GFP::GEI-12 on a Phos-tag gel (Kinoshita et al 2006). Whereas GFP::GEI-12 migrates as one band on SDS-PAGE, on 25 uM Phos tag it migrates as a weak smear that can be collapsed with addition of exogenous alkaline phosphatase (Figure 16C). This shows that GFP::GEI-12 is phosphorylated in vivo in embryos.

We next treated GFP::GEI-12 expressing worms with *mbk-2(RNAi)* and subjected embryonic lysates to Phos-tag analysis. We measured percentage unphosphorylated on the Phos tag gel and found that in *mbk-2(RNAi)*, GFP::GEI-12 is hypophosphorylated. GFP::GEI-12 in *pptr-1(tm3103)* background was hyperphosphorylated (Figure 16C). We conclude that *mbk-2* is required for GEI-12 phosphorylation and *pptr-1* is required for GEI-12 dephosphorylation in vivo.

GEI-12 and C36C9.1 are required for P granule dynamics

We had previously observed that P granule dynamics are dependent on the cell cycle (Gallo et al 2010). By observing fertilization events of oocytes in live mothers, we observed that P granule dynamics begin shortly after fertilization, when oocyte P granules disassemble throughout the fertilized zygote. Granules then reassemble throughout the entire embryo prior to the end of meiosis. In RNAi knockdowns of *gei-12* and *C36C9.1*, we find that oocyte P granules are not properly disassembled in *gei-*

12;C36(RNAi) embryos, and persist through the first few cell cycles. In addition, P granule reassembly is reduced throughout the entire embryo (Figure 17A). This results in a fertilized embryo with only a few, large P granules inherited from the oocyte that persist throughout the first few cell cycles (Fig 17B). In *gei-12;C36C9.1(RNAi)* zygotes after the establishment of polarity, granule disassembly and reassembly remain disrupted. In the anterior, many granules are not properly disassembled, and posterior assembly of large granules is reduced.

Disruption of granule disassembly and reassembly continues in subsequent cell cycles. For example, in the P1 cell at the 2 cell stage, granules are not properly disassembled in the anterior, nor properly assembled in the posterior, resulting in further missegregation of P granule proteins (Fig 17B). This results in the primodial germ cell, P4, receiving equal amounts of P granule components as somatic cells (Figure 17B). These effects are due to differences in P granule aggregation and segregation to the germ cell lineage, not total protein levels, as levels of endogenous P granule components remain the same in *gei-12;C36C9.1(RNAi)* embryos by Western blotting (Figure 18E). Consistent with missegregation of P granule components to both germline and soma, L1 larvae are born with less than a full complement of PGL-1 in Z2 and Z3 (Fig 17B). Over larval development, zygotic production of PGL-1 restores the full complement of PGL-1 to the germline (Data not shown).

One known RNA component of embryonic P granules, *nos-2*, is also missegregated. In *gei-12(RNAi)*, *nos-2* mRNA is symmetrically inherited by the germ lineage cell P3 and its sister C (Fig 17C). Thus, GEI-12 is required for segregation of P granule proteins and RNAs.

GEI-12 has two paralogues in the C. elegans genome: C36C9.1 and F52D2.12. To determine which of these paralogues are required for P granule segregation, we were able to specifically knock down C36C9.1 and F52D2.12 in a *gei-12* deletion mutant. In this mutant background, C36C9.1 is required for P granule dynamics, whereas F52D2.12 is not (Figure 18D). Thus, GEI-12 and C36C9.1 are redundantly required for P granule dynamics.

Despite these dramatic effects on P granule segregation, we note that key fate regulators, such as PIE-1 and MEX-5, remain properly segregated in *gei-12;C36C9.1(RNAi)* embryos, although they do not localize to P granules (Figure 18C). In addition, GEI-12 and C36C9.1 are specific for P granules, as they do not influence the distribution of PATR-1, a P body component (Figure 18B). Consistent with these observations, we find that loss of *gei-12/C36C9.1* does not result in embryonic lethality. However, these embryos grow to larvae with a low percentage of sterility at 24°C (Fig 17D), suggesting that germ cell proliferation is compromised.

To test whether *gei-12/C36C9.1* act downstream of the kinase *mbk-2 in vivo*, we knocked down *gei-12/C36C9.1* in *mbk-2* mutant embryos. We observed fewer, larger granules throughout the embryo as in the *gei-12/C36C9.1* knockdown, consistent with *gei-12/C36C9.1* acting downstream of *mbk-2* (Figure 18A).

MEG-1 is required for P granule disassembly

meg-1 and *meg-2* have previously be reported to affect P granule segregation in a percentage of fixed embryos (Leacock and Reinke 2008). During our initial characterizations, we knocked down both *meg-1* and *meg-2* by RNAi in live embryos.

We observed that P granule missegregation is cell-cycle dependent. At interphase, P granules are not properly disassembled in the anterior of *meg-1(RNAi);meg-2(RNAi)* embryos. During mitosis, P granules are missegregated to both somatic and germline daughter cells. Over the course of the following cell cycle, missegregated P granules are selectively disassembled in somatic daughters (Figure 19A).

To determine if *meg-1* and *meg-2* are required for the *pptr-1* phenotype, we performed genetic epistasis experiments. Loss of *pptr-1* results in P granule disassembly during mitosis and missegregation of P granules to all cells, such that the P4 blastomere cannot be distinguished from somatic cells. Loss of *meg-1* and *meg-2* results in the opposite phenotype: P granules are stabilized in both the P4 germline lineage as well as the P4 sister cell, D. We find that loss of *meg-1* and *meg-2* in *pptr-1* mutants results in a *meg-1/2*-like phenotype, such that large granules predominate in P4 and its sister D (Figure 19B). Thus, *meg-1* and *meg-2* act downstream of *pptr-1* in embryos.

To determine whether *meg-1* or *meg-2* are required for P granule segregation, we immunostained previously characterized deletion mutants in *meg-1(vr10)* or *meg-2(ok1937)* mutants. In *meg-1(vr10)*, we noted that P granules are not properly disassembled in the anterior of interphase cells, similar to *meg-1(RNAi);meg-2(RNAi)*. No such phenotype was seen in *meg-2(ok1937)* (Figure 19C).

GEI-12 and MEG-1 localize to sub P granule compartments

To understand how GEI-12 affects P granule dynamics, we determined its localization in both live and fixed worms. We created transgenic worms expressing GFP::GEI-12 under regulatory control of its own promoter and 3'UTR. GFP::GEI-12

localizes prominently to P granules in embryos, consistent with their role in regulating P granules during this developmental stage (Figure 20A). We confirmed this localization using an antibody specific for GEI-12. MEG-1 has also been previously reported to localize to embryonic P granules (Leacock and Reinke 2008).

Intriguingly, using our spinning disk confocal at 100x magnification, we noted that both GEI-12 and MEG-1 are not distributed uniformly throughout each granules. Within the P granule, we noted regions of high GEI-12 and MEG-1 concentration and regions with lower GEI-12 and MEG-1 concentrations (Figures 20B and 20C). To observe the subgranular distribution of GEI-12 and MEG-1 with higher resolution, we used light sheet microscopy developed by the Betzig lab at Janelia Farm Research Campus. The Betzig's lab's light sheet microscopy improves resolution in the z axis. Combined with structured illumination techniques, the Betzig lab's light sheet microscopy increases resolution in xyz planes (Gao et al 2012). We looked at GFP::GEI-12 in live embryos using structured illumination and found that GEI-12 forms doughnut-like structures with high density towards the edge and low density towards the interior. In contrast, GFP::PGL-1 appeared more uniformly distributed and did not form these structures (Figure 20D). By live imaging embryos co-expressing GFP::GEI-12 and mCherry::PGL-3 using sheet scanning mode without structured illumination, we noted that GEI-12 often formed enclosures around PGL-3 (Figure 20E). Thus, usage of spinning disk confocal microscopy, SR-SIM, and sheet scanning in live and fixed samples indicate that P granules are not homogeneous structures with equal mixing of all components. Instead, specific proteins form specific domains within the granule. Specifically, GEI-12 seems to form a scaffold-like enclosure around the core P granule

components PGL-1 and PGL-3. This imaging data, combined with the requirement of GEI-12 for P granule assembly, suggests that GEI-12 actively stabilizes P granules in the posterior in order for proper P granule segregation during embryogenesis.

Conclusions

We find that MBK-2 and $PP2A^{PPTR-1/2}$ are required for P granule dynamics and act downstream of known polarity regulators. In a yeast two hybrid screen for interactors of PPTR-1, we found three serine-rich, intrinsically disordered proteins: GEI-12, C36C9.1, and MEG-1. Knockdown of these genes by RNAi affects P granule dynamics but does not affect the overall polarity or viability of the embryo. We also find that GEI-12 and MEG-1 can be phosphorylated in vitro by MBK-2, and phosphorylation is dependent on known MBK-2 consensus sites. GEI-12 is phosphorylated in vivo in an *mbk-2* dependent manner, and dephosphorylated in a *pptr-1* dependent manner. Taken together, we propose that a phosphorylation/dephosphorylation of MEG-1, GEI-12 and C36C9.1 drives P granule dynamics during embryogenesis, ensuring that P granules are properly disassembled and reassembled in the cytoplasm. In this model, GEI-12 and MEG-1 are phosphorylated by MBK-2, and phosphorylated GEI-12 and MEG-1 are required for P granule disassembly in the anterior of the embryo. $PP2A^{PPTR-1}$ then acts to dephosphorylate GEI-12, and dephosphorylated GEI-12 is required for P granule reassembly in the posterior.

How does GEI-12 assemble P granules? Intriguingly, GEI-12 localizes to sub P granule domains surrounding P granule components, and knockdown of GEI-12 results in loss of P granule aggregation. Structured illumination imaging of GEI-12 and PGL-1

reveals that GEI-12 forms doughnut-like scaffolds around P granule components. One possibility is that in the non-phosphorylated state, GEI-12 forms a scaffold that stabilizes P granules. Consistent with this hypothesis, recombinant GEI-12 can bind to PGL-1, a core P granule component, by GST pulldown.

Because of the high serine content of GEI-12, C36C9.1, MEG-1, and MEG-2, one possibility is that an increase in overall protein charge following phosphorylation by MBK-2 disassembles the scaffold and drives P granule disassembly and reassembly. Our results suggest that there are multiple phosphorylated forms of GEI-12, only some of which are dependent on MBK-2. Further experiments are required to distinguish whether phosphorylation of key residues is required for P granule dynamics, or whether total protein charge plays a greater role in granule dynamics.

Two models have been proposed for RNA granule assembly: the liquid droplet model and the hydrogel model (Brangwynne et al 2009, Kato et al 2012). Intriguingly, our analysis of P granule dynamics does not fit neatly into either of these two models. The hydrogel model implicated specific low complexity domains as crucial to granule formation. None of our intrinsically disordered proteins contain these specific low complexity domains, and GEI-12 is not selectively precipitated by the biotinylated isox small molecule used in the hydrogel studies (Data not shown). In addition, the observation that P granules contain substructure, or regions of differing protein density, argues that these granules are not simple homogeneous liquid droplets, but instead undergo nonhomogeneous mixing. Instead, we propose that intrinsically disordered proteins, due to their conformational flexibility, may act as a scaffold for RNA granule assembly. Intriguingly, intrinsically disordered proteins have been implicated in

mammalian stress granule assembly (Kedersha et al 2013), suggesting that intrinsically disordered proteins may be conserved RNA granule regulators in multiple systems.

Experimental Procedures

Yeast two hybrid

Yeast two hybrid was performed using DUALhybrid kit (P01004, Dualsystems Biotech). All plasmids were converted to Gateway-compatible vectors (Invitrogen) and Gateway recombination was used to create N-terminally tagged pLexA-PPTR-1 bait vector, pY3H-PAA-1 bridge vector and candidate prey vectors. For library screening, yeast transformed with PPTR-1 bait and PAA-1 bridge were used with prey library from Dualsystems consisting of polyA+ cDNA from mixed stage C. elegans with 5.7e6 independent clones. Total transformation efficiency was 4.3e5 clones per ug DNA, with 2.1 times library coverage. Out of 1.2e7 total transformants, about 4500 positive colonies were obtained. 111 of these positive colonies were sequenced and correspond to 32 different genes.

RNAi-mediated Knockdown

RNAi was performed by feeding. Feeding constructs were obtained from the Ahringer or Openbiosystems libraries and sequenced, or newly cloned from *C. elegans* cDNA. HT115 bacteria transformed with feeding vectors were grown at 37º C in LB + ampicillin (100µg/mL) for 5 hours, induced with 5 mM IPTG for 45 minutes, plated on NNGM (nematode nutritional growth media) + ampicillin (100µg/mL) + IPTG (1mM), and grown overnight at room temperature before adding L4 worms at 24º C for 24-30 hours.

Live Imaging and Spinning-Disc Confocal Microscopy

Embryos were dissected from gravid adults into M9 and placed on a 3% agarose pad. For imaging of newly fertilized embryos, young adult mothers were anesthesized in 0.3mM levamisole for 15 minutes prior to mounting on 3% agarose pads. Time-lapse movies were acquired using a Zeiss Axio Imager fitted with a Yokogawa spinning-disc confocal scanner. Slices were taken every 1μm for a total of 8μm for time-lapse images. All images were acquired with Slidebook software (Intelligent Imaging Innovations).

In situ Hybridization

In situ hybridization of *nos-2* and mRNA was performed as described previously (Voronina et al 2012).

Antibody production

Peptide antibodies against GEI-12 were made by Covance using KLH conjugation in rabbits.

Immunostaining

Gravid adult hermaphrodites were laid on a slide coated with 0.01% poly-L-lysine and embryos, extruded by squashing with a coverslip, and frozen on pre-chilled aluminum blocks. Cover slips were removed and slides were incubated in -20 °C methanol for 15 minutes, followed by -20 °C acetone for 10 minutes. Slides were preblocked in PBS/0.1% Tween/0.1% BSA (PBT) for 30 minutes, and incubated with primary antibody

overnight at 4 °C. Primary antibodies were diluted in PBT as follows: K76 (1:10, DSHB), chicken anti-GLH-2 (1:200, gift from K. Bennett), rabbit anti GEI-12 (1:250, Covance), rabbit anti MEG-1 (1:200, gift from V. Reinke). Secondary antibodies were applied for 2 hours at room temperature. Images were acquired using a Zeiss Axio Imager fitted with a Yokogawa spinning-disc confocal scanner.

Transgenics

InFusion cloning (Clontech) was used for generation of all transgene plasmids. Transgenes were introduced into worms by microparticle bombardment (Praitis et al 2001).

GST pulldown

GST fusion proteins were cloned into pGEX6p1 (GE Healthcare) by restriction enzyme-mediated cloning. MBP fusion proteins were cloned into pJP1.09, a Gateway-compatible pMAL-c2x (Pellettieri et al 2003). Proteins were expressed in *E. coli* BL21 cells overnight at 16°C following induction with 0.4 mM IPTG. 200 mg of bacterial pellet of GST fusion proteins was resuspended in 10mM EGTA, 10mM EDTA, 500 mM NaCl, 0.1% Tween, PBS pH7.4 with protease and phosphatase inhibitors, lysed by sonication, and bound to GST beads. Beads were washed and incubated with MBP fusion proteins at 4°C for 1 hour in 50 mM Hepes pH7.4, 1 mM EGTA, 1 mM MgCl2, 500 mM KCl, 10% glycerol, 0.05% NP-40, pH7.4, protease and phosphatase inhibitors. After washing, beads were eluted with 10 mM reduced glutathione and loaded on SDS-PAGE.

Protein purification and in vitro kinase assay

MBP fusion proteins were cloned into pJP1.09, expressed and partially purified as previously described (Griffin 2011). In vitro kinase assays were performed as previously described (Cheng 2009).

Phos tag gel

Embryos were harvested from young adult worms and sonicated in 2% SDS , 65mM Tris pH7, 10% glycerol with protease and phosphatase inhibitors. Lysates were spun at 14000 rpm for 30 minutes and cleared supernatants treated with 100 U alkaline phosphatase (Roche). Samples were run on Phos tag gels (7% SDS-PAGE gels with 25 uM Phos-tag and 50 uM MnCl2) and SDS-PAGE (7%) at 30 mA for 2.5 hours. Gels were washed in transfer buffer with 1 mM EDTA twice for 10 minutes each, then washed in transfer buffer without EDTA. Western blot transfer was performed for 1 hour at 4°C onto nitrocellulose membranes. Membranes were blocked and washed in 5% milk, 0.1% Tween-20 in PBS and probed with JL-8 antibody (Clontech).

References

Brangwynne CP1, Eckmann CR, Courson DS, Rybarska A, Hoege C, Gharakhani J, Jülicher F, Hyman AA. Germline P granules are liquid droplets that localize by controlled dissolution/condensation. Science. 2009 Jun 26;324(5935):1729-32.

Campbell LE, Proud CG. Differing substrate specificities of members of the DYRK family of arginine-directed protein kinases FEBS Lett 510 (2002: 31–36.

Cheng KC, Klancer R, Singson A, Seydoux G. Regulation of MBK-2/DYRK by CDK-1 and the pseudophosphatases EGG-4 and EGG-5 during the oocyte-to-embryo transition. Cell. 2009 Oct 30;139(3):560-72.

Gallo CM, Wang JT, Motegi F, Seydoux G. Cytoplasmic partitioning of P granule components is not required to specify the germline in C. elegans. Science. 2010 Dec 17;330(6011):1685-9.

Gnad F, Ren S, Cox J, Olsen JV, Macek B, Oroshi M, Mann M. PHOSIDA (phosphorylation site database): management, structural and evolutionary investigation, and prediction of phosphosites. Genome Biol. 2007;8(11):R250.

Gao L, Shao L, Higgins CD, Poulton JS, Peifer M, Davidson MW, Wu X, Goldstein B, Betzig E. Noninvasive imaging beyond the diffraction limit of 3D dynamics in thickly fluorescent specimens. Cell. 2012 Dec 7;151(6):1370-85.

Griffin EE, Odde DJ, Seydoux G. Regulation of the MEX-5 gradient by a spatially segregated kinase/phosphatase cycle. Cell. 2011 Sep 16;146(6):955-68.

Himpel S, Tegge W, Frank R, Leder S, Joost HG, Becker W. Specificity determinants of substrate recognition by the protein kinase DYRK1A J. Biol. Chem 275 (2000):2431–2438.

Kato M, Han TW, Xie S, Shi K, Du X, Wu LC, Mirzaei H, Goldsmith EJ, Longgood J, Pei J, Grishin NV, Frantz DE, Schneider JW, Chen S, Li L, Sawaya MR, Eisenberg D, Tycko R, McKnight SL. Cell-free formation of RNA granules: low

complexity sequence domains form dynamic fibers within hydrogels. Cell. 2012 May 11;149(4):753-67.

Kedersha N, Ivanov P, Anderson P. Stress granules and cell signaling: more than just a passing phase? Trends Biochem Sci. 2013 Oct;38(10):494-506.

Kinoshita E1, Kinoshita-Kikuta E, Takiyama K, Koike T. Phosphate-binding tag, a new tool to visualize phosphorylated proteins. Mol Cell Proteomics. 2006 Apr;5(4):749-57.

Leacock SW, Reinke V. MEG-1 and MEG-2 are embryo-specific P-granule components required for germline development in Caenorhabditis elegans. Genetics. 2008 Jan;178(1):295-306.

Pellettieri J, Reinke V, Kim SK, Seydoux G. Coordinate activation of maternal protein degradation during the egg-to-embryo transition in C. elegans. Dev Cell. 2003 Sep;5(3):451-62.

Praitis V, Casey E, Collar D, Austin J. Creation of low-copy integrated transgenic lines in Caenorhabditis elegans. Genetics. 2001 Mar;157(3):1217-26.

Voronina E, Paix A, Seydoux G. The P granule component PGL-1 promotes the localization and silencing activity of the PUF protein FBF-2 in germline stem cells. Development. 2012 Oct;139(20):3732-40.

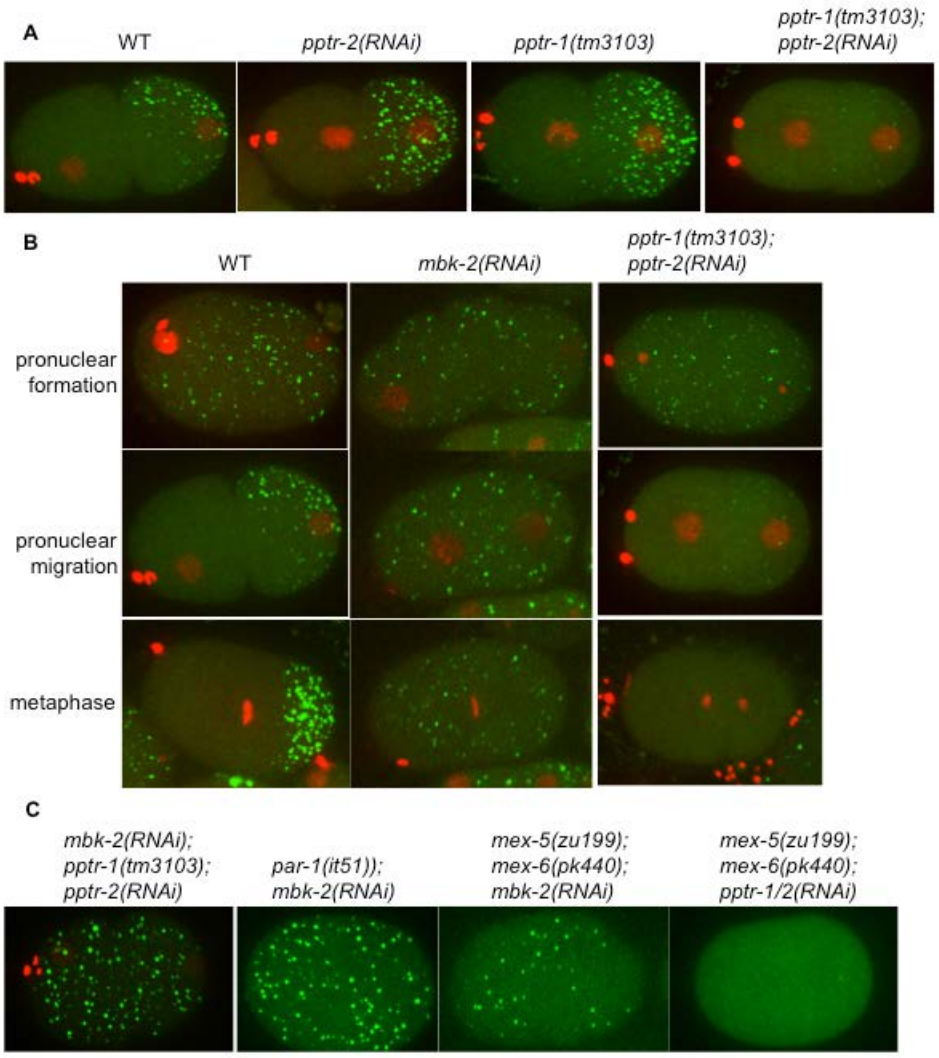

Figure 13. MBK-2 and PP2A$^{PPTR-1/2}$ are required for P granule dynamics

Maximum projections of half embryo (8 μm) stacks. P granules are labeled with GFP::PGL-1. (A) Pronuclear migration stage zygotes in wildtype, *pptr-2(RNAi)*, *pptr-1(tm3103)*, and *pptr-1(tm3103);pptr-2(RNAi)* backgrounds. (B) Time-lapse images of embryos expressing GFP::PGL-1 and mCherry::H2B in *mbk-2(RNAi)* conditions or *pptr-1(tm3103);pptr-2(RNAi)* conditions. (C) Indicated RNAis were applied to embryos for epistasis analysis.

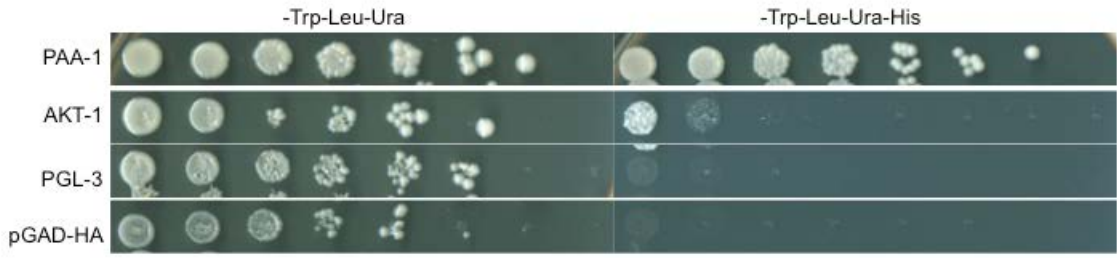

Figure 14. Screening conditions for yeast two hybrid

Yeast transformed with pLEXA-PPTR-1 (bait) and Y3H-PAA-1 (bridge) were subsequently transformed with pGAD-HA fused to the indicated prey proteins. Yeast colonies were grown on –Trp –Leu –Ura to select for transformation and plated in 10-fold serial dilutions on –Trp –Leu –Ura and –Trp –Leu –Ura -His. Conditions were chosen such that PPTR-1 interacted with positive controls (PAA-1 and AKT-1) but not with negative control (empty pGAD-HA vector). Note that PGL-3 does not interact with PPTR-1 in this assay.

Table 3. Hits from yeast two hybrid screen

ID	Name	Description and notes	Number of colonies	RNAi library	Change in wildtype P granules	Dominance over pptr-1(tm3103)	F1 phenotypes - RNAi efficacy
C27H6.3			44	JA:V-6P08	-	-	
Y71H2AM.20		Phosphatase activator	14	JA:III-7K04	-	-	3.8% emb
K02B9.1	meg-1	P granule component and regulator	10	JA:X-6D07	-	-*	63% sterile
Y37D8A.9	mrg-1	chromodomain protein; essential for germ cell survival	5	11068-E-12	-	-	100% sterile
M110.4	ifg-1	eIF4G	3	JA:II-6E05	Somatic granules persist	Somatic granules persist	Larval lethal
C36C9.1		Homology to gei-12	3	JA:X-1F01	-	-	
K02A4.1	bcat-1	branched-chain amino acid aminotransferase	3	JA:X-6G09	-	-	
C11E4.6		CASK-interacting adaptor protein (caskin)	2	JA: X-4D20	-	-*	
T09E8.2	him-17	required for recombination during meiosis	2	V:8B04; 10029-A-7	-	-	0/105 male
T24C4.6	zer-1	ubiquitin ligase substrate recognition subunit	2	JA: III-1E18	-	-	
F32H2.3	spd-2	centrosome maturation	2	JA: I-4O08	Mislocalized in P0	Enhanced	100% emb

ZK6.11			2	11206-D-5	-	-	
Y48E1C.1			2	11038-E -5	-	-*	
F46B6.7	ztf-7	small colony; Zinc finger putative Transcription Factor family	2	11004-A -2	-	-	
C27A12.3	tag-146	small colony; zinc finger protein	2	JA: I-2H04	-	-	
F29G9.2			2	JA: V-4D23	-	-	
T01H3.4	perm-1	required for eggshell formation	1	already have	Mislocalized to C and D	-	100% emb
W05B2.5	col-93	collagen; cannot distinguish from col-92 and col-94	1	JA: III-5H02	-	-	
F18A1.3?	lir-1?	LIN-26-like zinc-finger protein	1	JA: II-5B14	-	-	
F56F3.1	ifet-1	eIF4E transporter	1	10028-E-10	Pleiotropic	-*	79% emb
F52D2.4	gei-12	novel protein; homology to C36C9.1	1	11082-E -11	Mislocalized from P0	Mislocalized from P0	
C09D1.1	unc-89	small colony; required for organization of A bands in striated muscle	1	JA: I-1D10	-	-	
C09G5.5	col-80	small colony; collagen	1	JA: II-7B01	-	-	

Y24D9A.1	ell-1	small colony; ELL transcription elongation factor homolog	1	10015-E -3	-	-	dpy or small
W03C9.7?	mex-1	small colony; P granule component and regulator	1	Cloned	P granule mislocalization	-	98.8% emb
F26D10.3	hsp-1	small colony; HSP-70	1	JA: IV-8A12	-	-	P0 mothers egl
C28H8.12	dnc-2	small colony; member of the dynamitin family	1	Cloned	Pleiotropic	Pleiotropic	98% emb
C55B7.4	acdh-1	Small colony; Found in conjunction with meg-1	1	11019-F -7	-	-	
F59D8.1	vit-3	small colony; Found in conjunction with meg-1	1	11076-H -7	-	-	1.4% emb
Y39G10AR.7		small colony; Found in conjunction with meg-1	1	Cloned	-	-	4.4% emb
K03A1.6	his-38	small colony; Found in conjunction with meg-1	1	Cloned	-	-	6.6% emb
Y32H12A.5	paqr-2	small colony; Progestin and AdipoQ Receptor family	1	11203-H -1	-	-	6% emb

Table 1. Hits from yeast two hybrid screen.

111 individual colonies were picked from –Trp –Leu –Ura –His screening plates. Plasmid DNA was extracted and sequenced with pGAD-HA specific primers, and number of colonies are indicated. RNAi feeding vectors were then obtained from Ahringer or OpenBiosystems RNAi banks, or if unavailable, newly cloned into pL4440. P granule phenotypes were observed from at least 10 adult P0 worms treated >24 hours from L4, and F1s allowed to develop as a indicator of RNAi efficacy. P granule phenotypes are indicated. In 4 RNAi conditions, 1 worm out of >10 showed some rescue in *pptr-1(tm3103)*; these are indicated as -*. All other phenotypes were seen in a majority of treated worms. Note that under these conditions, *meg-1(RNAi)* did not result in P granule phenotypes in wildtype worms.

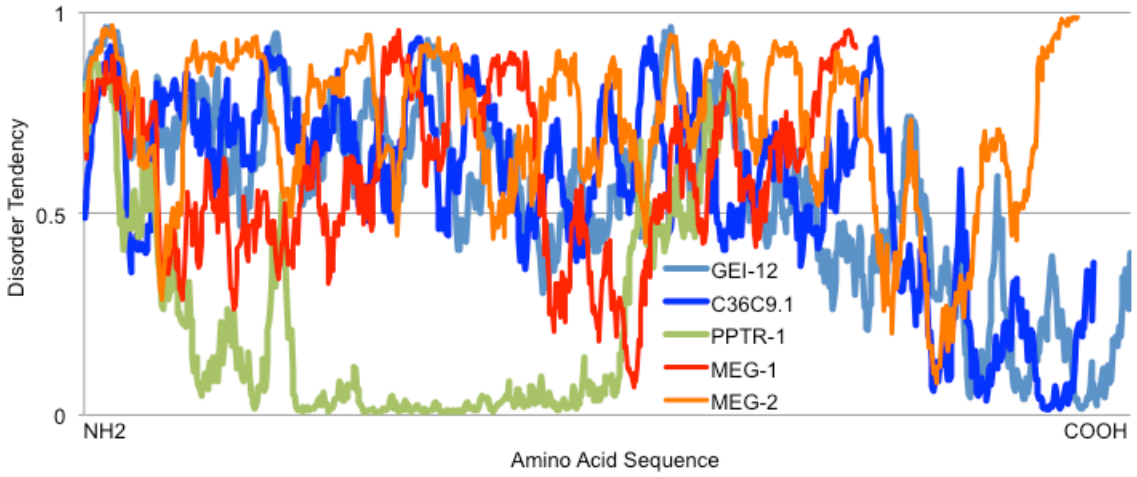

Figure 15. Disorder tendency

Disorder tendencies were plotted using IUPRED (http://iupred.enzim.hu/) using "long disorder" parameters.

	GEI-12 (862 aa)	C36C9.1 (832 aa)	MEG-1 (636 aa)	MEG-2 (819 aa)	PPTR-1 (542 aa)
Ala	5.9%	5.8%	8.0%	7.2%	6.1%
Arg	6.6%	6.7%	4.7%	6.8%	4.4%
Asn	**7.2%**	**8.2%**	**9.6%**	**9.5%**	3.7%
Asp	5.7%	5.9%	5.5%	5.4%	4.8%
Cys	1.6%	1.6%	0.3%	0.2%	1.3%
Gln	5.6%	4.9%	**8.2%**	**8.7%**	4.2%
Glu	4.9%	4.4%	3.8%	4.2%	7.9%
Gly	5.2%	6.6%	6.3%	7.1%	4.4%
His	2.3%	3.0%	3.3%	2.7%	2.6%
Ile	4.2%	3.7%	2.8%	2.4%	5.7%
Leu	6.4%	7.0%	7.4%	6.1%	11.4%
Lys	6.7%	5.5%	3.1%	0.6%	8.1%
Met	1.9%	1.6%	3.8%	3.3%	1.8%
Phe	3.6%	3.6%	3.9%	3.3%	5.9%
Pro	5.7%	5.5%	6.3%	7.3%	6.3%
Ser	**13.8%**	**14.1%**	**11.8%**	**14.3%**	6.1%
Thr	5.6%	5.0%	4.9%	4.6%	5.0%
Trp	0.8%	0.8%	0.6%	0.6%	0.9%
Tyr	2.0%	1.9%	2.4%	2.0%	2.8%
Val	4.4%	4.1%	3.3%	3.7%	6.5%

Table 4: Amino acid compositions.

Amino acid compositions were identified using Wormbase (Release WS241). Note high percentages of asparagine and serine in GEI-12, C36C9.1, MEG-1, and MEG-2. MEG-1 and MEG-2 also exhibit high percentages of glutamine, as documented by Leacock and Reinke 2008.

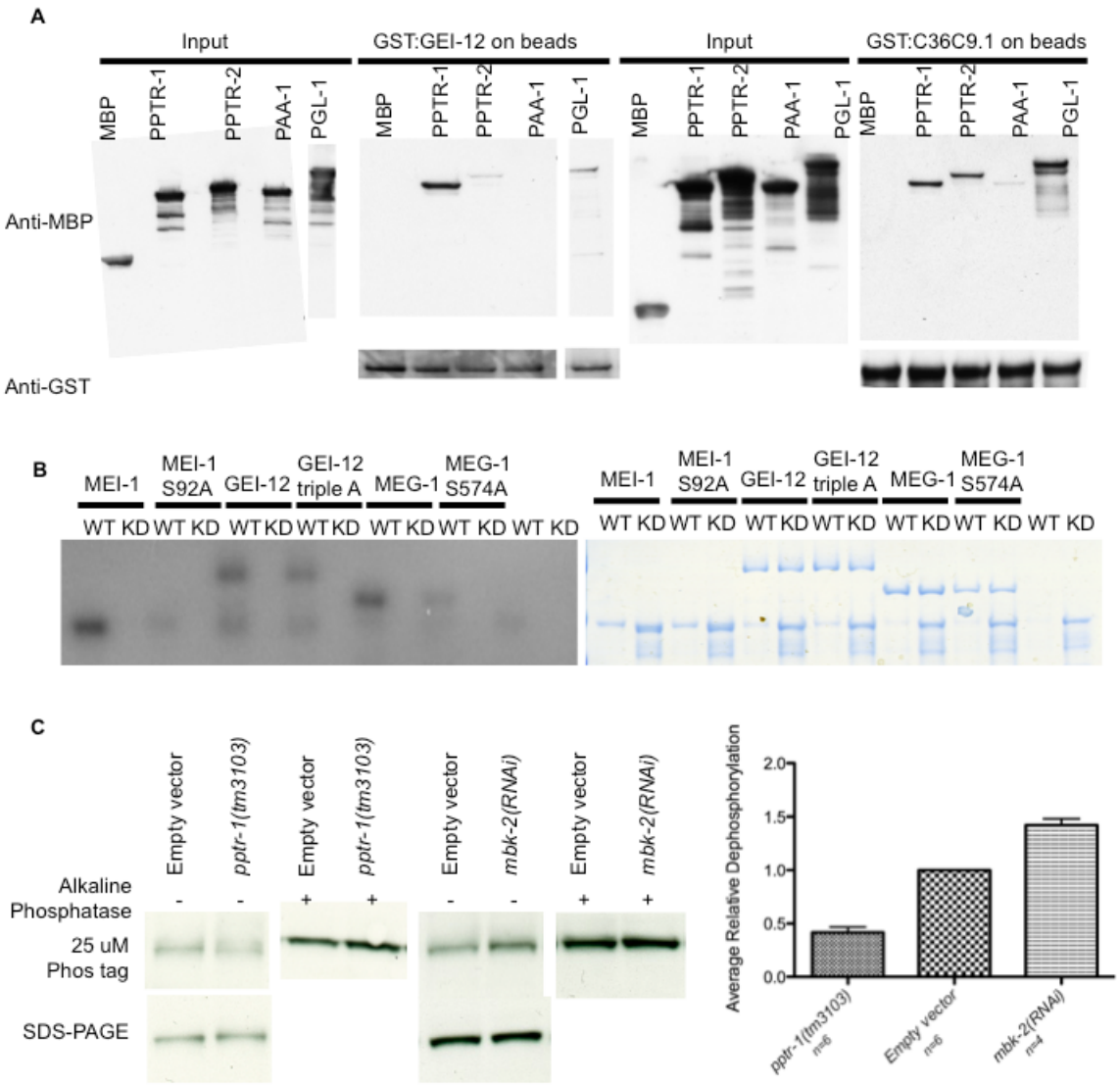

Figure 16. GEI-12 and C36C9.1 are substrates of MBK-2 and PP2A^{PPTR-1}

(A) GST pulldowns using GST:GEI-12 or GST:C36C9.1 as bait, and indicated MBP fusions as prey. Inputs are shown on left and pulldowns on right. Pulldowns were also probed with anti-GST antibody as a loading control. This panel was performed by Dominique Rasoloson.

(B) In vitro kinase assays with recombinant proteins using wildtype MBK-2 or kinase dead (K196R) MBK-2 on indicated substrates. Autoradiograph on left, Coomassie on

right. Phosphorylation is diminished in MEI-1 S92A, GEI-12 triple A (1.4 fold) and MEG-1 S574A (3.3 fold).

(C) In vivo analysis of phosphorylation using Phos-tag gels and embryonic lysates. Left, GFP::GEI-12 runs as one discrete band on SDS-PAGE, but as a weak smear on 25 uM Phos tag. The extent of the smear increases in *pptr-1(tm3103)* embryos and decreases in *mbk-2(RNAi)* embryos. All smears can be collapsed with addition of exogenous alkaline phosphatase prior to running on Phos tag. Right, quantitation of average relative dephosphorylation was obtained by quantitating strength of band on Phos tag versus SDS-PAGE gels and normalizing to empty vector controls. Number of technical replicates are indicated below. This panel was performed by Jarrett Smith.

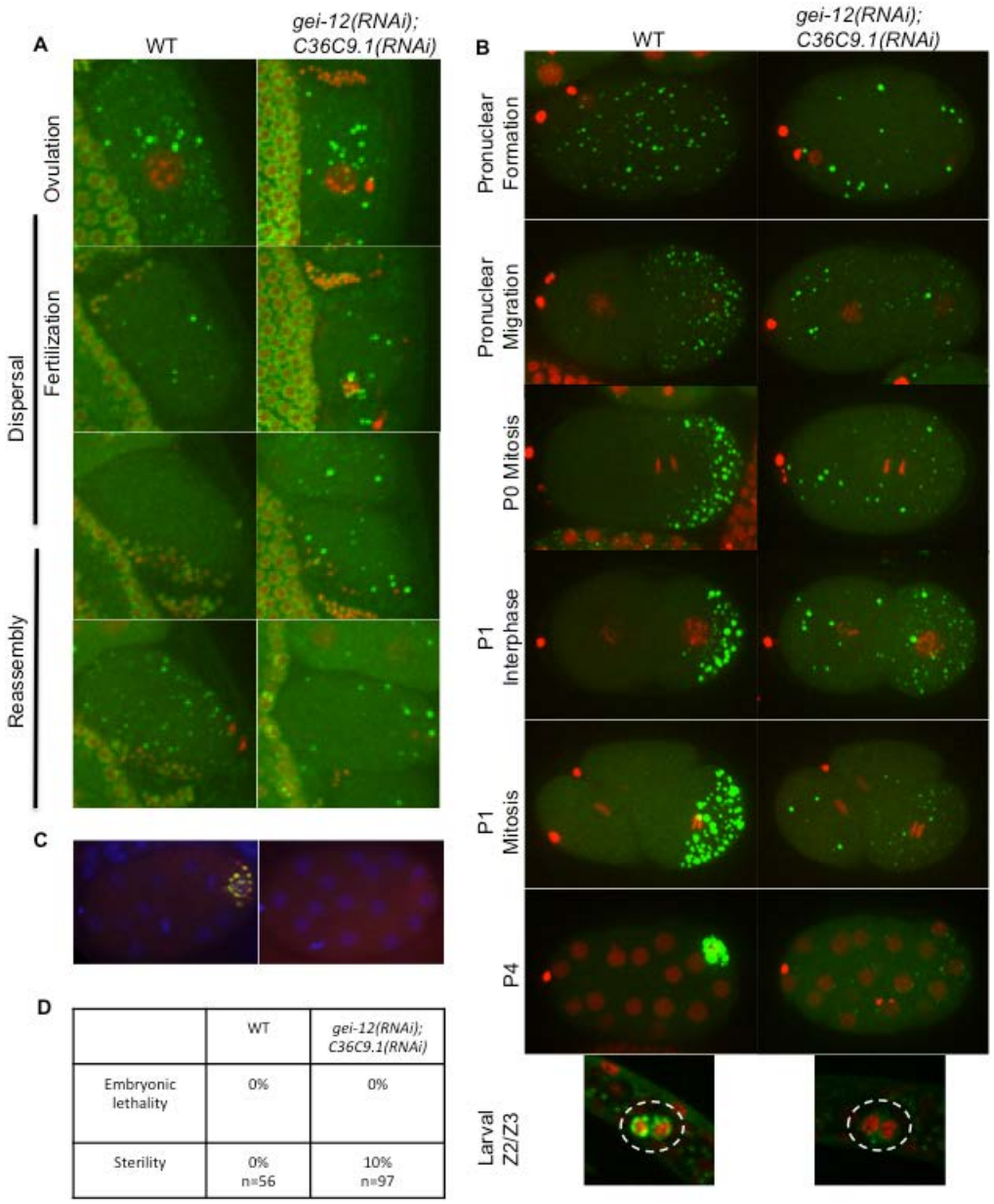

Figure 17. GEI-12 and C36C9.1 are required for embryonic P granule dynamics

(A and B) P granule phenotypes in wildtype (empty vector treated) versus *gei-12(RNAi);C36C9.1(RNAi)* embryos. P granules are labeled in green with GFP::PGL-1 and histones in red with mCherry::H2B. (A) Maximum projections of still frames of movies taken during ovulation and fertilization in live anesthetized worm mothers. Movies are staged using mCherry::H2B and time of fertilization. (B) Maximum

projections of individual embryos staged using mCherry::H2B. Images are 1 μm stacks taken through half the embryo. Bottom: single plane images of larval L1 stage Z2/Z3 germ cells. (C) In situ hybridization for P granule mRNA *nos-2* (red) and GFP:PGL-1 (green). This panel was performed by Alexandre Paix. (D) Embryonic lethality and sterility counts in F1 worms at 24°C.

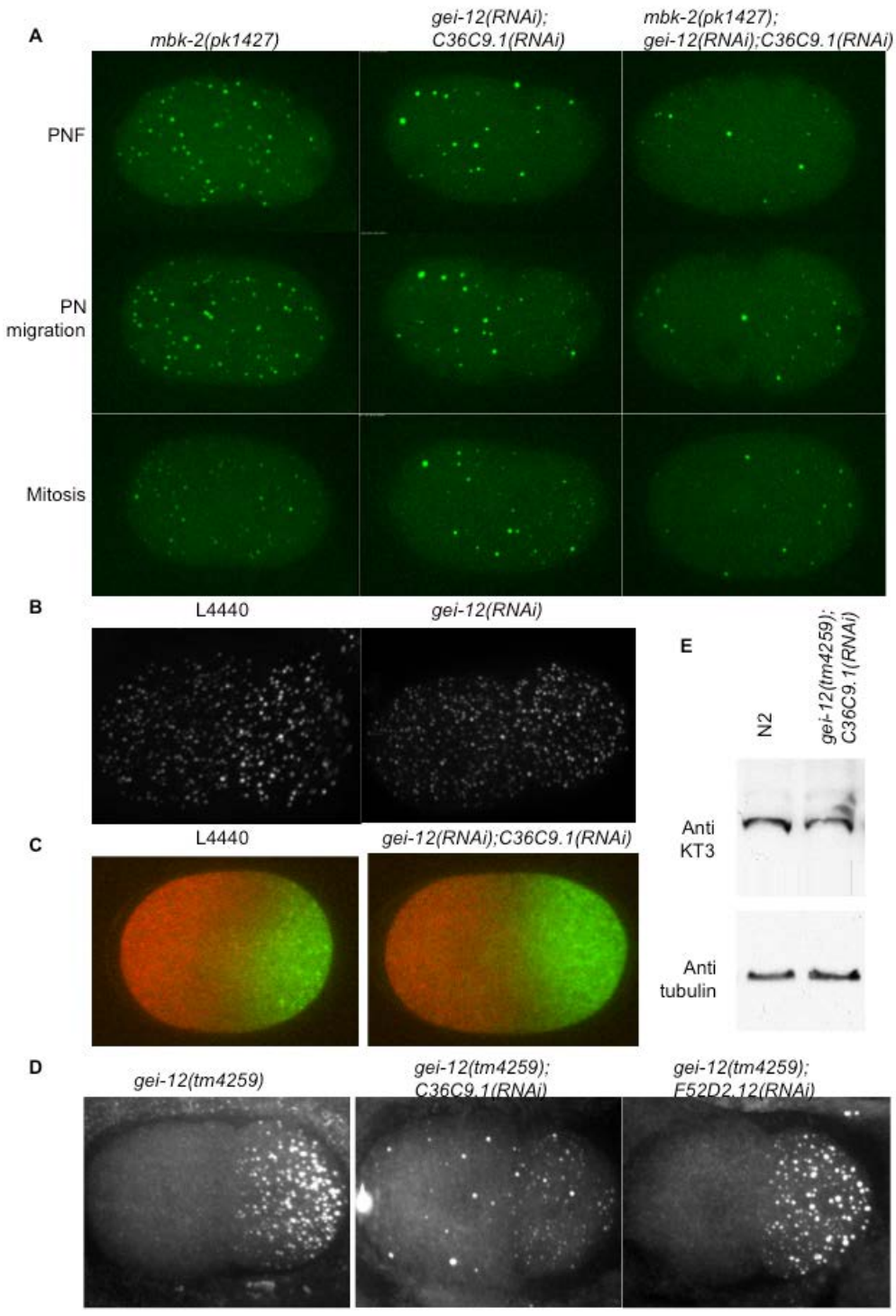

Figure 18. GEI-12 and C36C9.1 are required for MBK-2 activity and are specific for P granule dynamics

(A) Time-lapse images of embryos expressing GFP::PGL-1 in *mbk-2* null, *gei-12(RNAi);C36C9.1(RNAi)*, *mbk-2* null with *gei-12(RNAi);C36C9.1(RNAi)*.

(B) 2 cell stage embryos expressing GFP::PATR-1 were treated with empty vector control or *gei-12(RNAi);C36C9.1(RNAi)*.

(C) 1 cell stage embryos expressing GFP::PIE-1;mCherry::MEX-5 were treated with empty vector control or *gei-12(RNAi);C36C9.1(RNAi)*.

(D) 2 cell stage embryos immunostained with anti-GLH-2 antibody. *gei-12(tm4259)* worms were treated with empty vector control, or with RNAi specific against C36C9.1 or F52D2.12.

(E) Wildtype or *gei-12(tm4259);C36C9.1(RNAi)* embryonic lysates were run on SDS-PAGE and blotted for PGL-3 (KT3 antibody).

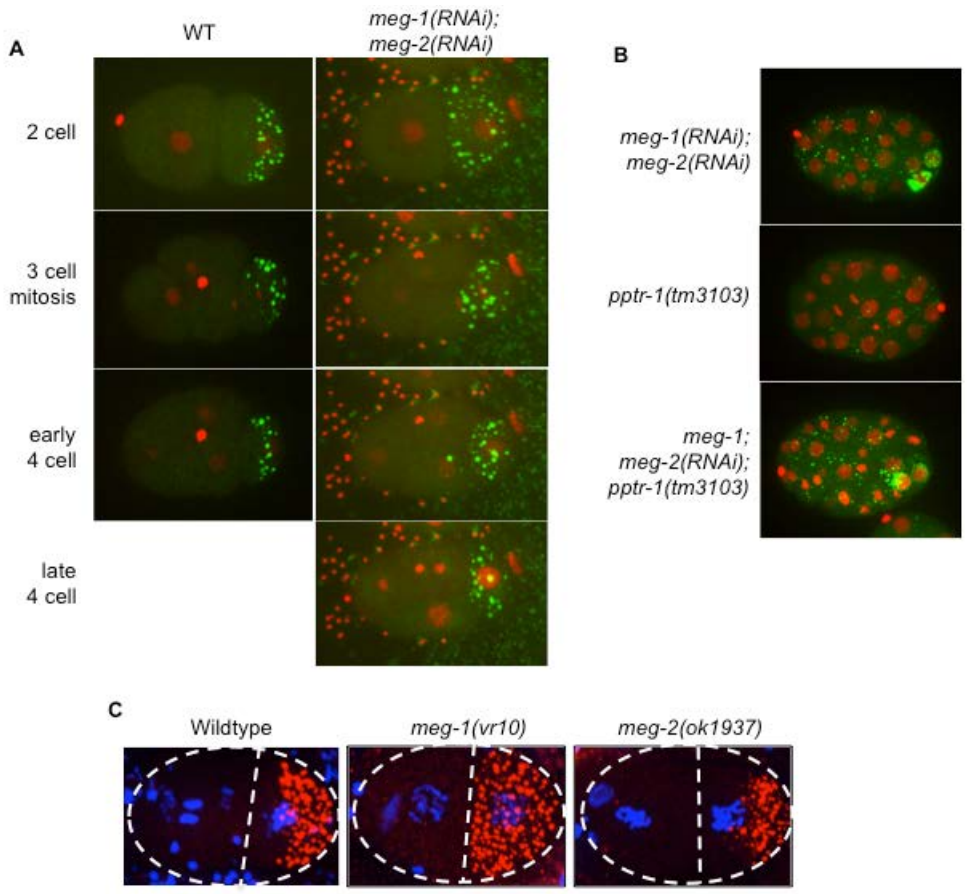

Figure 19. MEG-1 and MEG-2 are required for P granule dynamics

(A) Time-lapse movies of embryos treated with empty vector or *meg-1(RNAi);meg-2(RNAi)*. Embryos were staged from time of zygote mitosis. P granules are missegregated to EMS in *meg-1(RNAi);meg-2(RNAi)* but disassembled over the course of the cell cycle. (B) ~30 cell stage embryos treated with *meg-1(RNAi);meg-2(RNAi)* or empty vector. (C) Immunostaining of wildtype (N2) embryos, *meg-1(vr10)*, or *meg-2(ok1937)* embryos with K76 antibody. Dashed white lines outline the embryo boundary and cell/cell boundary.

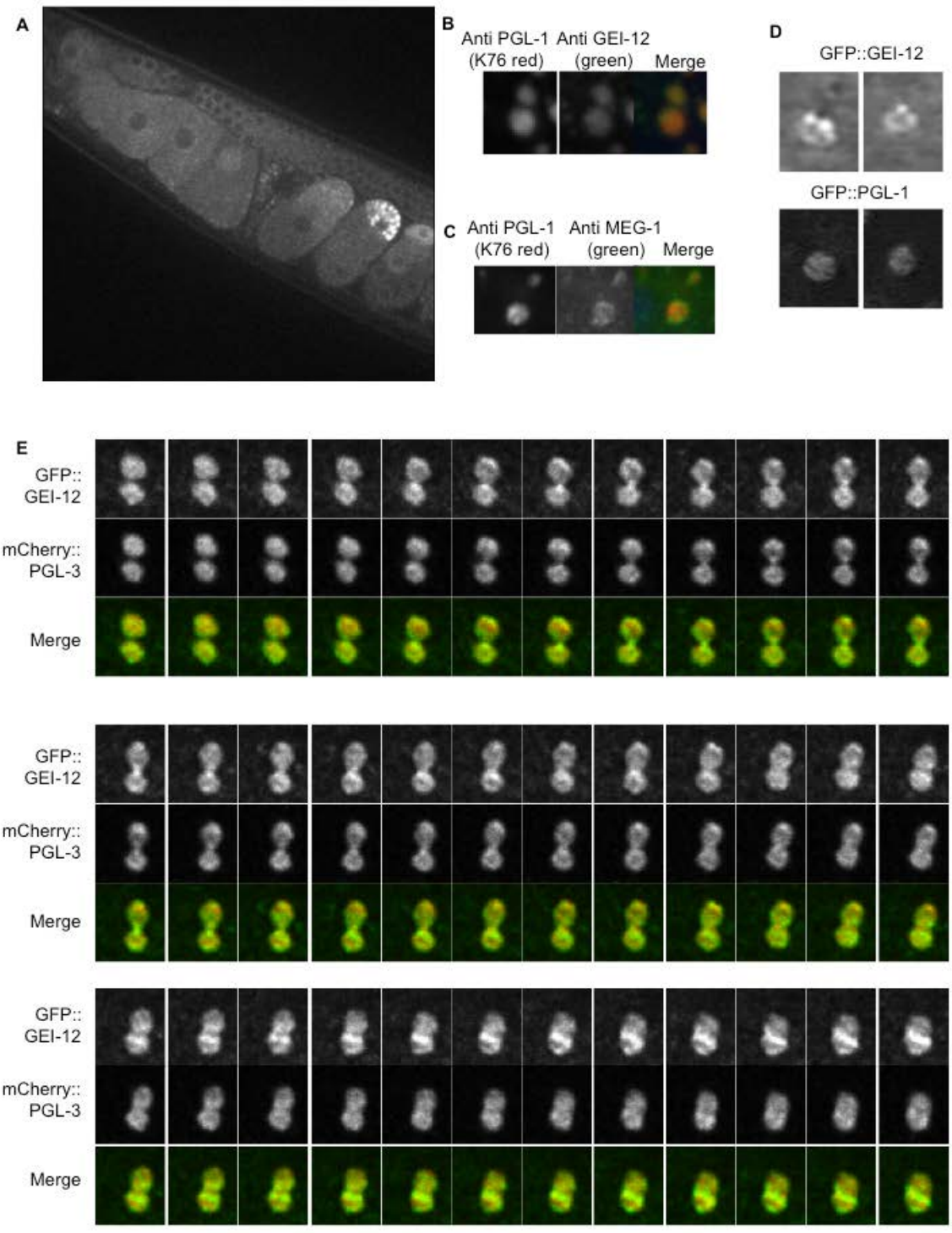

Figure 20. GEI-12 and MEG-1 localize to sub P granule domains

(A) Worm expressing GFP::GEI-12 under control of GEI-12 promoter and 3'UTR

(B) Immunostaining of endogeous GEI-12 and PGL-1 acquired on spinning disk confocal. Max projection of confocal stacks

(C) Immunostaining of endogenous MEG-1 and PGL-1 acquired on spinning disk confocal. Single plane images

(D) Sheet scan structured illumination of GFP:GEI-12 and GFP:PGL-1

(E) Sheet scan deconvolved images of 2 granules undergoing fusion. Embryos express GFP::GEI-12 and mCherry::PGL-3.

Chapter 3
Conclusions and future directions

In this thesis, I have used *C. elegans* P granules as a model system to understand the regulation and function of RNA granules during germline development. I showed that a PP2A regulatory subunit, PPTR-1, is specifically required for the stabilization of P granules during mitosis and the asymmetric segregation of P granule components to the germline. Characterization of the pptr-1 mutant revealed that asymmetric segregation of P granules is not required to distinguish soma and germline and is not required for the asymmetric segregation of other germline factors. I then used PPTR-1 as a tool to probe the mechanistic basis behind localized granule assembly and disassembly, and identified novel P granule components that scaffold P granules and regulate their dynamics in embryos.

Many intriguing questions arise from these results. I address three in this chapter: 1. How is germ plasm organized and localized? 2. What are the molecular mechanisms holding RNA granules together? 3. What is the role of asymmetric P granule segregation in development?

Organization and localization of germ plasm

Our evidence indicates that P granules may not be instructive cues in germ plasm organization. How, then, is germ plasm organized?

One candidate for an instructive cue in germ plasm organization is PAR-1. PAR-1 is asymmetrically localized to the posterior cortex and posterior cytoplasm of the embryo, and the cytoplasmic fraction of PAR-1 is sufficient for localization of downstream cell fate proteins such as MEX-5 (Griffin et al 2011). To directly test whether PAR-1 is

sufficient for germ plasm localization, it would be interesting to ectopically localize PAR-1, such as by optogenetic techniques, and observe germ plasm relocalization.

What are the downstream effectors of PAR-1? One possibility is that PAR-1 negatively regulates MEX-5/6 localization, which then regulates localization of MBK-2 (Figure 21). MBK-2 is required for asymmetric localization of other germ plasm components besides P granules, including PIE-1 and POS-1 (Pellettieri et al 2003), and unpublished observations from our lab have shown that it is asymmetrically localized in the early embryo. A series of experiments may be used to test this hypothesis. First, my experiments show that *mbk-2* is epistatic to *mex-5/6* for P granule localization. Is *mbk-2* epistatic to *mex-5/6* for localization of other germ plasm components? Second, could overexpression or activation of MBK-2, such as removal of a negative regulator, be sufficient to further restrict germ plasm assembly? Third, does MEX-5/6 regulate the localization or activity of MBK-2, for example its activity on substrates? If so, further work may be done to determine how MEX-5/6, two RNA-binding proteins, regulate MBK-2 localization, and whether MBK-2 directly phosphorylates each germ plasm component or phosphorylates an intermediate that helps segregate germ plasm.

In addition, the importance of PPTR-1 and PPTR-2 to germ plasm segregation has not been fully characterized. PPTR-1 and PPTR-2 redundantly regulate P granule localization, and I have observed that they are also required for PIE-1 localization (unpublished data). Whether PPTR-1 and PPTR-2 are required for localization of other germ plasm components is unknown. Do PPTR-1 and PPTR-2 exist in a cytoplasmic gradient, and/or do they exhibit a gradient of activity in the embryo? Is this gradient dependent on *mex-5/6*? Is *mbk-2* epistatic to *pptr-1/2* for germ plasm assembly? Could

overexpression of PPTR-1/2 be sufficient to assemble ectopic germ plasm? What proteins are dephosphorylated by PPTR-1/2 to achieve germ plasm assembly?

Finally, it is possible that PAR-1 may have an independent role in assembling germ plasm. When analyzing the roles of PAR-1 and MEX-5/6 on P granule assembly, we found that PAR-1 was capable of aggregating P granules independently of MEX-5/6. Does *par-1* assemble other germ plasm components independently of *mex-5/6*? If so, one possibility is that PAR-1 may regulate MBK-2 or PPTR-1/2 in parallel with MEX-5/6 (Figure 21). *In vitro* kinase assays may be used to determine whether PAR-1 directly phosphorylates MBK-2 or PPTR-1/2, and phosphomimic/nonphosphorylatable mutations can be used to test the importance of phosphorylation. An alternative is that PAR-1 may phosphorylate other unknown proteins to regulate germ plasm assembly, and future work may be performed to identify PAR-1 substrates.

Molecular mechanisms of granule assembly

One intriguing aspect of RNA-protein aggregates is that these structures exist without a limiting membrane and with constant flux of components, yet remain distinct structures within the cytoplasm. With the identification of protein components required for P granule assembly, we can start to identify the mechanistic basis behind granule assembly. Intrinsically disordered proteins have been hypothesized to aid in RNA granule formation due to their ability to flexibly interact with multiple protein components (Kedersha et al 2013). In order to directly test whether there are specific regions in GEI-12 and C36C9.1 that affect various aspects of P granule assembly, structure-function analyses may be performed in vivo or in vitro to identify domains required for function.

In vitro, these screens may include testing GEI-12 and C36C9.1 truncations for binding to PGL-1 or other P granule components. One intriguing truncation that may be made is a deletion of the more ordered C termini of GEI-12 and C36C9.1. These mutations may then be tested in vivo for P granule aggregation phenotypes. To gain a structural understanding of the function of intrinsically disordered proteins, these protein mutations can then be compared to wildtype by limited proteolysis, circular dichroism, and NMR (Johnson et al 2012). Other intrinsically disordered regions have been shown to undergo conformational change upon binding to macromolecular complexes and substrates (Dyson and Wright 2005), and one possibility is that the ability of GEI-12 and C36C9.1 to sample multiple structural conformations is crucial for P granule assembly. Ultimately, a minimal domain of GEI-12 and C36C9.1 sufficient to scaffold ectopic P granules would be informative to understanding the molecular mechanisms by which intrinsically disordered proteins act on RNA granules.

Roles of asymmetric P granule segregation

We began by addressing the role of asymmetric P granule segregation to the organism by characterizing the *pptr-1* mutant. We found that *pptr-1* mutants are more sensitive to high temperature stress conditions, but the importance of *pptr-1* to somatic processes (Padmanabhan et al 2009) precluded an exhaustic analysis of phenotypes that arise in the *pptr-1* mutant specifically due to P granule missegregation. With the identification of *pptr-1* substrates whose loss of function do not exhibit obvious somatic defects, we are now poised to address the role of asymmetric P granule segregation to organismal development.

First, it would be useful to characterize *gei-12;C36C9.1* loss of function phenotypes. We have observed 10% sterility at 24°C, and it would be informative to characterize whether this sterility is sensitive to differing temperatures and other stress conditions such as oxidative stress. It would also be important to try to characterize germ cell development under these conditions to identify the stages at which development and proliferation are inhibited.

Other phenotypes that may be tested include RNAi inheritance and germline immortality. We had originally tested the ability of *pptr-1* mutants to inherit RNAi, with the idea that perhaps asymmetrically segregated P granules are required for segregation of exogenous dsRNA to the germline. Although we did not observe defects in these preliminary experiments, it would be interesting to use the *gei-12;C36C9.1* knockdown situation to test this again, in order to bypass any potential somatic cell contributions. In addition, it would be intriguing to understand whether there may be cumulative defects in germ cells over generations when losing *gei-12* and *C36C9.1*, and whether P granules may act in establishing germline immortality.

One potential molecular mechanism through which P granules act is by regulation of RNAs. Thus, sequencing the transcriptome, as well as the small RNA-ome of *gei-12;C36C9.1* loss of function germ cells grown at stressed and non-stressed conditions would be incredibly informative. Cell sorting and RNA sequencing techniques pioneered by Chih-Yung Sean Lee in our lab would be instrumental in this type of analysis. Secondary screening approaches may then be used to test whether RNAs downregulated in *gei-12;C36C9.1* germ cells are required for P granule localization and/or germ cell development under different conditions, and whether RNAs upregulated in *gei-*

12;C36C9.1 germ cells may rescue sterility and/or P granule phenotypes. Sequence commonalities among the downregulated RNAs may be used to identify motifs for P granule enrichment. Furthermore, analysis of specific mRNAs and their protein products may give indications about the mechanisms by which P granules affect mRNA metabolism. For example, stress granules are known to form on translationally stalled mRNA complexes, and it would be interesting to directly test whether P granule biogenesis may be similar. Indeed, I have seen that GFP::GEI-12 localizes to *C. elegans* stress granules upon heat shock stress, and there may be a direct relationship between stress granules and P granules in the developing embryo (unpublished data). Further experiments in *C. elegans* and mammalian cells will help to elucidate these links.

References

Dyson HJ, Wright PE. Intrinsically unstructured proteins and their functions. Nat Rev Mol Cell Biol. 2005 Mar;6(3):197-208.

Griffin EE, Odde DJ, Seydoux G. Regulation of the MEX-5 gradient by a spatially segregated kinase/phosphatase cycle. Cell. 2011 Sep 16;146(6):955-68.

Johnson DE, Xue B, Sickmeier MD, Meng J, Cortese MS, Oldfield CJ, Le Gall T, Dunker AK, Uversky VN. High-throughput characterization of intrinsic disorder in proteins from the Protein Structure Initiative. J Struct Biol. 2012 Oct;180(1):201-15.

Kedersha N, Ivanov P, Anderson P. Stress granules and cell signaling: more than just a passing phase? Trends Biochem Sci. 2013 Oct;38(10):494-506.

Padmanabhan S, Mukhopadhyay A, Narasimhan SD, Tesz G, Czech MP, Tissenbaum HA. A PP2A regulatory subunit regulates C. elegans insulin/IGF-1 signaling by modulating AKT-1 phosphorylation. Cell. 2009 Mar 6;136(5):939-51.

Pellettieri J, Reinke V, Kim SK, Seydoux G. Coordinate activation of maternal protein degradation during the egg-to-embryo transition in C. elegans. Dev Cell. 2003 Sep;5(3):451-62.

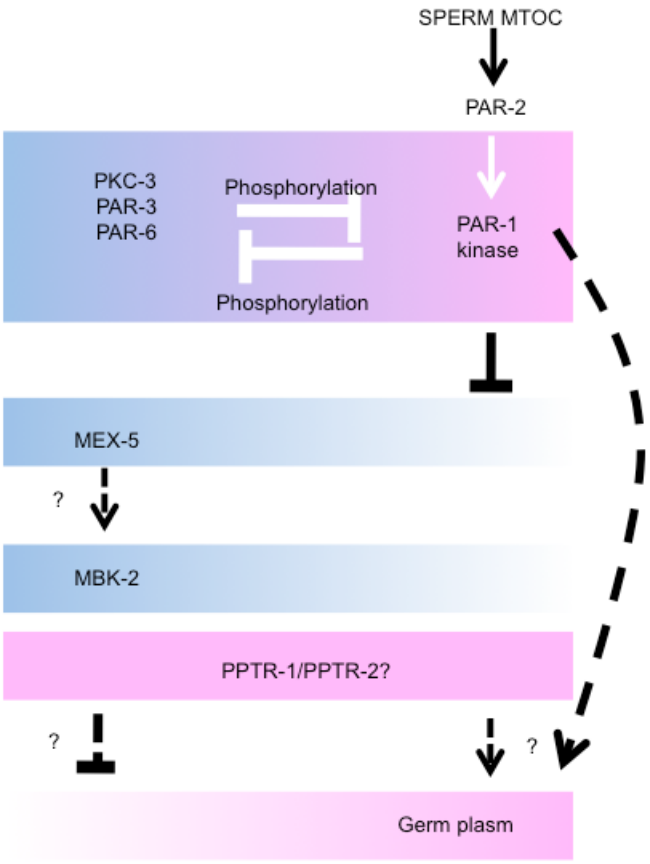

Figure 21. Proposed model for germ plasm assembly.

Dashed arrows represent proposed mechanisms. It is not known whether PPTR-1 and PPTR-2 are localized in a cytoplasmic gradient.

Curriculum Vitae

JENNIFER T. WANG

725 N. Wolfe Street / 706 PCTB
Baltimore, MD 21205
jwang110@jh.edu

Education:

Ph.D. expected	2014	Biochemistry, Cell and Molecular Biology	Johns Hopkins School of Medicine
B.S.	2005	Biology	MIT

Experience:

Research rotation	2008	Lab of Cynthia Wolberger, JHUSOM
Research rotation	2008	Lab of Elizabeth Chen, JHUSOM
Research rotation	2007	Lab of Geraldine Seydoux, JHUSOM
Research assistant	2005-2007	Lab of Sean Whelan, Harvard Medical School
Undergraduate Research Opportunities Program Student	2004-2005	Lab of Phil Sharp, MIT

Honors:

2014 Young Investigators' Day, Michael Shanoff Award, JHUSOM
2012 Outstanding Journal Club presentation, MBG, JHUSOM
2011 Outstanding Journal Club presentation, MBG, JHUSOM
2011 First place, oral presentation, BCMB program retreat, JHUSOM

Publications:

Wang Y., **Wang J.T.**, Rasoloson D., Stitzel M.L., O'Connell K., Smith H.E., Seydoux G (2014) Identification of suppressors of mbk-2/DYRK by whole-genome sequencing. *G3 (Bethesda)* 4(2):231-241. PMCID PMC3931558

Wang J.T., Seydoux G. (2013) Germ cell specification. Germ Cell Development in C. elegans, In: Advances in Experimental Medicine and Biology. 757:17-39. Book Chapter.

Gallo C.M.*, **Wang J.T.***, Motegi F., Seydoux G (2010) Cytoplasmic partitioning of P granule components is not required to specify the germline in C. elegans. *Science* 330(6011):1685-1689. *Equal contribution. PMCID PMC3072820

Bheda P., **Wang J.T.**, Escalante-Semerena J.C., Wolberger C (2011) Structure of Sir2Tm bound to a propionylated peptide. *Protein Sci*. 20(1):131-139. PMCID PMC3047069

Wang J.T.*, McElvain L.E.*, Whelan S.P. (2007) A sequence specific messenger RNA capping machine encoded by vesicular stomatitis virus. *J. Virol*. 81 (20):11499-11506. *Equal contribution. PMCID PMC2045530

Li J., **Wang J.T.**, Whelan S.P. (2006) A unique strategy for mRNA cap methylation used by vesicular stomatitis virus. *PNAS* 103 (22):8493-8. PMCID PMC1482520

Abstracts:

Wang J.T., Seydoux G. (2013) Asymmetric segregation of P granules requires granule remodeling by two novel serine-rich proteins. International C. elegans Meeting, Los Angeles, CA, June 27 2013. Poster.

Wang J.T., Seydoux G. (2012) Regulation of P granule dynamics by phosphorylation. Germ Cell Meeting, Cold Spring Harbor, NY, October 3 2012. Platform.

Wang J.T., Seydoux G. (2011) Germ granules: fate determinants or fate byproducts? BCMB Program Retreat, Towson, MD, October 7 2011. Platform.

Wang J.T., Gallo C.M., Seydoux G. (2011) The PP2A phosphatase subunit PPTR-1 is required to stabilize embryonic P granules during mitosis. International C. elegans Meeting, Los Angeles, CA, June 24 2011. Poster.

Wang J.T., Gallo C.M., Seydoux G. (2010) Regulation of Germ Granule Integrity by the Phosphatase PP2A. ASCB, Philadelphia, PA, December 12 2010. Poster.

Wang J.T., Seydoux G. (2010) Cytoplasmic Partitioning of P granule components is not required to specify the germline in Caenorhabditis elegans. ASCB Special Interest Subgroup, The Cell Biology of Metabolic Pathways, Philadelphia, PA, December 11 2010. Platform.

Wang J.T., Gallo C.M., Seydoux G. (2010) Cytoplasmic partitioning of P granule components is not required to specify the germline in C. elegans. Germ Cell Meeting, Cold Spring Harbor, NY, October 6 2010. Poster.

Wang J.T., Gallo C.M., Seydoux G. (2009) Regulation of P granule Integrity by the Phosphatase PP2A. ASCB, San Diego, CA, December 6 2009. Poster.

Wang J.T., Gallo C.M., Seydoux G. (2009) Regulation of germ granules by a phosphatase. Germ Cell Meeting, Cold Spring Harbor, NY, October 2 2009. Poster.

Wang J.T., Gallo C., Voronina E., Seydoux G. (2009) Regulation of P granule integrity by a phosphatase. International C. elegans Meeting, Los Angeles, CA, June 27, 2009. Poster.

Service:

2008-2011	Tutor, Dyslexia Tutoring Program, Baltimore, MD
2009	Teaching assistant, Fundamentals of Genetics, JHUSOM
2010	Teaching assistant, Fundamentals of Genetics, JHUSOM
2012-2014	Peer Mentor, Peer Mentoring Program, JHUSOM